

**Institut für Experimentelle Genetik
GSF-Forschungszentrum für Umwelt und Gesundheit
Neuherberg**



**Changes in the kidney proteome of vitamin D
receptor knock-out mice**

Daniela Perovic

Vollständiger Abdruck der von der Fakultät Wissenschaftszentrum
Weihenstephan für Ernährung, Landnutzung und Umwelt der Technischen
Universität München zur Erlangung des akademischen Grades eines

Doktors der Naturwissenschaften

genehmigten Dissertation.

Vorsitzender: Univ.-Prof. Dr. Alfons Gierl

Prüfer der Dissertation: 1. Univ.-Prof. Dr. Johannes Buchner
2. Univ.-Prof. Dr. Wolfgang Wurst

Die Dissertation wurde am 13.02.2003 bei der Technischen Universität München
eingereicht und durch die Fakultät Wissenschaftszentrum Weihenstephan für
Ernährung, Landnutzung und Umwelt am 15.04.2003 angenommen.

Table of content

Abstract	5
Zusammenfassung	7
Abbreviations	9
1. INTRODUCTION	11
1.1. Vitamin D	11
1.1.1. Metabolism	11
1.1.2. The role of vitamin D	13
1.1.3. Mechanism of action	13
1.2. Nuclear vitamin D receptor (VDR)	16
1.3. Vitamin D deficiency	17
1.3.1. Phenotypic characteristics of VDR knock-out mice	17
1.3.1.1. Impact of VDR deficiency on renal tubular calcium reabsorption	18
1.4. Aim of the study	19
2. RESULTS	21
2.1. Two-dimensional electrophoresis	21
2.1.1. Isoelectric focusing	21
2.1.2. SDS-polyacrylamide gel electrophoresis	22
2.1.3. PDQuest software analysis of 2-D electrophoresis gels	26
2.1.4. 2-D electrophoresis in a narrow pH range	32
2.2. Protein identification	34
2.2.1. Visualization	34
2.2.2. MALDI-TOF mass spectrometry	36
3. DISCUSSION	47
3.1. Two-dimensional electrophoresis (2-D electrophoresis) as a method of choice in different protein expression analysis	47
3.1.1. 2-D electrophoresis limitations	48
3.1.2. Improvement possibilities	50
3.2. Identified changes in protein expression and connection to vitamin D	51
3.3. Conclusions	55

4. MATERIALS AND METHODS	57
4.1. METHODS	57
4.1.1. Two-dimensional electrophoresis	57
4.1.1.1. First dimensional isoelectric focusing	60
4.1.1.2. Second-dimension SDS-PAGE	64
4.1.1.3. Visualization	66
4.1.1.4. Pattern evaluation	67
4.1.2. In-gel digestion	68
4.1.3. MALDI-TOF mass spectrometry	69
4.2. MATERIALS	75
4.2.1. Buffers and solutions	75
4.2.2. Chemicals	79
4.2.2.1. General	79
4.2.2.2. Standards	80
4.2.3. Enzymes	80
4.2.4. IEF material	80
4.2.5. SDS-PAGE material	80
4.2.6. Other material	80
4.2.7. Animals	81
4.2.8. Software	81
4.2.9. Devices	81
Literature	83
<i>List of figures</i>	91
<i>List of tables</i>	93
5. APPENDIX	95
5.1. Protein concentration measurement	95
Acknowledgements	99

Abstract

Vitamin D is a steroid hormone whose main function in organism is regulation of Ca^{2+} metabolism. The hormone acts in various tissues, but mostly in kidney, bone and intestine, either directly, influencing genomic and nongenomic responses, or indirectly via regulation of Ca^{2+} homeostasis. To exert its genomic actions vitamin D binds to the vitamin D receptor (VDR), whereupon liganded receptor binds to vitamin D response elements (VDRE) in target gene promoter regions and activates transcription. The mechanism of nongenomic responses, which take only seconds/minutes and modulate different signalling pathways, is still unclear.

VDR belongs to the steroid hormone receptor superfamily and contains several domains common to all members of the family, including an N-terminal DNA binding domain, a ligand binding domain, a transcription factor domain and a C-terminal domain responsible for interactions with cofactors.

In this study, VDR knock-out mice were examined, in which the DNA binding domain of VDR was partially deleted, thus disabling DNA binding, but the receptor was expressed and had an intact ligand binding domain. This mutation caused ablation of both, genomic and nongenomic responses in mice. Therefore, changes in the expression level of a large number of different proteins, which are regulated by vitamin D, or involved in vitamin D mediated response, were expected. Hence 2-dimensional electrophoresis was used to investigate changes in the kidney proteome of VDR knock-out mice. This approach enables an unbiased exploratory survey of a huge number of proteins at the same time.

Using this technique a number of differentially expressed proteins were identified: VDR, cytosolic malate dehydrogenase, lactate dehydrogenase, hydroxyacid oxidase and adenosine kinase. Except VDR, all of them were significantly downregulated in VDR knock-out mice and they were generally involved in central metabolic processes in the cell. Taken together, downregulated expression of these enzymes implied lower energy supplies in kidneys of VDR deficient animals. However, no major functional abnormalities in VDR knock-out mice could be observed.

Identification of VDR itself provided additional evidence that the receptor was expressed, even with partially deleted DNA binding domain, and therefore points to the importance of the N-terminal part of the protein in vitamin D response.

Zusammenfassung

Vitamin D ist ein Steroidhormon, dessen Funktion hauptsächlich in der Regulation des Calciummetabolismus besteht. Hierfür wirkt es in zahlreichen Geweben, aber vor allem in der Niere, in den Knochen und im Darm. Vitamin D kann direkt (genomische und nicht-genomische Wirkweise) oder indirekt (Einfluss auf die Calciumhomöostase) wirken. Die genomische Wirkung wird durch die Bindung und des Vitamin D an den Vitamin D-Rezeptor (VDR) vermittelt. Dieser Komplex bindet an Vitamin D-Response-Elemente (VDRE) in Promotoren von Zielgenen und aktiviert so deren Transkription. Der Mechanismus der nicht-genomischen Reaktionen, die innerhalb von Sekunden oder Minuten ablaufen und verschiedene Signalwege modulieren, ist immer noch unklar.

VDR gehört zur Steroid-Rezeptor-Superfamilie und enthält mehrere Domänen, die allen Mitgliedern gemeinsam sind. Dazu gehören eine N-terminale DNA-Bindungsdomäne, eine Liganden-Bindungsdomäne und eine C-terminale Region, die für die Wechselwirkung mit Cofaktoren zuständig ist.

In der vorliegenden Arbeit wurden VDR-*knock out*-Mäuse (VDR-*k.o.*-Mäuse) untersucht. Diese zeichnen sich durch eine teilweise verkürzte DNA-Bindungsdomäne des VDR aus. Der Rezeptor wird zwar exprimiert, kann aber nur Vitamin D und nicht mehr VDREs binden. Erstaunlicherweise fallen dadurch sowohl die genomischen als auch die nicht-genomischen Reaktionen komplett aus. Deshalb wurde angenommen, dass sich das Expressionsniveau zahlreicher Proteine, die entweder von Vitamin D reguliert werden oder an der Vitamin D-Antwort beteiligt sind, ändern sollte. Um diese Veränderungen zu untersuchen, wurde das Nieren-Proteom von VDR-*k.o.*-Mäusen mit zwei-dimensionaler Elektrophorese analysiert. Durch diesen Ansatz wird die Analyse einer großen Zahl von Proteinen in einem einzigen Experiment auf unvoreingenommene und umfassende Art ermöglicht.

Eine Reihe unterschiedlich exprimierter Proteine wurde mit Hilfe dieser Technik identifiziert: Neben VDR waren dies u.a. die zytosolische Malatdehydrogenase, die Laktatdehydrogenase, die Hydroxysäureoxidase und die Adenosinkinase. Mit Ausnahme von VDR sind alle diese Proteine, die an zentralen intrazellulären Stoffwechselprozessen beteiligt sind, in den untersuchten VDR-*k.o.*-Mäusen signifikant herunterreguliert. Diese Daten weisen auf eine mangelhafte Energieversorgung in der Niere der VDR-defekten Tiere hin. Allerdings wurden keine signifikanten Funktionsstörungen beobachtet.

Die Beobachtung, dass auch VDR selber in VDR-*k.o.*-Mäusen fehlreguliert ist, lieferte einen zusätzlichen Hinweis, dass der Rezeptor exprimiert wird, auch wenn ihm Teile der DNA-Bindungsdomäne fehlen. Das bestätigt die wichtige Funktion der N-terminalen Rezeptor-Domäne für die Vitamin D-Antwort.

Abbreviations

1 α ,25-(OH) ₂ D ₃	1 α ,25-dihydroxyvitamin D ₃
2-D electrophoresis	two-dimensional electrophoresis
25-OH-D ₃	25-hydroxyvitamin D ₃
A ₆₆₀	absorbance at 660 nm
ACTB	β -actin
ACTH	adenocorticotrophic hormone
ADH	alcohol dehydrogenase
ADK	adenosine kinase
AF-2 domain	affinity function domain
AMP	adenosine monophosphate
ATP	adenosine triphosphate
ATPB	ATP synthase β -chain
BSA	bovine serum albumin
CaR	extracellular Ca ²⁺ (Ca _o ²⁺)-sensing receptor
COOH terminus	carboxyl terminus
CYP1 α	25-hydroxyvitamin D-1 α -hydroxylase
CYP24	25-OH-D ₃ -24-hydroxylase
CYP27	vitamin D ₃ -25-hydroxylase
DAG	diacylglycerol
DBP	vitamin D binding protein
DIGE	difference gel electrophoresis
DNA	deoxyribonucleic acid
DTE	dithioerythritol
DTT	dithiothreitol
EcaC -1 and -2	epithelial calcium channels 1 and 2
ERK1/ERK2	extracellular signal-regulated kinase 1 and 2
HAO3	hydroxyacid oxidase 3
HCCA	α -cyano-4-hydroxycinnamic acid
IEF	isoelectric focusing
IL-4	interleukin-4
IL-18	interleukin-18
IP ₃	inositol-1,4,5-trisphosphate
IPG strip	ready-made Immobiline DryStrip gels
ko	knock-out
kVh	kilovolt-hour
LDHB	L-lactate dehydrogenase B-chain
MALDI-TOF	matrix assisted laser desorption/ionization time-of-flight
MAP kinase	mitogen activated protein kinase
MDHC	cytosolic malate dehydrogenase

MEK1/MEK2	Raf kinases
mRNA	messenger ribonucleic acid
MS	mass spectrometry
M _w	molecular weight
NACH	nucleic acid conducting channel
NADH	<i>reduced</i> nicotinamide adenine dinucleotide
NADPH	<i>reduced</i> nicotinamide adenine dinucleotide phosphate
NC	nitrocellulose
n.c.	negative control
NCoR	nuclear corepressor
NH ₂ terminus	amino terminus
PBS	phosphate buffered saline
pI	isoelectric point
PIP ₂	phosphoinositoldiphosphate
PKC	protein kinase C
PLC	phospholipase C
PMF	peptide mass fingerprint
POL II	RNA polymerase II
ppm	parts per million
PTH	parathyroid hormone
RNA	ribonucleic acid
RXR	retinoid acid receptor
SDS-PAGE	sodium dodecylsulfate polyacrylamide gel electrophoresis
SELDI	surface enhanced laser desorption/ionization
Shc	steroid hormone coactivator
SMRT	silencing mediator for retinoid and thyroid hormone receptors
Src	steroid receptor coactivator
V	volt
VDR	vitamin D receptor
VDR ^{mem}	putative vitamin D membrane receptor
VDRB1	vitamin D receptor with extended amino terminus
VDRE	vitamin D response elements
TFA	trifluoroacetic acid
TGF-β1	transforming growth factor-β
TNF-α	tumor necrosis factor-α
UV	ultraviolet radiation
wt	wild type

1. INTRODUCTION

1.1. Vitamin D

1.1.1. Metabolism

Formation of vitamin D₃ from 7-dehydrocholesterol represents the first step in vitamin D metabolism. The process is taking place in the skin, by exposure to ultraviolet light. Alternatively, vitamin D, in the form of either vitamin D₂ or vitamin D₃ can be derived from dietary sources. The biologically active form, 1 α ,25-dihydroxyvitamin D₃ (1 α ,25-(OH)₂D₃) is formed in two further activation processes, involving first 25-hydroxylation in the liver, followed by 1 α -hydroxylation in the kidney. The product of the 25-hydroxylation step, 25-OH-D₃ is the major circulating form of vitamin D, due to its strong affinity toward vitamin D binding protein in blood (DBP). Its further metabolic fate depends on the calcium requirement in the organism.

Metabolic activation of vitamin D₃ is catalysed by specific cytochrome *P*-450-containing enzymes, the vitamin D₃-25-hydroxylase (CYP27) and the 25-hydroxyvitamin D-1 α -hydroxylase (CYP1 α) in the renal proximal tubular cell, with the later one being tightly regulated by the levels of plasma 1 α ,25-(OH)₂D₃ and calcium (**Jones G. et al. 1998**). In addition to its final metabolic activation in kidney, 25-OH-D₃ can be also inactivated by action of the 25-OH-D₃-24-hydroxylase (25-OH-D-24-OHase). In early '90s, this cytochrome *P*-450 containing enzyme, CYP24, was cloned and it was reported that it performs the 24-hydroxylation and subsequent reactions leading to inactivation of both 1 α ,25-(OH)₂D₃ and 25-OH-D₃ (**Akiyoshi-Shibata M. et al. 1994; Beckman M.J. et al. 1996**). The mechanisms of vitamin D activation and inactivation processes are shown in **Figure 1**.

In response to hypocalcaemia, the parathyroid glands, the main calcium sensing organs in vertebrates, secrete parathyroid hormone (PTH), which induces 25-hydroxyvitamin D-1 α -hydroxylase (**Shinki T. et al. 1998**). At the same time, PTH suppresses 25-OH-D-24-OHase (**Shinki T. et al.; 1992**). This leads to further increment in 1 α ,25-(OH)₂D₃ plasma level.

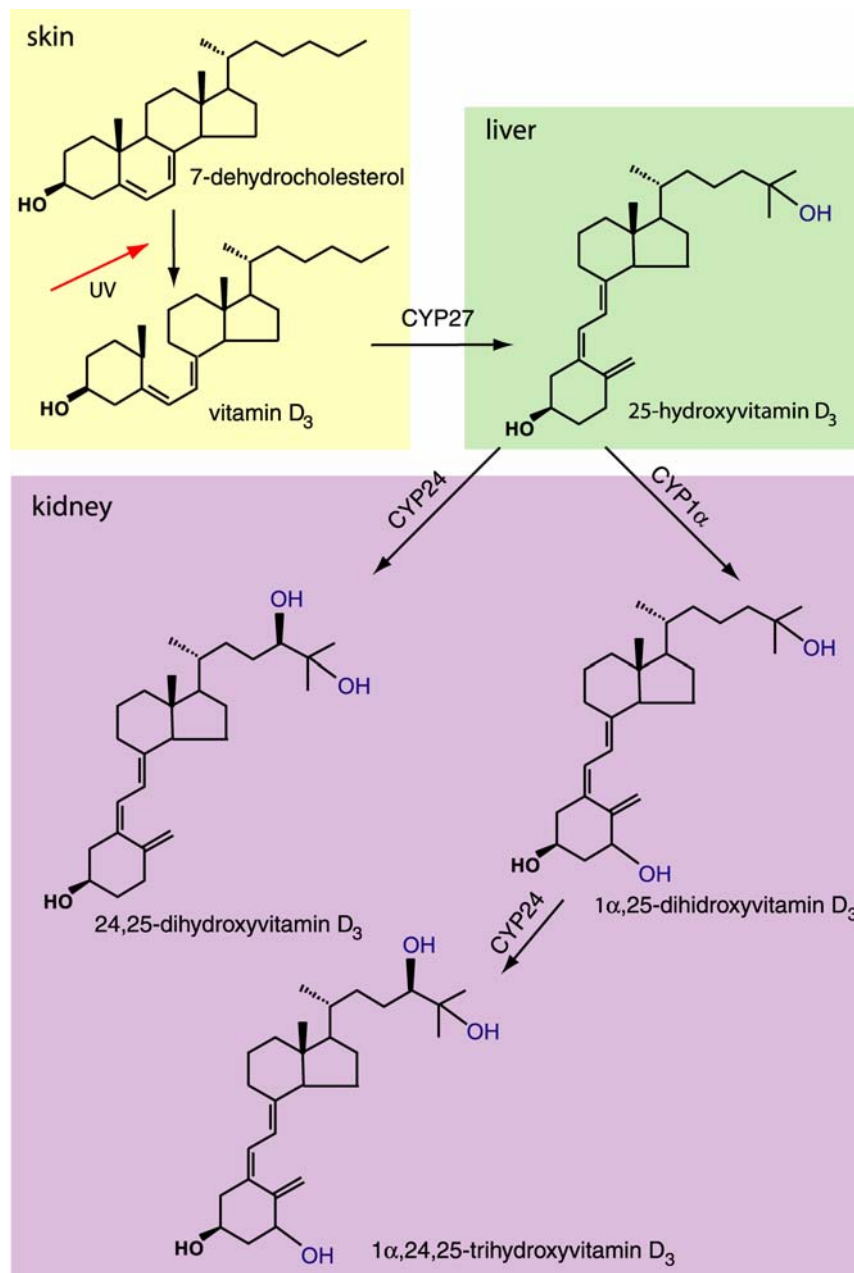


Figure 1. Activation and inactivation steps in vitamin D metabolism. The first step in vitamin D metabolism is conversion of 7-dehydrocholesterol to vitamin D₃ under the influence of UV light in the skin. Active form of vitamin D is formed in two subsequent steps, 25-hydroxylation step catalysed by specific vitamin D₃-25-hydroxylase (CYP27) in liver, followed by additional hydroxylation step catalysed by 25-hydroxyvitamin D-1α-hydroxylase (CYP1α) in kidneys. Inactivation of both 25-hydroxyvitamin D₃ and 1α,25-dihydroxyvitamin D₃ is catalysed by the same enzyme, 25-hydroxyvitamin D-24-hydroxylase (CYP24) in kidneys.

1.1.2. The role of vitamin D

The major role of vitamin D in the organism is calcium mobilization. Elevation in $1\alpha,25\text{-(OH)}_2\text{D}_3$ plasma levels causes increased intestinal calcium absorption involving calbindin and possible other proteins by so far unknown mechanisms (**Jones G. et al. 1998**). At the same time PTH and $1\alpha,25\text{-(OH)}_2\text{D}_3$ stimulate bone resorption by promoting differentiation of osteoclast. This mechanism involves osteoblast mediated activation of RANK on the osteoclast surface and triggering of several downstream signalling cascades, which causes osteoclast to resorb bone (**Jones G. et al. 1998; Purroy J. and Spurr N.K. 2002**). The action of vitamin D in stimulating bone resorption is not only to provide bone calcium for the plasma, but to complete bone-remodelling required for bone shaping and repairing processes.

Recently, additional roles of vitamin D have been discovered in various organs like pancreas, skin, ovaries, parathyroid gland, as well as mammary epithelium, neuronal tissue, macrophages and T-lymphocytes. In parathyroid gland, vitamin D suppresses PTH secretion, and in T-lymphocytes, it suppresses production of $\text{TNF-}\alpha$ and $\text{interferon-}\gamma$ by stimulating production of $\text{TGF-}\beta 1$ and IL-4 (**Cantorna M.T. et al. 2000**). In skin, vitamin D induces keratinocyte differentiation. Vitamin D also influences insulin secretion from the pancreas by raising plasma calcium concentration (**Chertow B.S. et al. 1983**). Additionally, studies performed on vitamin D deficient mice revealed possible vitamin D involvement in both, male and female fertility (**Yoshizawa T. et al. 1997**).

1.1.3. Mechanism of action

Vitamin D acts *via* specific vitamin D receptor(s) (VDR) and elicits two different kinds of responses, a fast nongenomic response in a time range of seconds/minutes, and a slower genomic response, which needs hours or days. The mechanism of genomic action is very well known and it is a result of vitamin D association with nuclear VDR, which leads to binding to and activation of the vitamin D response element (VDRE) in various gene promoter regions. The functional form of nuclear VDR is heterodimer with retinoid acid receptor (RXR). Binding of this heterodimer to the response element induces a bend in the DNA of the promoter and interaction with other transcription factors, which act as coactivators of transcription (**Kimmel-Jehan C. et al. 1999; Kimmel-Jehan C. et al. 1997**). Recent research implied that these coactivator proteins might possess intrinsic histone acetylase activity (**Chen H. et al. 1997**). Thus binding of VDR in promoter region and recruitment of its coactivators, might result in histone acetylation and subsequent release from DNA. This in turn leads to the opening of the promoter to the transcriptional machinery (**Figure 2**).

INTRODUCTION

Except as an activator, VDR may act as a repressor of transcription as well (**Figure 2**), but the mechanism of repression is less understood. A current model suggests that class II nuclear receptors, to which VDR belongs, form complexes with corepressors when ligand is not present. Therefore, all nuclear hormone-responding genes are initially in repressed state, due to the chromatin condensation (**Torchia J. et al. 1998**).

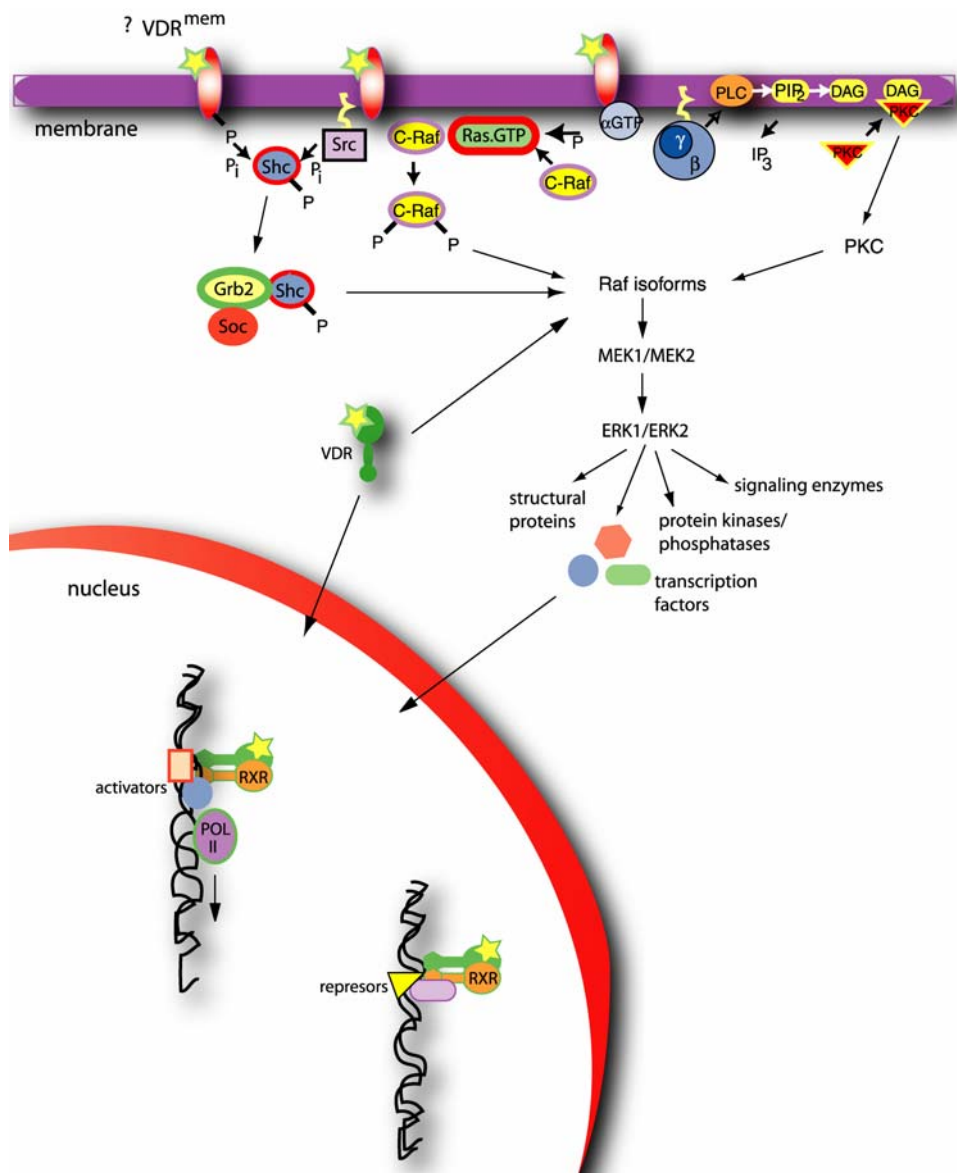


Figure 2. Vitamin D mediated genomic and nongenomic response. The nongenomic response is proposed to be mediated *via* a putative vitamin D membrane receptor (VDR^{mem}), as well as classical nuclear vitamin D receptor (VDR). In both cases binding of the $1\alpha,25-(OH)_2D_3$ (presented with a star) results in activation of mitogen activated protein (MAP) kinases ERK1 and ERK2, which in turn phosphorylate a number of proteins involved in regulation of processes in nucleus and cytosol. The signal transduced *via* membrane receptor(s) can utilize 3 possible mechanisms: membrane receptors with intrinsic tyrosine kinase activity that can interact with Shc/Grb2/Soc and then Raf; membrane receptors without intrinsic tyrosine kinase activity, which utilize Src to phosphorylate Shc that consequently interacts with Grb2/Soc and activates Raf; or those that activate G-proteins to generate either membrane Ras.GTP or activate PLC to generate PIP_2 and DAG, which is further linked to activation of PKC. Genomic response on $1\alpha,25-(OH)_2D_3$ can result in either activation or repression of transcription. In both cases VDR forms homo- or hetero-dimers, the later one usually with retinoic acid receptor (RXR). After the binding to the vitamin D responsive element (VDRE) in promoter region, it recruits activation factors, which in turn leads to activation of transcription. The more detailed explanation can be found in the text. In the case of repression it is suggested that VDR/RXR heterodimer recruits repressors when $1\alpha,25-(OH)_2D_3$ is not present. However, it was observed that on some promoters, repressors stay bound even after binding of $1\alpha,25-(OH)_2D_3$ to its receptor. Shc - steroid hormone coactivator; Src – steroid receptor coactivator; PLC – phospholipase C; PIP_2 – phosphoinositoldiphosphate; DAG – diacylglycerol; PKC – protein kinase C; IP_3 – inositol-1,4,5-trisphosphate; MEK1/MEK2 – Raf kinases; ERK1/ERK2 – extracellular signal-regulated kinase 1 and 2; POL II – RNA polymerase II.

VDR homo- and hetero-dimers were reported to interact with nuclear corepressor (NCoR), silencing mediator for retinoid and thyroid hormone receptors (SMRT) and Alien (**Tagami T. et al. 1998; Polly P. et al. 2000**). It was shown however, that addition of $1,25-(OH)_2D_3$ causes incomplete dissociation of repressors from VDR, suggesting that another mechanism of repression, by which VDR can serve as a downregulator of transcription might exist (**Polly P. et al. 2000**).

Until now, even less is known about mechanisms of nongenomic response to vitamin D. The nongenomic response is believed to be mediated *via* putative vitamin D membrane receptor (VDR^{mem}) (**Norman A.W. et al. 2001**). So far, a wide array of rapid responses to $1\alpha,25-(OH)_2D_3$, including activation of protein kinase C (PKC), activation of MAP kinases, opening of Ca^{2+} and Cl^- channels in varieties of tissues have been reported (**Zanello L.P. and Norman A.W. 1997; Beno D.W. et al. 1995; Song X. et al. 1998**). These rapid actions have been postulated to regulate cell biologic function and potentially to interact with other membrane mediated-kinase cascades, or to cross talk with the cell nucleus to control the genomic responses associated with cell differentiation and proliferation (**Berry D.M. et al. 1996**). The suggested mechanism for the nongenomic response is shown in **Figure 2**.

1.2. Nuclear vitamin D receptor (VDR)

The VDR is generally expressed at relatively low levels *in vivo*, although target tissues, such as bone, kidney, intestine, may have relatively high levels of the receptor in comparison to the other tissues. Like the other nuclear receptors, VDR can be divided into several functional domains as shown in **Figure 3**. At the NH₂ terminus is an A/B domain of ~20 amino acids, followed by the DNA binding domain comprised of two zinc finger motifs. It was shown that the A/B domain of estrogen, progesterone and glucocorticoid receptors has much longer amino acid sequence and functions as a transcriptional activation domain (**Wilson J.D. and Foster D.W. 1992**), while its function in VDR is still unknown. The ligand binding domain of the protein is a complex region responsible for high-affinity binding of ligand, for dimerization with RXR, and for binding to the basal transcription machinery (**Jones G. et al. 1998**). The COOH-terminal portion of the protein, termed the AF-2 domain, has been shown to be critical for transcription. Removal of this domain results in decreased ligand-binding affinity and loss of transcriptional activation, due to inability to interact with other transcription factors. In contrast to many related receptors, VDR is predominantly nuclear already in the ligand-free state and it has to form heterodimers (mostly with RXR) to be able to bind efficiently to its response elements in promoter region. The regulation of transcription is modulated by the subsequent binding of coactivators or corepressors as already described. Recently a new form of VDR, named VDRB1 with an extended N-terminus was reported. It was found to be expressed exclusively in kidney, osteoblasts and intestine and it was characterized by reduced transactivation activity and a ligand-responsive speckled intranuclear localization (**Sunn K.L. et al. 2001**).

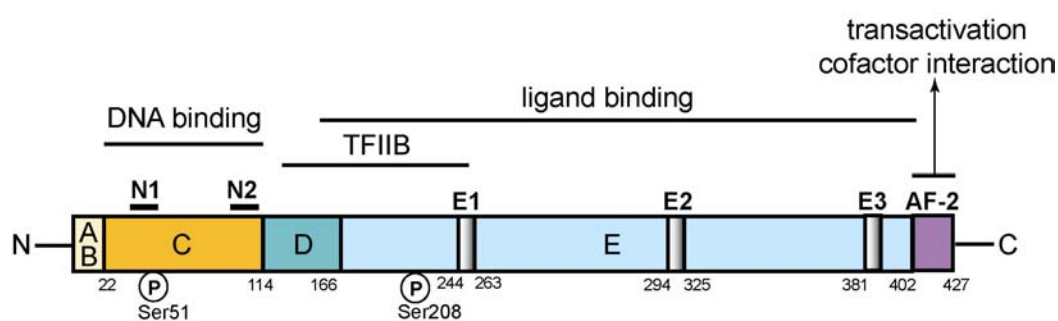


Figure 3. Schematic structure of vitamin D receptor. The most important domains are: DNA binding domain (C), ligand binding domain (E) and affinity function domain (AF-2) that is responsible for interaction with cofactors. DNA binding domain contains two zinc finger motifs (N1 and N2), and one phosphorylation site (Ser51). Additional phosphorylation site is at Ser208. Transcriptional factor (TFIIB) binds overlapping the ligand binding domain (D-E1), and at the N-terminal part of the receptor are ~20 amino acids (A/B) with still unknown function.

1.3. Vitamin D deficiency

Since vitamin D plays a major role in Ca^{2+} metabolism and bone mineral homeostasis, the most prominent feature of vitamin D deficiency, either by acquired or hereditary defects in the metabolic activation of the vitamin D to its hormonal form, or in the subsequent functions of the hormone in target cells, is defect in bone mineralization, characterized by impairment of skeletal growth in rickets and a number of rachitic syndromes. As already mentioned, vitamin D might play additional roles in other tissues, but its precise function there is still unclear.

Further insights in physiological actions of $1\alpha,25\text{-(OH)}_2\text{D}_3$ became possible after generation of vitamin D receptor deficient mice.

1.3.1. Phenotypic characteristics of VDR knock-out mice

Currently, three mouse models with VDR deficiency are available. Heterozygous mice show no apparent difference in comparison to wild type (WT) animals. Homozygous mutant mice are normal until weaning, but then display reduced body weight and growth retardation throughout life. Severe secondary hyperparathyroidism develops during the growth phase, accompanied with hypocalcaemia. All animals show histological signs of rickets and alopecia. No impact was observed on both male and female fertility, except in case of mice generated by Yoshizawa et al., but this is believed to be a consequence of genetic background rather than direct vitamin D involvement (**Yoshizawa T. et al. 1997; Kinuta K. et al. 2000; Erben R.G. et al. 2002; Li Y.C. et al. 1997**). The consequences of vitamin D deficiency were also seen in the immune system. Recent studies showed that production of interleukine 18 (IL-18), which is a Th1-promoting cytokine was reduced in macrophages from VDR deficient homozygous mice. In accordance with that, antigen-stimulated spleen cells from those animals showed an impaired Th-1 response (**O'Kelly J. et al. 2002**).

The impact of vitamin D on development and especially development of the nervous system was also investigated. Although VDR was expressed in E11.5 embryos in the neural tube, telencephalon, mesencephalon, rhombencephalon and spinal nerves as well as in other organs, its deficiency had no impact on ontogenesis, implying that the absence of VDR during development can be compensated by other still unknown factors (**Erben R.G. et al. 2002**).

At least some of the described effects of VDR deficiency are shown to be caused by hypocalcaemia rather than receptor deficiency itself, and could be corrected by rescue diet enriched with calcium. This diet normalized growth and prevented the development of rickets and parathyroidism, but not alopecia (**Li Y.C. et al. 1998**).

It was already mentioned that vitamin D invokes rapid, nongenomic responses, probably *via* a putative membrane receptor that differs from the classical nuclear VDR. Recent studies performed on mice, in which deoxyribonucleic acid (DNA) binding domain of VDR was partially deleted, thus disabling DNA binding but maintaining receptor expression and ligand binding, revealed impairment in both genomic and nongenomic functions, despite a presumably intact VDR^{mem}. The rapid response to 1 α ,25-(OH)₂D₃ was completely absent in osteoblasts from those mice, as well as responses in skin, bone, intestine, parathyroid glands and kidney, implying that vitamin D signalling pathways other than those mediated through the classical nuclear receptor are of minor physiological importance (**Erben R.G. et al. 2002**).

1.3.1.1. Impact of VDR deficiency on renal tubular calcium reabsorption

In accordance with previous findings that vitamin D facilitates renal calcium reabsorption, recent studies on VDR knock-out mice given the Ca²⁺ reach rescue diet, confirmed increased Ca²⁺ excretion in the urine (**Erben R.G. et al. 2002**). One of the possible mechanisms by which 1,25-(OH)₂D₃ can execute this stimulatory action may involve induction of the intracellular calcium-binding proteins calbindin D_{9k} and calbindin D_{28k} (**Bouhtiauy I. et al. 1994a and 1994b**). In the kidney of VDR deficient mice, the mRNA levels of calbindin D_{9k} were found to be strongly downregulated, while those of calbindin D_{28k} were only moderately decreased or unchanged (**Yoshizawa T. et al. 1997; Van Cromphaut S.J. et al. 2001; Li Y.C. et al. 1997**). Furthermore, the recently cloned and characterized apical epithelial calcium channels (EcaC-1 and -2) may also play an important role in vitamin D renal calcium absorption, since its mRNA and protein levels were shown to be decreased in the kidney of vitamin D-deficient rats (**Hoenderop J.G. et al. 2002**). However, recent data published by Van Cromphaut et al. and Erben et al. showed the involvement of EcaC-1 and -2 in renal calcium reabsorption to be unlikely, since its levels were either unchanged in VDR deficient animals or corrected by a rescue diet. Furthermore, the observed changes in mRNA levels of calbindin D_{9k} and calbindin D_{28k} in VDR deficient mice, fed with either normal or rescue diet (**Erben R.G. et al. 2002**), can not explain efficiently the molecular defect of the renal calcium reabsorption.

1.4. Aim of the study

From the data presented in the previous chapters it is clear that vitamin D exhibits complex actions in various tissues, either directly, influencing genomic and nongenomic responses, or indirectly *via* regulation of Ca^{2+} homeostasis. It acts *via* VDR that is able to form complexes with variety of transcription factors, which in turn modulate different signalling pathways.

The main vitamin D-responsive tissues are bone, kidney, and intestine. They are involved in Ca^{2+} mobilization and absorption. Until now, a little is known about exact mechanisms and proteins involved in triggering those events, especially in case of renal calcium reabsorption. Although, based on the present data, calbindin $\text{D}_{9\text{k}}$ represents a possible candidate involved in this process, further studies are necessary to support those findings.

In this study, changes in kidney proteome (the expressed protein complement of a genome) were investigated by 2-dimensional electrophoresis (2-D electrophoresis) of mice in which the DNA binding domain of VDR was partially deleted but the truncated receptor was expressed and could bind the ligand (**Erben R.G. et al. 2002**).

Proteome analysis should be particularly suited to characterize the molecular mechanism of rapid, nongenomic actions of vitamin D, which would escape classical mRNA-based approaches, as it is, e.g., able to identify changes in protein phosphorylation that underlie many rapid intracellular signalling pathways. At the same time, fluctuations at the message level that are not represented at the translated protein level will be filtered out, providing a more specific picture of vitamin D-related changes than mere genomic techniques.

The focus was on kidney as a first target, not only because large samples of sufficiently homogenous tissue were readily available to optimize the technical parameters (various for each tissue), but also because in this tissue rapid, nongenomic vitamin D responses are supposed to play a prominent role. This approach should give a better insight into mechanisms that are underlying the pathologically relevant aspects of vitamin D action in kidney.

2. RESULTS

Two-dimensional electrophoresis (2-D electrophoresis) was used to investigate changes in the kidney proteome of vitamin D receptor (VDR) knock-out mice. In order to achieve an optimised protocol for our study, it was necessary to optimize the complex 2-D electrophoresis technique, including several modifications in protein sample preparation, and as well in the second dimension separation (sodium dodecyl sulphate polyacrylamide gel electrophoresis; SDS-PAGE). After separation it was possible to identify a number of differentially expressed proteins by matrix assisted laser desorption/ionization time-of-flight (MALDI-TOF) mass spectrometry (MS). Many of these genes were related to cellular energy metabolism and are remarkably downregulated in VDR knock-out mice.

2.1. Two-dimensional electrophoresis

Vitamin D receptor knock-out mice, as already mentioned, have ablated genomic and nongenomic actions of vitamin D in the organism (**Erben R.G. et al. 2002**). Considering the fact that vitamin D affects many different pathways in different cells of the organism, changes in the expression level of many proteins involved in these actions were expected. Therefore, the 2-D electrophoresis method was used, since it enables screening of large number of proteins at the same time and studying of differential protein expression.

2.1.1. *Isoelectric focusing*

Considering the high susceptibility of the isoelectric focusing (IEF) method to the amount of protein applied on the Immobiline DryStrip (IPG Strip), it was important to know the protein concentration of the sample. Therefore, colorimetric assay based on copper ions and Folin-Ciocalteu's phenol reagent for phenolic groups, was used. According to the average concentration (see Appendix), all kidney protein isolates were diluted in lysis buffer to a final concentration of 10mg/ml of total proteins.

RESULTS

2.1.2. SDS-polyacrylamide gel electrophoresis

In contrast to the IEF, whose protocol was easily established, the second dimension separation (SDS-PAGE) required several optimisation steps to achieve reliable results.

Although protein separation on the gel was good, first results brought in question the problem of proteolysis in lower molecular weight (M_w) region that influenced accuracy of results. Red box on **Figure 4a** indicate the region with huge number of small protein spots with low M_w that pointed to the sample proteolysis. Better results couldn't be achieved even after inclusion of proteinase inhibitor Pefabloc in lysis buffer during protein isolation (**Figure 4b**). Again red box indicates the same area on the gel, where no reduction in proteolysis level can be seen. Therefore, protein isolation protocol was changed. First step was *homogenisation* of the frozen kidneys in solution of *proteinase inhibitor* cocktail in water, and *lyophilization* over the night. The next day lyophilised tissue was *resuspended* in lysis buffer and *ultracentrifuged* to remove DNA, salts and other interfering components. In that way proteolysis was reduced, and good protein separation on the gels (**Figure 5a and 5b**) was not disturbed.

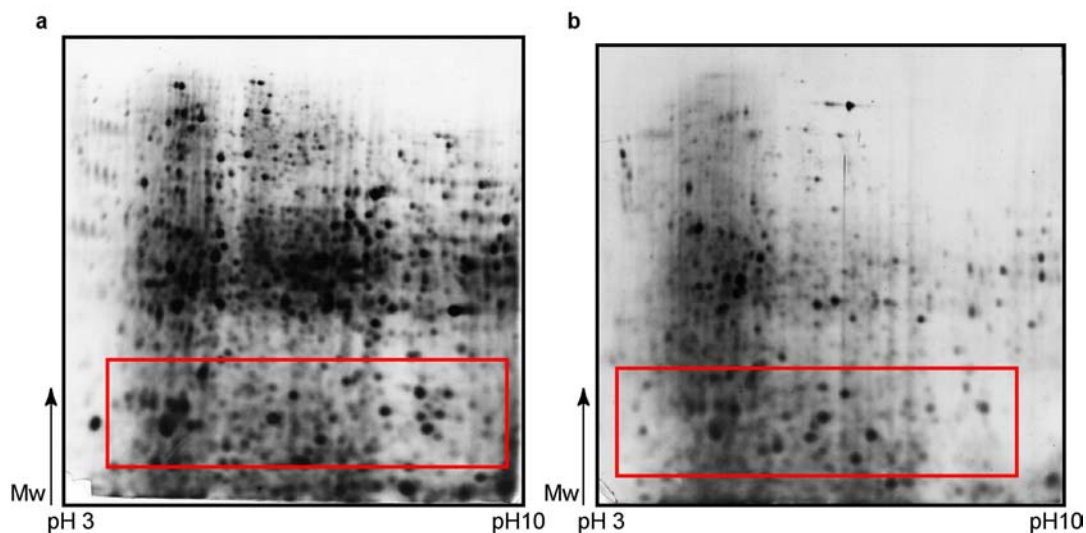


Figure 4. Analysis of wild type mice kidney proteome by 2-D electrophoresis. First dimension has been done on a wide pH range (pH 3-10), at 180mm - separation distance, and sample application made by in-gel rehydration. Isoelectric focusing (IEF) was done up to 36 kVh. Second dimension was vertical SDS-PAGE on 12% polyacrylamide gel. Proteins were visualized by silver staining. Samples were prepared: **a** – without proteinase inhibitor; **b** – with 10 mM Pefabloc proteinase inhibitor included in lysis buffer. Red marked boxes indicate low molecular weight regions with prominent proteolysis.

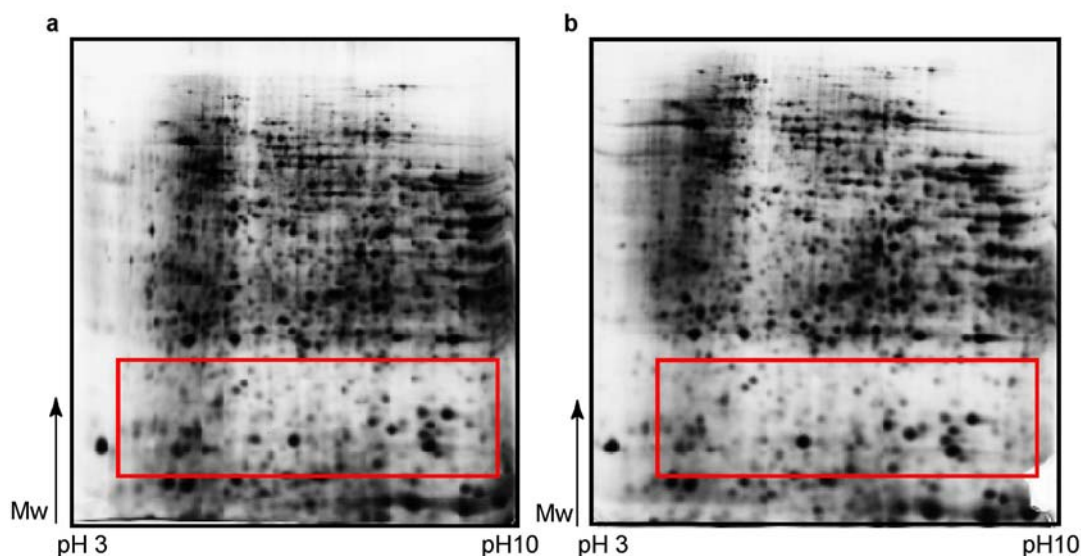


Figure 5. Analysis of wild type mice kidney proteome by 2-D electrophoresis. First dimension has been done on a wide pH range (pH 3-10), at separation distance of 180 mm. Sample application was made by in-gel rehydration and IEF was done up to 41 kVh. Second dimension was vertical SDS-PAGE on 12% polyacrylamide gel. Proteins were visualized by silver staining. **a** and **b** – proteinase inhibitor cocktail, used in the first step of protein isolation, and lyophilization step, reduced the level of sample proteolysis that can be noticed in the reduced number of small blur protein spots in red box's marked area on the gels, compared to **Figure 4**.

Still, the problem of protein diffusion in the protein spots on the gels, during SDS-PAGE, was present. It was necessary to focus spots better in order to enlarge the amount of protein in the protein spot, so that more sample would be available for further analysis on MALDI-TOF MS. The subsequent set of experiments was done with following modifications: in current (mA) or voltage (V) used for run, temperature of gel holders (cooling of the cores), and temperature at which run was done (room temperature or in the cold room).

1) First run was done at constant voltage (80V), in the cold room (+4°C), without additional cooling, but the time acquired to complete the run was too long (24:15 hrs), so protein diffusion was still strong. Arrows on the **Figure 6a** are pointing on the protein spots with emphasized protein diffusion.

2) At constant current (20 mA/gel), in the cold room, without additional cooling, focusing was better, but the “smile”-effect appeared on the gels. Orange lines on the **Figure 6b** show the distortion of protein pattern (“smile”-effect) that reduced reproducibility and made the comparison of results impossible.

RESULTS

3) When cooling (+4°C) of the gel holders was included, but electrophoresis run was done at room temperature, at constant current (40mA/gel), it was expected that buffer ions mobility would not be impaired, although gels are cold. Surprisingly, results were even worse, showing the strong “smile”-effect, which is marked on **Figure 6c**.

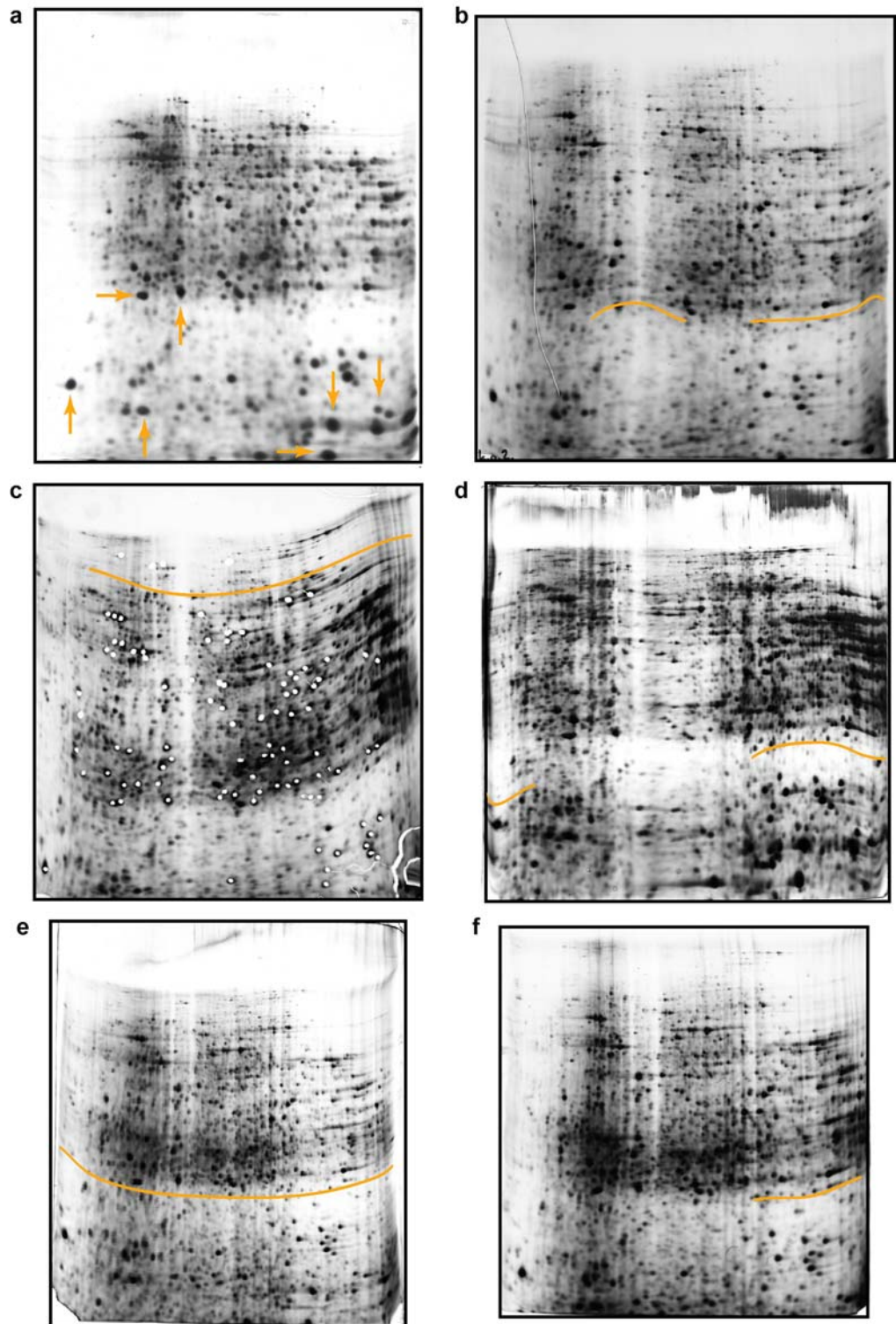
4) The same conditions (cooling of the cores at +4°C; room temperature run) were repeated, but this time with lower current, only 20 mA/gel. Still, the “smile”-effect was strong in higher pH range (**Figure 6d**).

5) Combination of the last two conditions (3 and 4), showed that 40 mA/gel in the cold room with additional cooling of the cores to +4°C, could not improve focusing and caused bad pattern reproducibility, due to distortions in protein migration over the whole pH range (**Figure 6e**).

6) Therefore, constant voltage instead of constant current was applied, and the run was carried out in the cold room, together with cooling of the cores (+4°C), first at 250V for 5 hours, and then it was completed at 300V for 1 hour. It was now easier to compare the gels, but the constant “smile”-effect, present in high pH range, was not removed (**Figure 6f**).

7) The last introduced modifications were constant voltage during the whole run (100V), carried on room temperature, with cooling of the gel holders at +15°C. In this way, duration of the run was reduced and protein diffusion avoided. Arrows on the **Figure 7** are pointing at the protein spots that are not blurred anymore, and orange lines stress the disappearance of “smile”-effect, due to low voltage applied. Since proteolysis was not aggravated by these modifications (**Figure 7**, red box), these parameters were applied for all following experiments.

Figure 6. Set of 2-D electrophoresis gels with differentially modified second dimension SDS-PAGE. For all gels, first dimension was done at high pH range (pH 3-10) at separation distance of 180 mm, and sample application was made by in-gel rehydration. IEF was done up to ~40 kWh. Second dimension was vertical SDS-PAGE at 12% polyacrylamide gel, and proteins were visualized by silver staining. Figures **a-f** represent different modifications used in the experiment. The run was done **a** – with constant voltage (80V) applied in the cold room (4°C). Arrows are pointing on strong protein diffusion in the protein spots; **b** – with constant current (20mA/gel), applied in the cold room (4°C). Lines are indicating distortions in the protein pattern; **c** – with constant current (40mA/gel) applied at room temperature, with cooling of gel holders (4°C). Note even stronger distortions on the gel. The gel was scanned after the excision of test protein spots; **d** – with applying lower current (20mA/gel) at room temperature, without cooling of the cores. Note that distortions remained in the very low and high pH range areas, marked by orange lines; **e** – with constant current (40 mA/gel), in the cold room, and with cooling of the gel holders (4°C). “Smile”-effect is visible through the whole pH range; **f** – with constant voltage (250V) for 5 hours that was then switched to 300V for an additional hour. The entire run was carried on in the cold room and has included the cooling of gel holders (4°C). Note that no improvement in the results could be observed.



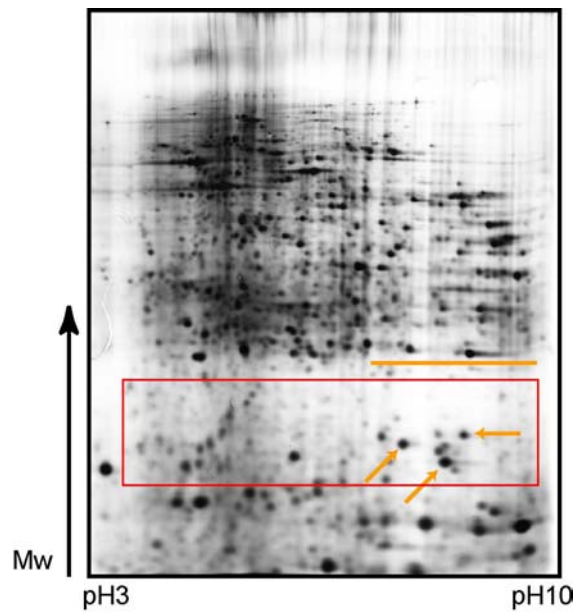


Figure 7. 2-D electrophoresis gel with reduced proteolysis and protein diffusion. First dimension separation was done on a wide pH range (pH 3-10), at separation distance of 180 mm, with sample application made by in-gel rehydration. IEF was done up to 37 kVh. Second dimension was vertical SDS-PAGE on 12% polyacrylamide gel, and proteins were visualized by silver staining. Running conditions were: constant voltage (100V), applied at room temperature, with cooling of the gel holders at 15°C. Red box indicates reduced proteolysis in low M_w region of the gel and arrows are pointing on spots with lowered protein diffusion. There is no distortion in protein pattern on the gel, which can be especially noticed in higher pH range (stressed with orange line).

2.1.3. PDQuest software analysis of 2-D electrophoresis gels

To ensure that differential expression is not due to biological noise, many samples for each condition were analysed. Kidneys were isolated from 5 wild type, and 5 VDR knock-out mice and each sample was analysed separately, in triplicates, by 2-dimensional electrophoresis. Beside genomic difference between animals of the same type, this approach also excluded slight changes due to experimental procedure.

Using 2-D electrophoresis analysis software (PDQuest, BioRad) the original gel scan was filtered and smoothened to clarify the spots. The background was subtracted and spots were automatically identified by creating the gaussian spots from the clarified spots, with help of "Spot Detection Wizard". A gaussian spot is a precise three-dimensional representation of an original scanned spot, where gaussian curves are fitted to the scanned spot in the x and y dimension.

All separately processed gels of the wild type (**Figure 8a and 8b**), or knock-out samples (**Figure 9a and 9b**), were combined in a matchset gel, respectively (**Figure 8c and 9c**). A matchset gel is an abstract, higher level gel, which presents combination of two or more gels showing equal protein spots or differentially expressed protein spots. In this study a matchset of all wild type samples, and a matchset of all knock-out samples, were compared on the higher level, and differentially expressed proteins were identified.

Figures 8a and 8b are showing 2-D electrophoresis gels of two independent kidney samples from wild type mice. Both of them have proteins separated in a wide pH range (pH 3-10) and protein pattern doesn't show significant difference, as it was expected. Blue triangles on the figures mark some of equally expressed proteins that are used as landmarks in PDQuest analysis. According to these spots gels were overlaid, and small differences caused by gel shrinking or twisting, during the experimental work, were overcome. Usually, the number of landmarks per gel is about 10% of total number of protein spots on the gel. After setting the landmarks, all spots were automatically matched and corrections, when necessary, were done manually.

Green squares, marked with numbers 1 and 2 (**Figures 8 and 9**), represent positive control spots that were chosen according to the SWISS-2D polyacrylamide gel electrophoresis map of human kidney (http://www.expasy.ch/cgi-bin/map2/def?KIDNEY_HUMAN). These two proteins were highly expressed and showed no difference in expression between wild type and VDR knock-out mice. Red circles, numbered 3-9, mark protein spots that were chosen for further analysis.

On **Figure 9** 2-D electrophoresis gels of two independent kidney samples from VDR knock-out mice are shown. The analysis of gels and combining in a matchset was done in the same way as for wild type samples. Again, the landmarks are marked by blue triangles, positive control with green squares (numbers 1 and 2), and differentially expressed proteins with red circles, numbered 3-9.

Figures 8c and 9c present matchsets that contain equal protein spots, of wild type and VDR knock-out samples, respectively. When comparing gels in a matchset, there are often some variations in spot size and intensity signal between gels that is not due to differential protein expression. These nonexpression-related variations in spot intensity can be compensated by normalization. The normalization was performed according to the method specified by PDQuest software, where the raw quantity of each spot (intensity of each spot) in a member gel was divided by the total quantity of the valid spots in the gel.

RESULTS

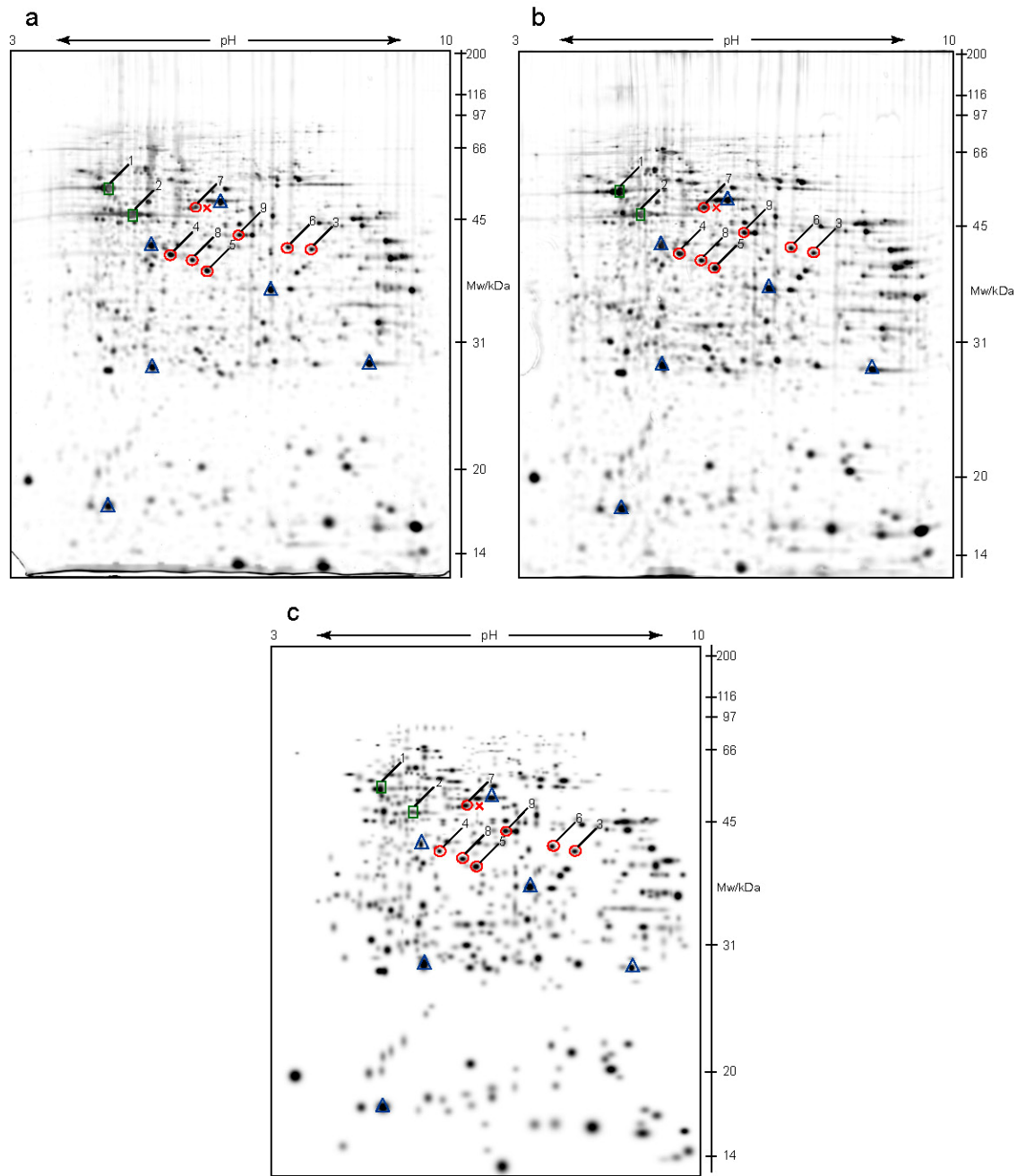


Figure 8. PDQuest analysis of wild type 2-D electrophoresis gels. **a** and **b** are filtered images of two independent gels made on a wide pH range separation (pH 3-10), at separation distance of 180 mm, and IEF up to 37 kVh. Second dimension was vertical SDS-PAGE on 12% polyacrylamide gel, which were then stained with silver. **c** represents a matchset image of wild type gels with equal protein spots. Marked by blue triangles are landmark spots with the same level of expression on both, wild type and VDR knock out gels. Green squares, numbered 1 and 2, designate protein spots taken as a positive control, and red circles with numbers 3-9, mark differentially expressed proteins, taken for MALDI-TOF MS identification. Red cross shows the position at which protein 7 was shifted in some gels (see text for details).

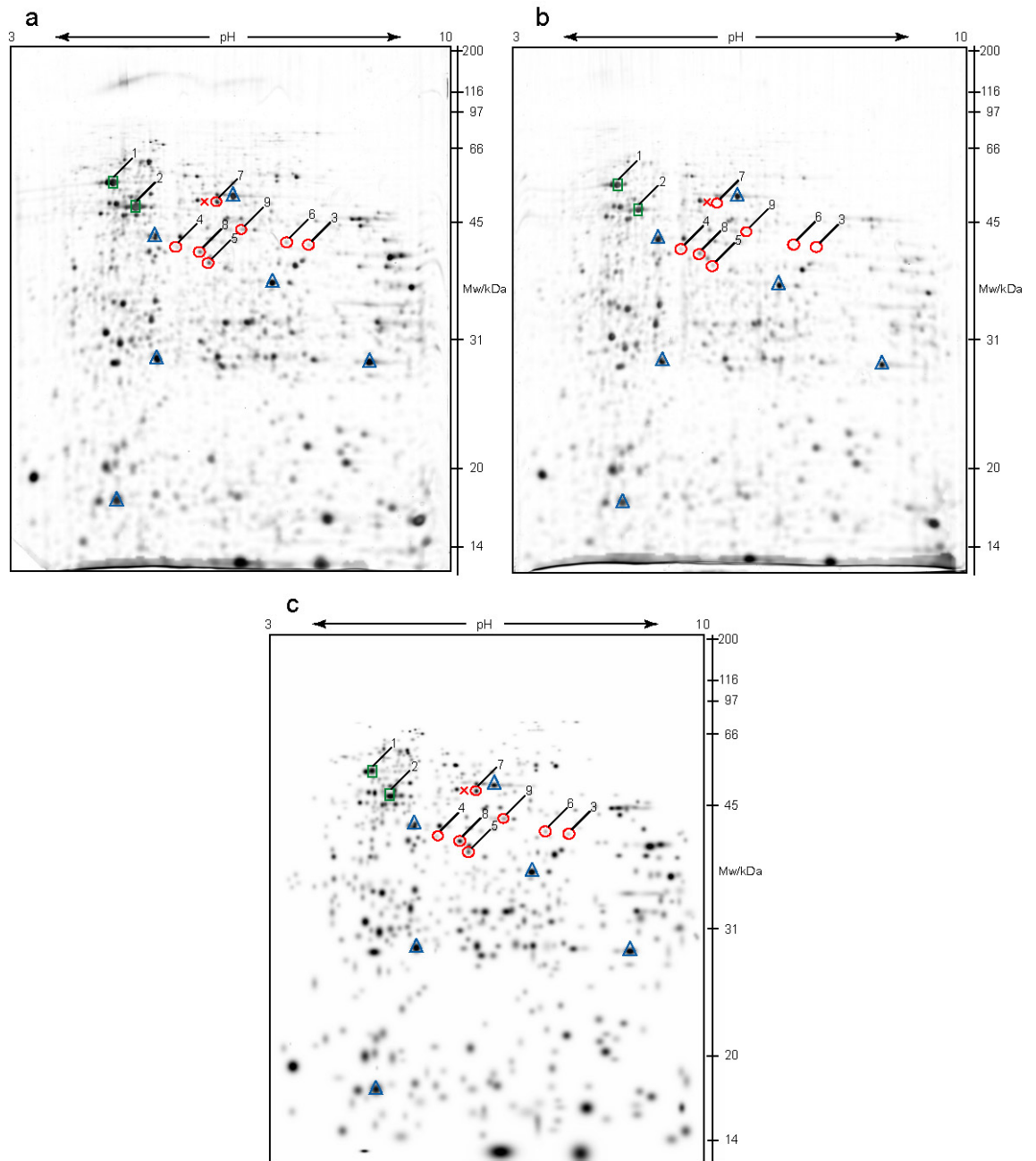


Figure 9. PDQuest analysis of knock-out 2-D electrophoresis gels. Filtered images of two independent gels are presented in **a** and **b**. First dimension separation was done on a wide pH range (pH 3-10), at 180 mm separation distance, with IEF up to 37 kVh. Second dimension was vertical SDS-PAGE on 12% polyacrylamide gel, and visualization of protein spots was done by silver staining. **c** is a matchset of VDR knock-out gels, made of equal protein spots. Blue triangles mark landmark spots, green squares (1 and 2) emphasize positive control protein spots, and with red circles (numbers 3-9) differentially expressed proteins (compared to the wild type gels) are marked. Red cross designate position where protein 7 was expressed in wild type gels presented in **Figure 8**.

RESULTS

After comparison of wild type and VDR knock out matchsets, there were many proteins identified as differentially expressed. Even after the normalization was done, some of the differentially expressed proteins were found to be false positives, due to the method reproducibility, which was never 100%. To confirm these findings, each protein spot was checked also by visual comparison of all gels, on each gel separately (15 wild type – gels and 15 VDR knock-out – gels). In the end, 7 proteins (**Figures 8 and 9**, numbers 3-9), that showed differential expression both on matchset gels and on separate gels, were taken for further analysis by mass spectrometry.

Protein 3 was highly expressed in almost all wild type samples. Only in 3 gels the expression level was a bit lower. In 8 of 15 VDR knock-out gels, the expression of the same protein was downregulated three times or more, while in the remaining 7 gels, it was downregulated more than two-fold. Protein number 4 showed at least three times lower expression in all VDR knock-out gels when compared to the wild type gels. In case of protein spot 5, there was not such a big difference noticed, but it was about two times downregulated in all VDR knock-out samples examined, in comparison to high expression in all wild type samples analysed. Number 6 was equally expressed in all wild type samples, while in 11 of 15 VDR knock-out gels the expression level was two times lower, and in the remaining 4 of 15 gels around three times lower, in comparison to the wild type.

Protein number 7 had unexpected pattern, that differed from gel to gel, no matter if wild type or a VDR knock-out sample was analysed. In 5 wild type gels, the protein spot showed normal expression, while in 9 gels it was not visible at all. In one case, it was present, but shifted to a higher pH region. On the other hand, in 5 VDR knock-out gels the expression was the same as in wild type samples. In 3 gels, the expression level was two times lower, and in 6 gels it was not present at all. Similar to the wild type, in 1 VDR knock-out gel the expressed protein was shifted to a higher pH, to the same position as on the wild type gel. A shift might be caused by a posttranslational modification or due to irregularities in the sample preparation. This pattern can be seen on **Figures 8 and 9**. In both wild type gels, presented on **Figures 8a and 8b**, the protein spot can be observed at the same position (red circle, number 7), and the position to which it was shifted is marked by red cross. On the contrary, first VDR knock-out gel (**Figure 9a**) shows shifted position of the protein (red circle, number 7), while on the second gel (**Figure 9b**) it was not present at all. Surprisingly, in the matchset gel (**Figure 9c**), the spot was present. This was due to the creation of the matchset with equal protein spots, where all spots from many gels are combined in one matchset. Therefore, it was of high importance to check each gel separately, to exclude the false positives. Considering the interesting and unusual pattern, this protein was also taken for further analysis.

Both protein spot 8 and 9 were showing high expression in all wild type gels examined. Number 8 expression was two times lower in all VDR knock-out gels, while number 9 showed only two times downregulation in 10 gels, out of 15, and more than three times downregulation in rest of the gels. Unfortunately, neither protein 8, nor protein 9, could be identified, due to insufficient amount of peptides, after the in-gel digestion of proteins from the protein spot.

Downregulation level (n-fold)							
Protein	3	4	5	6	7	8	9
ko1	>2x	~3x	~2x	~2x	n.p.	~2x	~2x
ko1	>2x	~3x	~2x	~2x	n.d.	~2x	~2x
ko1	>2x	~3x	~2x	~2x	n.d.	~2x	~2x
ko2	>3x	~3x	~2x	~3x	~2x	~2x	>3x
ko2	>3x	~3x	~2x	~3x	n.p.	~2x	>3x
ko2	>3x	~3x	~2x	~3x	n.p.	~2x	>3x
ko3	>3x	~3x	~2x	~2x	n.d.	~2x	~2x
ko3	>3x	~3x	~2x	~2x	~2x	~2x	~2x
ko3	>3x	~3x	~2x	~3x	~2x	~2x	>3x
ko4	>2x	~3x	~2x	~2x	n.p.	~2x	>3x
ko4	>3x	~3x	~2x	~2x	n.p.	~2x	~2x
ko4	>2x	~3x	~2x	~2x	n.p.	~2x	~2x
ko5	>2x	~3x	~2x	~2x	n.d.	~2x	~2x
ko5	>2x	~3x	~2x	~2x	n.d.	~2x	~2x
ko5	>3x	~3x	~2x	~2x	shifted	~2x	~2x

Table 1. List of proteins that were differentially expressed in the VDR knock-out kidney samples. Proteins are designated by the same numbers as on both matchset and separate gels. Downregulation level is expressed in n-fold, relative to the wild type samples analysed. In the case of protein number 7, where some irregularities in expression pattern were observed (see text for more details), additional symbols are used: **n.p.** for protein **n**ot **p**resent at all, **n.d.** for protein **n**ot **d**ownregulated in comparison to the wild type gels, and “**shifted**” for a shift of the protein to a higher pH region. ko1-ko5 are VDR knock-out kidney samples that were analysed in triplicates by 2-D electrophoresis.

2.1.4. 2-D electrophoresis in a narrow pH range

Selected proteins were additionally tested on so called “zoom-in” gels, where protein separation was done in a narrow pH range. The isoelectric focusing was done in two different overlapping pH ranges. The first one was pH 4-7 (**Figure 10**), and the second one pH 6-9 (**Figure 11**), while the second dimension separation (SDS-PAGE) was done in the same way as for pH range 3-10.

Compared at **Figure 10** are two representative gels, wild type (**Figure 10a**) and VDR knock-out (**Figure 10b**). Again, differentially expressed proteins taken for further analysis, are marked by red circles and designated by the same numbers as on **Figures 8 and 9**. Small blue square in high molecular weight region of the VDR knock-out gel (**Figure 10b**) represents the small region of the “clear gel”, containing no protein spots, that was taken as a negative control for MALDI-TOF MS analysis. Often, there are impurities in the gel that can interfere with peptide analysis in mass spectrometry and with protein identification in the database. Therefore, a “clear gel” section was processed the same way as the protein samples, and its spectrum was used to exclude false positives.

On **Figure 11**, two gels are presented with pH 6-9 separation range, showing two spots already identified at broad pH range separation experiment, that are marked again by the same numbers.

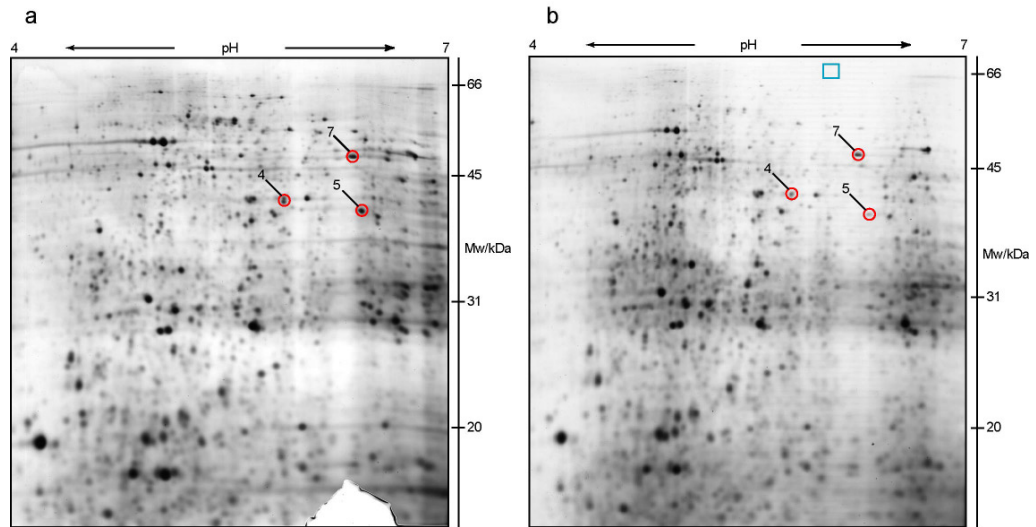


Figure 10. “Zoom-in” 2-D electrophoresis gels of wild type (a) and VDR knock-out (b) kidney proteome, that are separated at narrow isoelectric focusing range (pH 4-7), but on wide separation distance (180 mm), with 47 kVh in total. Red circles emphasize the same differentially expressed proteins, as identified on wide pH range (Figures 8 and 9), designated by the same numbers. Blue square at figure b marks small piece of gel without any protein spots, that was taken as a negative control for MALDI-TOF MS analysis.

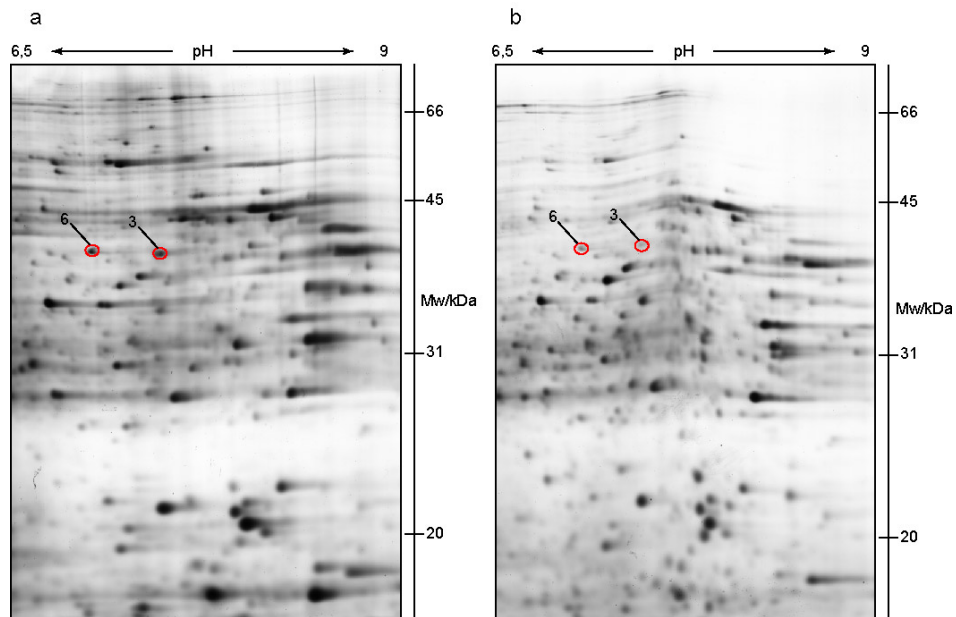


Figure 11. “Zoom-in” 2-D electrophoresis gels at narrow pH range (6-9), with wide separation distance (180 mm), of wild type (a) and VDR knock-out (b) kidney proteome. Isoelectric focusing was done up to 47 kVh and second dimension separation was vertical SDS-PAGE at 12% polyacrylamide gel. Two differentially expressed proteins (3 and 6), marked by red circles, have confirmed the results achieved on a wide pH range (pH 3-10), seen at Figures 8 and 9.

2.2. Protein identification

2.2.1. Visualization

After PDQuest analysis of all gels, differentially expressed proteins were cut from the gels and peptides were isolated by in-gel digestion. Before further analysis by MALDI-TOF MS was done, the system sensibility was checked by applying different molecular weight markers in specified concentrations.

They were separated on polyacrylamide gel, stained with Coomassie Blue (**Figure 12**) and peptides were isolated by the same in-gel digestion method as it was done for 2-D electrophoresis proteins. Identification was successful for different markers, applied in different amount of peptides, by MALDI-TOF MS analysis. In case of albumin (45 kDa protein), bovine serum albumin (66 kDa) and alcohol dehydrogenase (150 kDa), 30 ng was enough for identification, while for β -amylase (20 kDa) approximately 600 ng was the lowest amount of protein that could be identified.

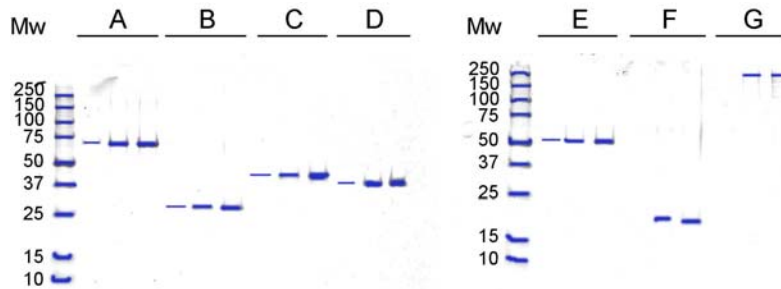


Figure 12. PAGE of different molecular weight protein markers. Each sample was applied in three different amounts, 100 ng, 500 ng and 1 μ g, respectively. Separation was done at 10% polyacrylamide gel and proteins were visualized by Coomassie stain. A - bovine serum albumin; B - carboanhydrase; C - albumin; D - alcohol dehydrogenase; E - β -amylase; F - apoferritin; G - thyroglobulin.

When first test sample, cut out from silver stained gel, was analysed, spectrum revealed no peaks that could be matched to the peptides in the database (**Figure 13**). Only peaks coming from matrix (M/z 845,17; 863,74), trypsin (M/z 1033,00; 1045,00; 2211,96) and adenocorticotrophic hormone, used as an internal standard (ACTH; M/z 2465,13), were achieved. Although MALDI-TOF is considered to be a “soft” ionisation technique, there are often some peaks coming from double charged ions, as it is the peak at M/z 1279,46 that is ACTH-double charged peak, present in almost all spectra.

Another peak ($M/z \sim 1074$) was showing up in many samples, even in the negative control spectrum (**Figure 15c**), which could be coming from some impurities in the gel, or chemicals used in sample preparation, for example trifluoroacetic acid.

Silver staining was used for visualization of the protein spots on the gel because Coomassie staining method was not sensitive enough (**Figure 14**). The detection limit between 1 and 10 ng for silver staining was much better applicable for 2-D electrophoresis, compared to the 50 to 100 ng for the Coomassie staining. The additional advantage of silver staining, in contrast to staining by dyes, is that it does not act by binding to the protein, and therefore decreases the number of necessary washing steps (**Rabilloud T. 1990**).

But the main disadvantages are that a very good visible spot on the gel does not guarantee sufficient amounts of peptides for the analysis, and that the silver staining technique includes protein treatment with a strong oxidizing agent that leads to oxidative attack on the protein and can cause chemical modifications or destruction. To avoid that, the silver nitrate treatment was performed at 4°C in order to minimize oxidation reactions (**Shevchenko et al. 1996**) and the sensitization treatment with sodium thiosulfate, necessary to obtain completely transparent gel background, was used, and it was found to be harmless toward protein molecules.

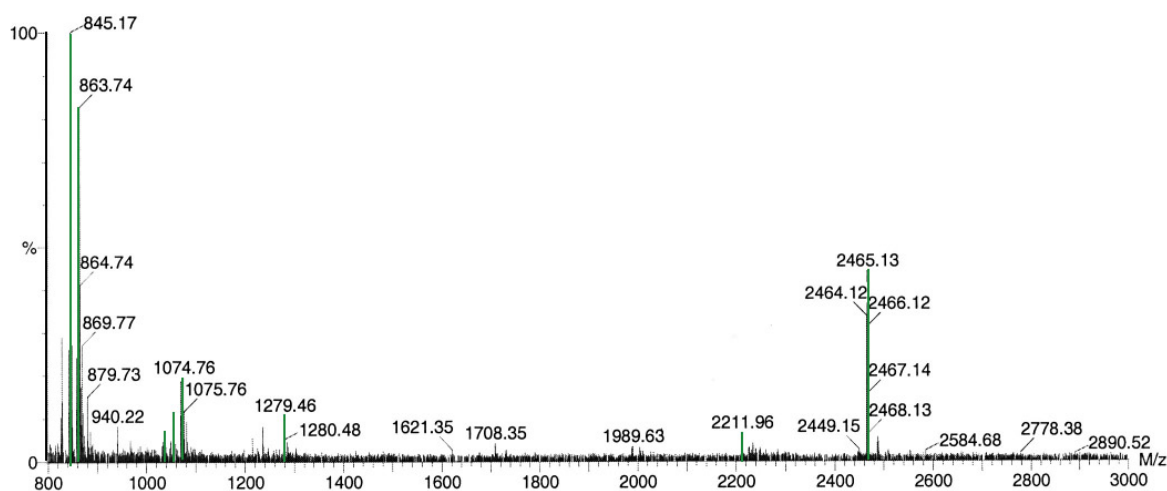


Figure 13. Reflectron MALDI-TOF MS spectrum of test protein spot. Peptides were obtained by in-gel digestion of the spot cut from a wild type gel. Presented spectrum is in range M/z 800-3000 and peak intensities are relative to the strongest signal present. Marked in green are peaks that correspond to matrix (M/z 845,17; 863,74), trypsin (M/z 1033,00; 1045,00; 2211,96), ACTH (M/z 2465,13; 1279,46) and one peak, present probably due to impurities (M/z 1074,76).

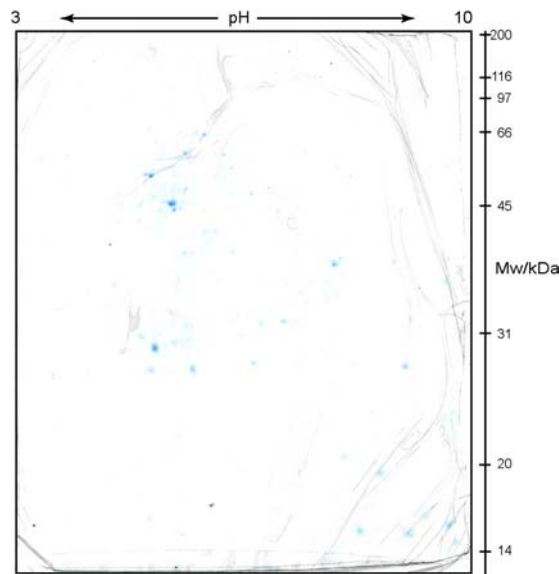


Figure 14. 2-D electrophoresis gel of a wild type mouse kidney proteome. First dimension separation was done in a wide pH range (pH 3-10), at separation distance 180 mm, with IEF up to 26 kVh. Second dimension separation was vertical SDS-PAGE on a 12% polyacrylamide gel, and visualization of proteins was done by Coomassie stain. Only a few spots are visible on the gel due to the insufficient Coomassie stain sensitivity.

2.2.2. MALDI-TOF mass spectrometry

In peptide mass fingerprint (PMF) analysis, as it was used here, a group of experimentally obtained peptide masses are compared to theoretical mass fingerprints of protein sequences available in databases. As a consequence, this type of analysis strongly depends upon the availability of the protein sequence in the database. Especially when working with proteins originating from species of which only a limited amount of genomic sequence data is available, as it is the case for most mammalian organisms, the success rate of this approach can be rather low.

Beside that, detection sensitivity in MALDI-TOF MS is limited not only by the absolute analyte quantity available, but also by chemical noise, which derives from sample contaminants. This can be seen also in **Figure 17**, where strong background noise is present, so it is hard to distinguish between peptide peaks and contaminants. Therefore, the best signal-to-noise ratio was obtained when only a portion of the spot at the center of staining intensity, where the analyte-to-background ration is the highest, was used for analysis. Also, to increase the amount of peptides, the same spots were cut from three separate gels and all three were combined together in one trypsin digest.

The results were now much better and spectra revealed high intensity signal for highly expressed proteins, used as a positive control (**Figures 15a and 15b**). Positive control spots were chosen according to the SWISS-2D PAGE map of human kidney, and identified proteins corresponded to those from human kidney map, according to their position on the gel and protein identity. That was confirmed by database search that identified huge number of matched peptides (**Table 2**) with protein of expected molecular weight and pI (**Table 3**).

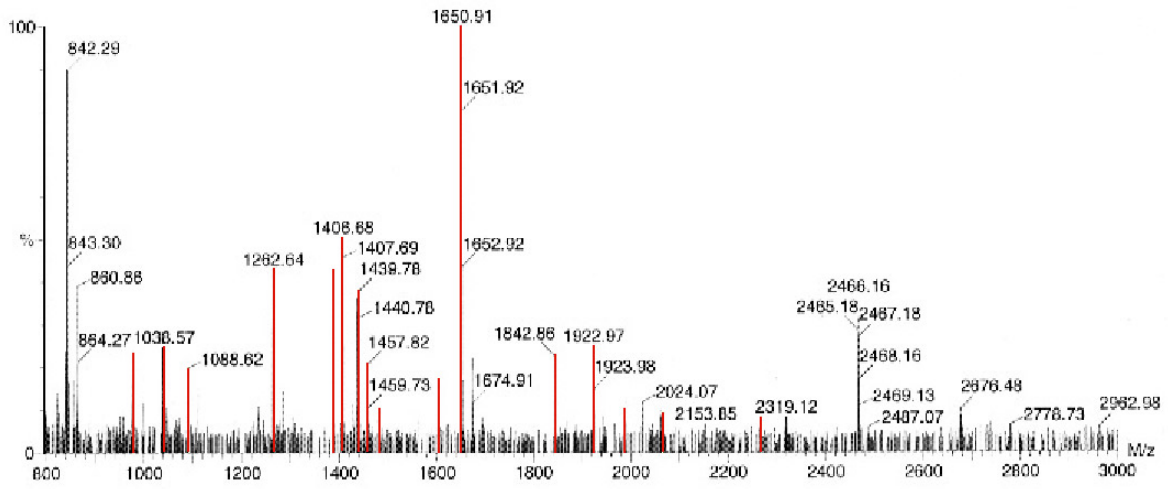
The first positive control was ATP synthase β -chain (ATPB; **Figure 15a**), 56 kDa protein, with pI 5.2 that is designated by number 1 on **Figures 8 and 9**, and the second one, marked as number 2, was β -actin (**Figure 15b**), 41 kDa cytoplasmic protein, in similar pH range (pI 5.4) as ATPB. For both proteins a huge number of peptides was identified, due to the large amount of tryptic peptides in the analysed samples. Consequently, protein sequence coverage was high (**Figure 19**). Although β -actin was first identified as a human protein, additional database searches revealed the presence of mouse β -actin with 100% sequence homology (**Figure 20**).

Test sample	n.c.	1 ATPB	2 ACTB	3 HAO3	4 LDHB	5 MDHC	6 ADK	7 VDR
845,17	861,18	975,54	976,47	1009,53	913,64	1026,53	919,47	900,75
863,74	1033,00	1038,57	998,48	1115,74	957,61	1178,69	1200,38	985,18
1033,00	1045,00	1088,62	1014,47	1139,65	959,56	1371,71	1299,62	1087,98
1045,00	1072,28	1262,64	1132,65	1423,76	1011,56	1387,69		1103,83
1074,76	1277,16	1378,60	1161,70	1561,72	1248,62	1393,69		1284,00
1279,46	1324,69	1385,70	1171,71	1579,84	1253,65	1757,91		1378,53
2211,96	1332,77	1406,68	1198,78	2978,72	1269,68			1433,98
2465,13	1380,48	1435,75	1516,76		1931,78			1647,98
	1396,76	1439,78	1791,04		1964,01			2312,82
	1450,71	1457,82	1998,94		2312,34			2417,84
	2208,99	1473,71	2215,76					
	2292,81	1601,89						
	2305,49	1650,91						
	2309,43	1842,86						
	2466,55	1922,97						
		1988,03						
		2060,93						
		2134,90						
		2266,06						

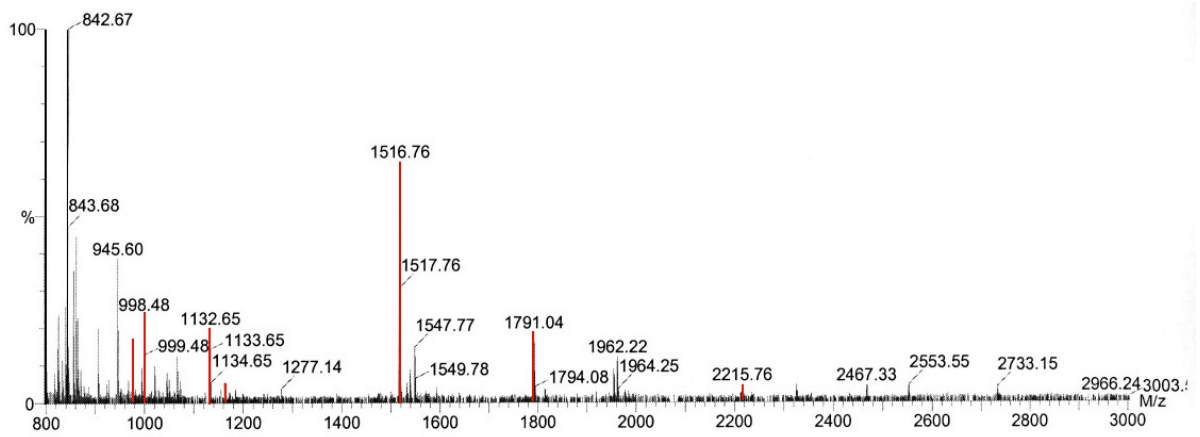
Table 2. List of tryptic peptide fragments peaks of all analysed protein samples. The measured masses of the peptides are within 150 ppm of the corresponding predicted peptide masses. Marked in green are matrix, trypsin and ACTH peaks, that are present in all spectra, but here are listed only for test sample (**Figure 13**) and negative control spectrum (n.c.) In red are tryptic peptides fragments that are main peaks in MALDI-TOF spectra of analysed proteins. All other numbers present the rest of tryptic peptides that are also part of protein fingerprint identified in the database, but are not highly visible in spectra. ATPB – ATP synthase β -chain; ACTB - β -actin; HAO3 – hydroxyacid oxidase 3; LDHB – L-lactate dehydrogenase, B-chain; MDHC – malate dehydrogenase; ADK – adenosine kinase; VDR – vitamin D receptor.

RESULTS

a



b



c

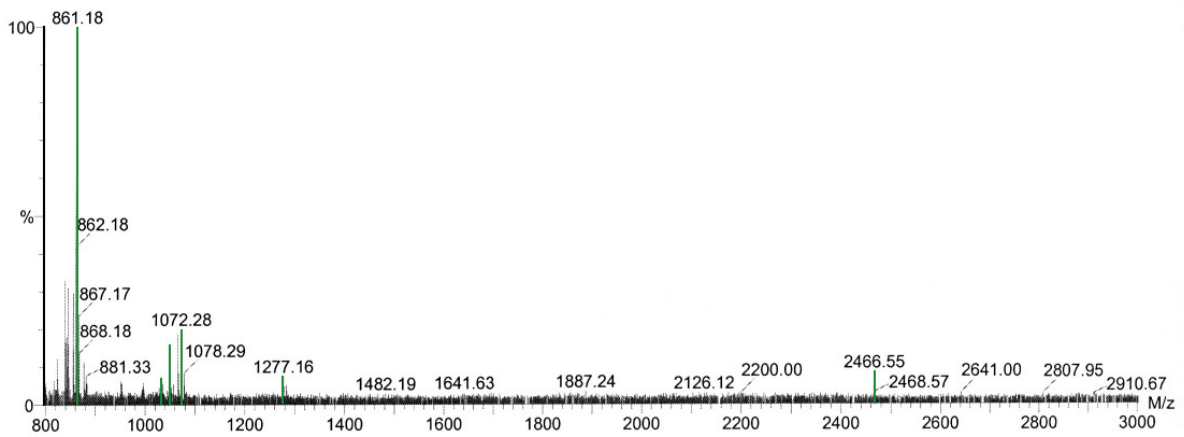


Figure 15. Reflectron MALDI-TOF mass spectrometry of peptides obtained by in-gel trypsin digestion of 2-D electrophoresis gel spots. Presented is MALDI-TOF spectrum of M/z 800-3000 region, while peak intensities are relative to the strongest signal present. Five percent of total digest was taken for MALDI analysis, using thin-layer α -cyano-4-hydroxycinnamic acid (HCCA)/nitrocellulose sample preparation. The measured masses are within 150 ppm of the corresponding predicted peptide masses. Marked peaks correspond to tryptic peptides of the protein analysed (**a** and **b**), or to matrix, trypsin and ACTH (**c**) components in the sample. **a** – ATP synthase β -chain; **b** – β -actin; **c** – negative control spectrum.

After analysing tryptic peptides of small “clear piece” of the gel, taken as a negative control, by MALDI-TOF MS, main peaks in spectrum were, like in the case of the test sample, coming only from matrix, trypsin and ACTH, that was used as an internal standard (**Figure 15c**). After the database search, a false identification revealed nucleoprotein, from the rest of peptide masses in the spectrum. This was taken in consideration when other proteins spectra were analysed.

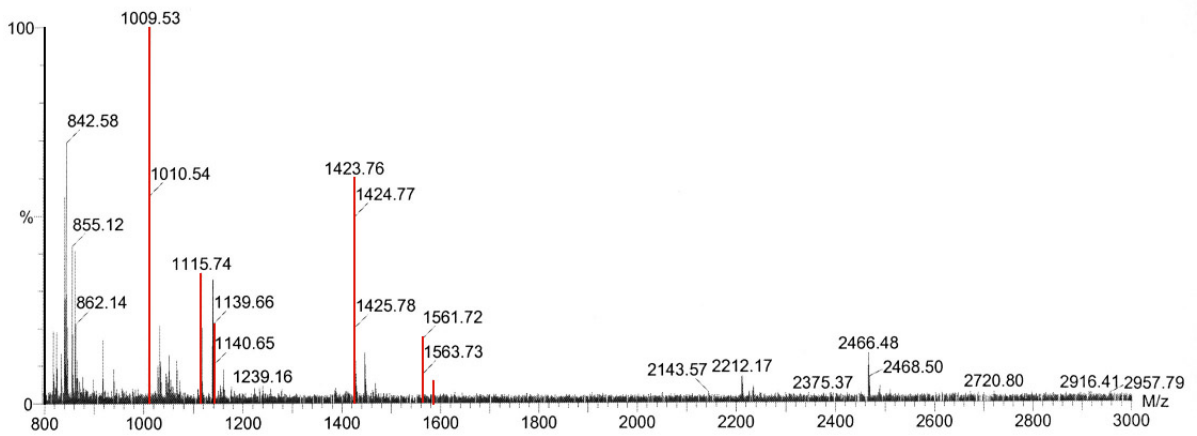
Unfortunately, spectra for differentially expressed proteins, in general, did not show the high peak intensities seen for positive control spectra, but that was expected, considering that positive control proteins are highly expressed in cells, while tested proteins can be present in very low concentrations. Beside that, only a small amount of sample-matrix mixture (0,5 – 1 μ l) can be deposited on the target plate. Such sample preparation therefore strongly limits the overall sensitivity of the technique and also impose restrains on the peptide concentration that can be analysed. Anyway, matched peptide peaks were good enough to search the database and after the search, many different parameters were checked to confirm protein identification (**Table 3**).

No.	Protein	Origin	Accession No.	Mw/kDa	pI
1	ATP synthase β -chain (ATPB)	mouse	P56480	56,361	5.2
2	Actin, cytoplasmic 1 (ACTB)	human	P02570	41,718	5.4
3	Hydroxyacid oxidase (HAO3)	mouse	Q9NYQ2	38,681	8.0
4	L-lactate dehydrogenase, B-chain (LDHB)	mouse	P16125	36,423	6.0
5	Malate dehydrogenase, cyt. (MDHC)	mouse	P14152	36,328	6.5
6	Adenosine kinase (ADK)	human	P55263	40,527	6.6
7	Vitamin D receptor (VDR)	mouse	P48281	47,833	6.1

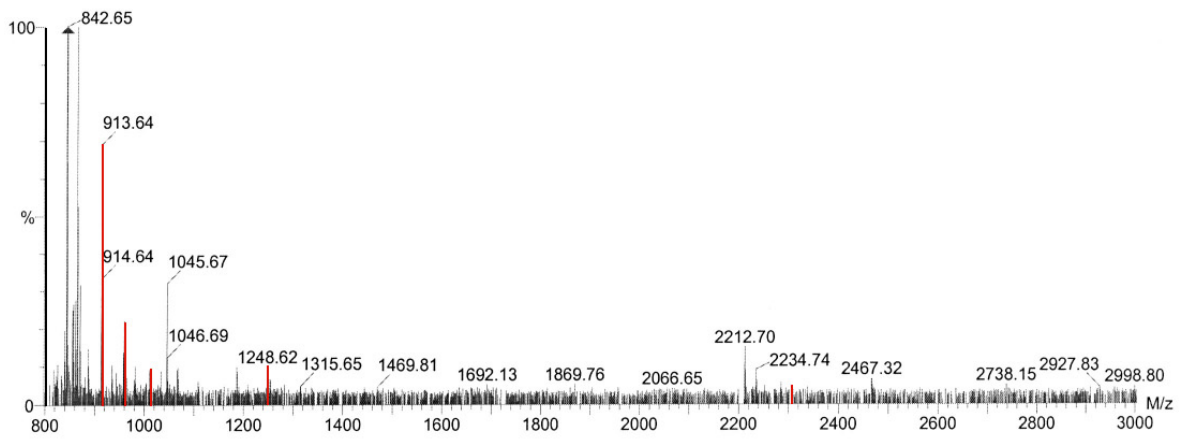
Table 3. List of different parameters for all proteins identified by MALDI-TOF MS. Numbers given are the same as marked on 2-D electrophoresis gels (Figures 9 and 10). For each protein, the origin of first identified protein in the database is stated, and accession numbers of corresponding proteins. Molecular weight and pI values are calculated from theoretical data, found in the same database (SWISSPROT).

RESULTS

a



b



c

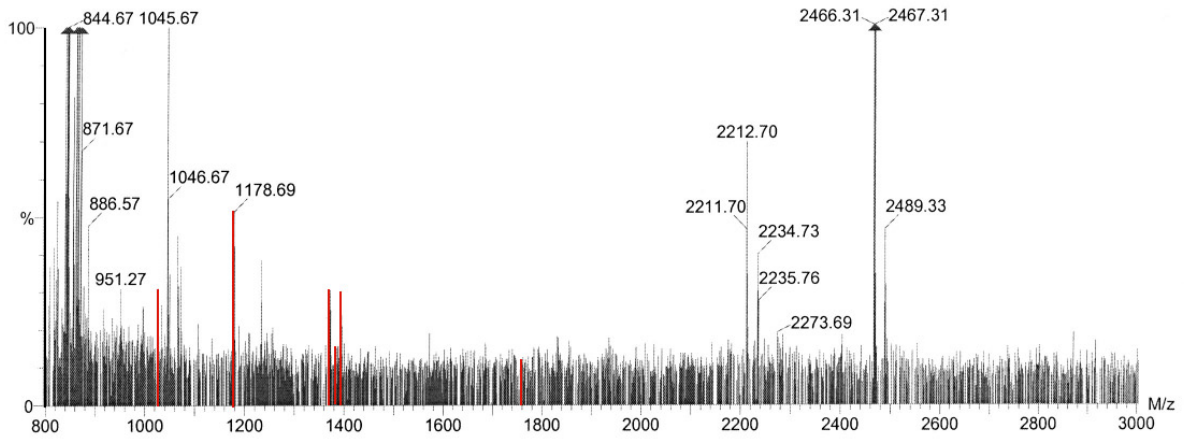


Figure 16. Reflectron MALDI-TOF mass spectrometry of peptides obtained by in-gel trypsin digestion of 2-D electrophoresis gel spots. Presented is MALDI-TOF spectrum of M/z 800-3000 region, while peak intensities are relative to the strongest signal present. Five percent of total digest was taken for MALDI analysis, using thin-layer HCCA/nitrocellulose sample preparation. The measured masses are within 150 ppm of the corresponding predicted peptide masses. Marked peaks are main tryptic peptides of proteins analysed, used for PMF analysis. **a** – hydroxyacid oxidase 3; **b** – L-lactate dehydrogenase B-chain; **c** –malate dehydrogenase MS spectrum.

Organism of origin of the entry was considered the most important criterion. If the database match was a protein from mouse or human, it was taken in further comparison, and if any other origin was noted, the match was excluded from further analysis. After that, the “score” parameter was checked. The entry with the highest score (the top score) on the list of entries received from the database presents the sequence which is the most likely to match with analysed peptides, based on the number of matching peptide fragment masses (**Table 2**), percent coverage (**Figure 19**) and mass difference. As entries were listed according to the score, the first entry on the list was considered as a “good match”. Molecular weight (M_w) and pI were compared to the position of the protein on the gel, and they fitted for all tested proteins (**Table 3**). In the end, spectrum was checked visually, if matched peptide fragment peaks were main in the spectrum, and none of them belonged to the matrix, trypsin or ACTH peaks.

Protein spot number 3, that was highly downregulated in VDR knock-out mice samples, revealed clear spectrum (**Figure 16a**) with high peak intensity signal of a hydroxyacid oxidase 3 (a murine peroxisomal protein), and all parameters checked (**Table 3**) confirmed the finding.

Although the next two differentially expressed proteins, L-lactate dehydrogenase B-chain (protein spot 4; **Figure 16b**) and malate dehydrogenase (number 5; **Figure 16c**), had not such high signal intensity, the PMF analysis was made of the main peptide peaks in the spectra, and all parameters fitted well to the identified proteins. Both of them are cytosolic proteins that are involved in cellular metabolism pathways.

RESULTS

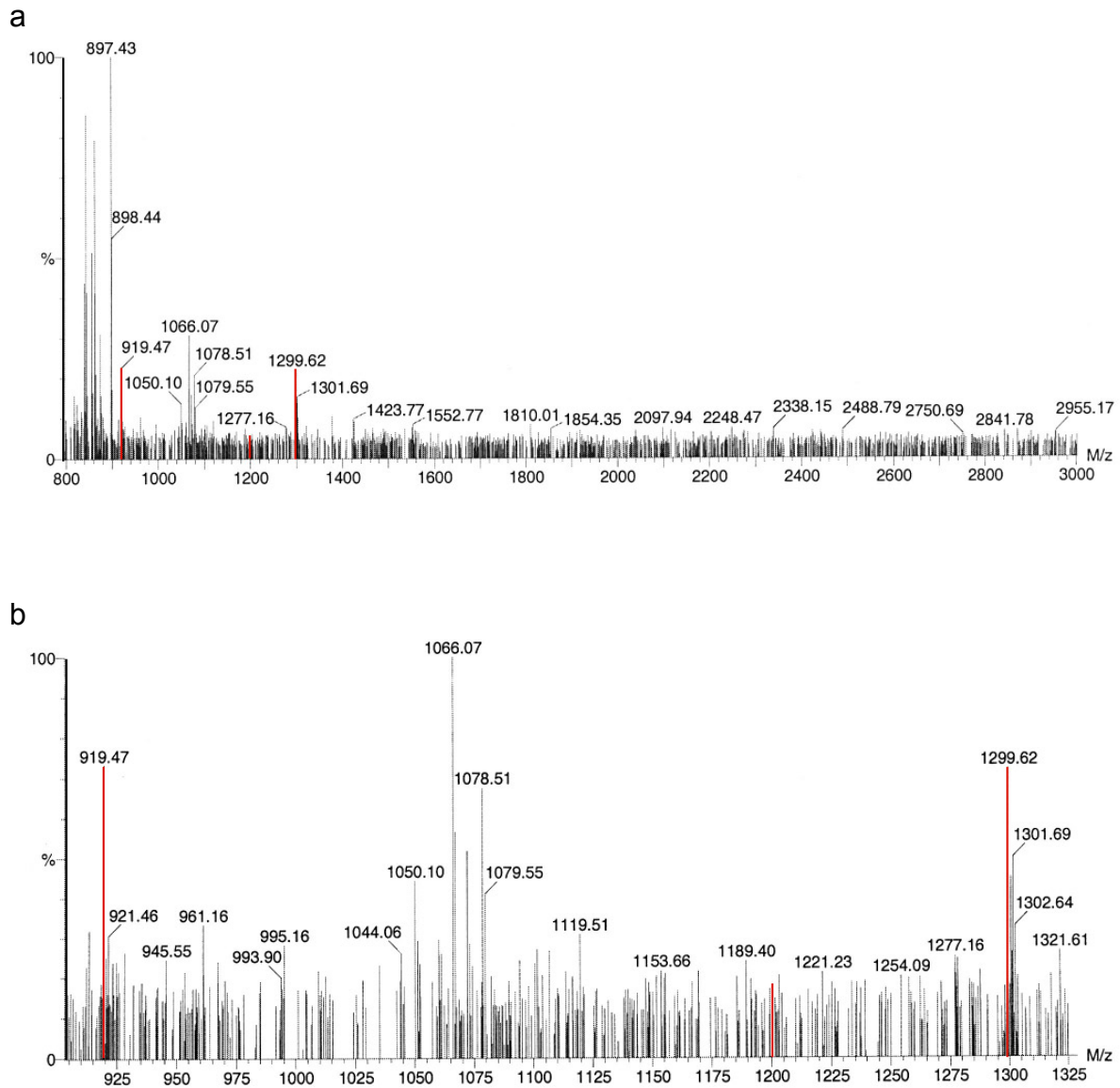


Figure 17. Reflectron MALDI-TOF mass spectrometry of adenosine kinase peptides.

After tryptic in-gel digestion of protein spot 6, five percent of total digest was taken for MALDI analysis, using thin-layer HCCA/nitrocellulose sample preparation. The measured masses are within 150 ppm of the corresponding predicted peptide masses. **a** – wide M/z range, 800-3000, of obtained spectrum had a strong background noise, that even ACTH peak was hardly noticeable. Enlarged view of spectrum in range of 900-1325 M/z, on figure **b**, focuses identified tryptic peptides.

On the **Figure 17** is the MALDI-TOF spectrum of adenosine kinase, the human counterpart of the mouse protein identified from tryptic peptides isolated from the protein spot 6 (**Figures 8 and 9**). As a strongly downregulated protein it was of great interest, so although its spectrum had high background noise, other parameters were carefully checked and proved the protein identity. Since a human protein was originally identified, the mouse counterpart was retrieved from the database and protein sequences were aligned. The alignment result revealed high overall similarity (87%) in protein sequence, and 100% identity within the identified peptides (**Figure 20**).

The last spectrum (**Figure 18**) presents the PMF of spot number 7 that had strange protein expression pattern on 2-D electrophoresis. Most surprisingly, the protein identified was vitamin D receptor itself! Although only few tryptic peptides were included in PMF, they were the main peaks in the spectrum, beside usual matrix, trypsin or ACTH peaks. Also, the pI (6,1) differed a little from the expected value, according to the position on the gel, but considering the fact that expression pattern differed exactly in the pH at which protein was present, and all other data (**Table 3; Figure 19**) confirmed the protein identity, it was taken as a true positive.

Enlarged views of adenosine kinase and VDR spectra (**Figure 17b and 18b**) were focused to the mass to charge (M/z) range of main tryptic peptides peaks. It can be noticed that identified tryptic peptides peaks have small intensities, but as already mentioned this was due to the small amount of peptides isolated by in-gel digestion of protein spots from 2-D electrophoresis gels, even after combining few samples. It can also be noticed that ACTH peak in both spectra (**Figures 17 and 18**) was hardly distinguishable, which was not the case for other spectra, and always the same amount of internal standard (ACTH) was added during the sample preparation.

RESULTS

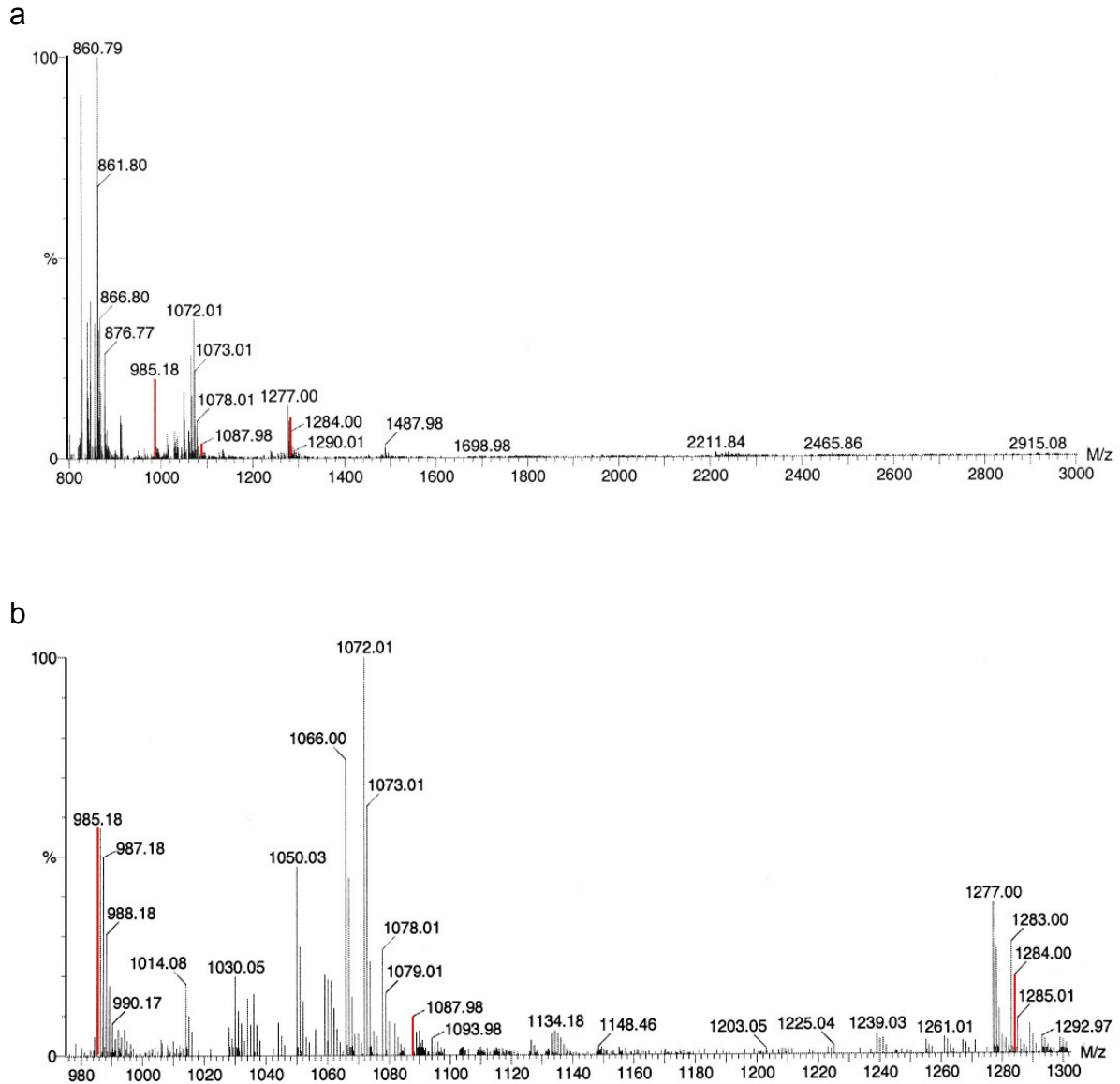


Figure 18. Reflectron MALDI-TOF mass spectrometry of vitamin D receptor peptides. After the protein spot 7 was digested by trypsin in-gel digestion method, five percent of total digest was taken for MALDI analysis, using thin-layer HCCA/nitrocellulose sample preparation. The measured masses are within 150 ppm of the corresponding predicted peptide masses. **a** – wide M/z range, 800-3000, revealed two stronger peaks belonging to the protein peptides. But compared to the ACTH peak that was present always in the same amount in all samples analysed, they showed higher signal intensity. **b** – focused view into the 980-1300 M/z area of the same spectrum.

1 - ATP synthase β -chain, mitochondrial precursor (ATPB_mouse)

mllsvgrvas asagralgl spsaalppaq llraapagv hpardyaaqa saapkagat grivavigav vdvqfdegip pilnalevqg rdsrlvleva qhlgestvrt iamdgteglv rgqkvldsga pikipvgpet lgrimnvige pidergpikt kqfapihaea pefiemsveq eilvtgikvv dllapyakgg kiglfggagv gktvlmeli nnvakahggy svfagvgert regndlyhem iesgvlnkd atskvalvyg qmneppgara rvaltgitva eyfrdqegqd vllfidnifr ftqagsevsa llgripsavg yqptlatdmg tmqerittk kgsitsvqai yvpaddltdp apattfahld attvisraia elgiypavdp ldstsrmdp nivgnehydv argvqkilqd yklsqdiiai lgmldelseed kltsvrarki qrfsqpfqv aevftghmgk lvpkietikg fqilageyd hlpeaqfymv gpieeavaka dklaeehgs

2 – Actin, cytoplasmic 1 (β -actin; ACTB_human)

mdddiaalv dngsgmckag fagddaprav fpsivgrprh qgvvmvnggqk dsyvgdeaqs krgiltkyp iehgvtvndw dmekiwhhtf ynelrvapee hpvllteapl npanrekmt qimfetfntp amyvaiqavl slyasgrttg ivmdsgdgvv htvpieggya lphailrldl agrdltidym kiltergyysf ttaereivr dikeklyva ldfeqemata assssleky elpdgqviti gnerfrcpea lfqpsfngme scjihettfn simkcdvdir kdlyantvls ggttmyppgia drmqkeital apstmkikii apperkysvww iggsilasls tfqqmwiskq eydesgpsiv hrkcf

3 – Hydroxyacid oxidase 3 (HAO3_mouse)

msllcladfk aqaqkqlskt swdfiegead dgityndnla afrirrlrpr yldrsvskidt rtiqqqein apicisptaf hsiawadgek stakaaqkan icyvissyas ytvedivaaa pggllhwfqlv vqpdwdinkq mvqriealgf kalvvtvdap vlnrrngnr sildleanik lkdrlspges ksglptplsm pssscwndl plqsmtrlp iilkgitke daelavkhni rgiivsnhgg rqidevpasi dalrevvaav ngkievymdg gvtgndvdk alalgarcif lgrpiiwgla kgedgvkev ldlkeelht cmalsgcrsv aeispdliqf srl

4 – L-lactate dehydrogenase B-chain (LDHB_mouse)

matlkekli svaddeavp nnkitvvvgv qvgmacaisi lgksladela lvdvledkik gemmdlqhggs lfiqtpkiva dkdysvtans kivvvtagvr qqegesrlnl vqrvnvnvfk iipqivkyssp dctiivvsnp vdiityvtwk lsglpkhrvi gsgcnldsar frylmaeklg ihpsschgw igehgdssva vwsgrnvagv slqelnpemg tdndsenwke vkhmvvdsay eviklkgytn waiglsvadl iesmlknlsr ihpvstmvkg mygienevfi slpcilnarg ltsvinqkik ddevaqlrks adtlwdiqkd lkd

5 – Malate dehydrogenase, cytoplasmic (MDHC_mouse)

msepirlvt gaagqiaysl lysignsvf gkdqpiilvl lditpmmgvl dgvlmelqdc apllqdvia tdkeeiafkd ldvavlvgs mprregmerkd llkanvkfk sqgtalekya kksvkvivvg npantnclta sksapsipke nfcsltridh nraksqialk lgtvaddvkn viiwgnhsst qypdvnhav klgqkevgyv ealkddswik gefittvqqr gaavikarki ssamsaakai adhirdiifg tpegefvs mg visdgnsygv pddllyslpv viknktwkfv eglpindfser ekmdltakel teeketafef lssa

6 – Adenosine kinase (ADK_human)

maaaeeepk kklkveapqa irenilfgmg nplldisavv dkdldkysl kpdnqilaed khkelfdelv kfkvevhag gstqnsikva qwmiiqqphka atffgcigid kfgeilkrka aeahvdahyy eqneqptgtc aacitgdnrs lianlaaanc ykkekhlde knwmlvekar vcyiagfflt vspesvlkva hhasennrif tlnsapfis qfykesimkv mpyvdilfng eteaatfare qgfetkdi ke iakktqalpk mnskrqrivi ftqgrddtim atesevtafa vldqdqkeii dtngagdavv ggflsqvlsvd kpltecirag hyaasiirr tgctfpekpd fh

7 – Vitamin D receptor (VDR_mouse)

meamaastsl pdpgdfdrnv pricgvcgdr atgfhnamt cegckgffr smkrkalftc pfngdcritk dnrrhcqacr lkrcvdigmm kefildteev qrkremimkr keeekaldsl rpklseeqgh iailldahl ktydptyadf rdfrrpirad vstgysprp tlfsgdsss nsdlytpsld mmepasfstm dlineegsddp svtdlspis mlphladlvs ysiqkvigfa kmipgfrdit sddqivllks saievimlrs nqsfmddms wdcgsqdyky ditdvsragh tielieplik fqvgllklnl heeehvlma icivspdrpg vqdaklveai qdrslntlqt yirchrpppg shqlyakmiq kladlrslne ehskqyrsls fqpensmklt plvlevfne is

Figure 19. Amino acid sequences of proteins identified by MALDI-TOF MS. Proteins are listed by the full name and abbreviation (consisting of official gene symbol and organism of origin). Marked in blue are peptides identified in PMF analysis, that emphasize protein sequence coverage.

RESULTS

Actin, cytoplasmic 1 (β -actin; ACTB_human) Actin β mouse (ATMSB)

mdddiaalvvdngsgmckagfagddapravfpsiogrprhggvmvngmqkdsyvgdeaqskrgiltkypiehgivtnw
mdddiaalvvdngsgmckagfagddapravfpsiogrprhggvmvngmqkdsyvgdeaqskrgiltkypiehgivtnw

ddmekiwhhhtfyneirvapeehpvllteaplnpkanrekmtqimfetfntpamyvaiqavlslyasgrttgivmdsgdgvtht
ddmekiwhhhtfyneirvapeehpvllteaplnpkanrekmtqimfetfntpamyvaiqavlslyasgrttgivmdsgdgvtht

vpiyegyalphairldlagrdldtdylmkiltergysfttaeivrdikeklcyvaldfeqemataassssleksyelpdgqvitiq
vpiyegyalphairldlagrdldtdylmkiltergysfttaeivrdikeklcyvaldfeqemataassssleksyelpdgqvitiq

nerfrcealfqpsflgmescgihettfnsmkcdvdirkdlyantvlsqggtmypiadrmqkeitalapstmkikiapperky
nerfrcealfqpsflgmescgihettfnsmkcdvdirkdlyantvlsqggtmypiadrmqkeitalapstmkikiapperky

svwiggsilaslstfqmwiskqeydesgpsivhrkcf
svwiggsilaslstfqmwiskqeydesgpsivhrkcf

Adenosine kinase (ADK_human) Adenosine kinase mouse (ADK_mouse)

maaaeeepkpkllkveapqalrenilfgmgnplldisavvdkdldkyslkpndqilaedkxkelfdelvkkfkveyhaggst

qnsikvaqwmiqqphkaatffgcigidkfgelkrkaeahvdahyyeqneqptgtcaacitgdnrslianlaaancykke
nsmkvaqwmiqephraatffgcigidkfgelkskaadahvdahyyeqneqptgtcaacitgdnrslianlaaancykke

hldleknwmlvekavrcyiaffltvsvpsvlkvahasennrftlnlsapfisqfykeslmkvmpyvdiifgneteaatfareq
hldlennwmlvekavrcyiaffltvsvpsvlkvaryaaennrftlnlsapfisqffkealmavmpyvdiifgneteaatfareq

gfetkdikeiakktqalpkmnskrqrivftqgrddtimatesevtafavlddqkeiidngagdafvggflsqvlsdkpltecir
gfetkdikeiarktqalpkvnskrqrivfnqgrddtivatgndvtafpvldenqeeivdngagdafvggflsqvlsdkpltecir

aghyaasiiirtgctfpekpdfh
aghyaasviirtgctfpeknfh

Figure 20. Amino acid sequence alignments of human and mouse proteins. Peptides in the human counterpart are marked with blue colour, and represent the sequences of tryptic peptides identified by MALDI-TOF MS. The same sequences are emphasized in mouse proteins in grey. It is clearly visible that identified peptides have the same amino acid sequence in proteins of both organisms.

3. DISCUSSION

3.1. Two-dimensional electrophoresis (2-D electrophoresis) as a method of choice in differential protein expression analysis

Since the first introduction of two-dimensional electrophoresis (2-D electrophoresis) by O'Farrel and Klose in 1975, the method went through the number of modifications and finally in 80-ies it became significant and widely used biochemical separation technique in the proteome analysis. It was found to be useful in detection of disease markers, monitoring therapies, drug discovery, purity checks, cancer research and in general for monitoring differential protein expression in cells, as it enables to screen a large number of proteins at the same time.

In this study 2-D electrophoresis was used to monitor changes in kidney proteome of vitamin D receptor (VDR) knock-out mice. Vitamin D acts upon various tissues via VDR(s), where it triggers two different kind of responses – a rapid nongenomic response and a much slower genomic response. The classical genomic response involves transcription of genes that contain specific vitamin D response element (VDRE) in their promoter sequences. On the other hand, the nongenomic response involves a number of different proteins as shown in **Figure 2**, and usually combines different signalling pathways, which in the end lead to expression of a variety of genes and not only those with VDRE containing promoters (**Zanello L.P. and Norman A.W. 1997; Beno D.W. et al. 1995; Song X. et al. 1998; Berry D.M. et al. 1996**). Since it was reported that the VDR knock-out mice used in this study have ablated both genomic and nongenomic responses (**Erben R.G. et al. 2002**), the intention was to analyze and identify differentially expressed proteins in kidney, one of the major vitamin D target tissue. Considering the fact that vitamin D affects many different pathways, changes in expression levels and/or posttranslational modification of many proteins were expected. However, as shown in the results, the number of significant changes was relatively restricted – partly due to the specific features of the method, but partly representing the limited number of changes that may be sufficient for pathogenesis.

3.1.1. 2-D electrophoresis limitations

PROTEIN SEPARATION

The first major technical limitation was the establishment of run conditions to achieve good protein separation and at the same time avoid protein degradation and distortions like the “smiling” effect. This is essential in order to achieve the precise reproducibility necessary for PDQuest analysis. Although, after optimization the reproducibility was sufficiently high, it was not absolute, and in some cases it was very difficult to determine spots identities and associated changes in expression level. Therefore, each of 5 samples of both, wild type and knock-out animals, were processed in triplicates and separated in a wide pH range first, and after protein identification, the samples were additionally checked on so called “zoom in” gels with a narrow pH range to confirm the results.

Nevertheless, some of the differentially expressed proteins, like protein number 7 (VDR) show an unexpectedly variable pattern that differed from gel to gel, irrespective of the sample. The expression of VDR in VDR knock-out mice provided an additional evidence that the receptor was expressed, although the first zinc finger motif (part of the DNA binding domain) was deleted (**Erben R.G. et al. 2002**). Different expression levels of VDR observed in the same group of animals can be due to differences between individual animals. Since vitamin D influences calcium homeostasis and therefore overall mineral ion homeostasis in organism, which is tightly regulated by feedback mechanisms in tissues like bone, intestine and kidney, it is to be expected that VDR expression level would differ according to changes in Ca^{2+} level, and this can vary between individual animals. However, complete absence of the protein, which was observed on number of gels was not expected and can not be explained by individual differences.

PROTEIN MODIFICATIONS

Unexpected protein shifts in a pH range, as observed in the case of VDR, can be due to a posttranslational modification. If a protein is phosphorylated, it will contain more negative charges and it will be shifted to a lower pH region. VDR contains two phosphorylation sites as shown in **Figure 3**, and impaired phosphorylation could consequently cause a shift to a higher pH region. Beside phosphorylation, some proteins carry an N-terminal signal peptide that can be cleaved off after the protein translation. As a consequence, the pI value of the mature protein will differ from the theoretical pI value in the database, and the protein will be present at a different position in the gel than otherwise expected.

Additionally, protein shifts in a pH range or in Mw were previously reported as possible, due to the sample preparation (**Lottspeich F. and Zorbach H. 1998**). Deamination of amino acids can cause a shift to lower pH up to one unite. At the same time, even in conditions when high molar urea is used for sample preparation, some groups can be shielded and protein can be shifted in a pH range. In case of Mw shifts, they are often caused by protein complexes that are not completely destroyed by denaturing conditions, used in sample preparation. Such complexes are moving more slowly in the gel and reside in the area with higher Mw. Furthermore, as already mentioned in results, one of the problems is protein degradation, which leads to the protein fragmentation to different positions in the gel. Taken together, these effects make correct protein identification - first by gel comparison and then by MALDI - even more difficult.

PDQuest SOFTWARE ANALYSIS

The second method limitation is selection and comparison of the gels. This is done by different software packages available commercially. In this case the proteins were identified by PDQuest software from BioRad. Several normalization steps should be performed on each set of gels separately, to achieve a better comparability of independent experiments, which are then combined to obtain high level matchset gels as described in results. Since the landmarks used for matching are set according to the personal impression, like all further manual corrections, and are highly subjective, reliability and reproducibility of the results are called into question.

VISUALIZATION AND IDENTIFICATION

The third limitation of the widely used silver stained gels is connected to the high sensitivity of the staining, which is good for detection and/or monitoring the expression changes of low expressed proteins, but represents a limit when it comes to protein identification. In case of two proteins (number 8 and 9) with identified expression changes in kidneys from knock-out animals, the amount of peptides was insufficient to obtain good spectra with matrix assisted laser desorption/ionization time-of-flight mass spectrometry (MALDI-TOF MS). High-quality spectra were obtained only for highly expressed control proteins (**Figure 15 a and b**). In rest of the cases good quality spectra were very hard to obtain and unfortunately rare (**Figures 16 and 17**), which made protein identification very difficult and uncertain.

3.1.2. *Improvement possibilities*

Even with all above described limitations of 2-D electrophoresis, this method is still the method of choice for monitoring global protein expression changes. The problems can be partly overcome by using a modified 2-D electrophoresis technique, called difference gel electrophoresis (DIGE). In this method two protein samples are pre-labeled with two cyanine dyes, thus enabling it to run two different samples on the same gel, in both dimensions. Therefore the two samples are subjected to the same procedure and environment throughout the whole experiment. Protein spots can be detected by fluorescence imaging immediately after the electrophoresis with a sensitivity equal to silver staining, and differences in protein expression can be detected with higher reliability and reproducibility (**Ünlü M. et al. 1997**).

When specific proteins are identified, the results can be additionally verified and more subtle changes in protein modification like phosphorylation, glycosylation etc. can be observed by surface enhanced laser desorption/ionization (SELDI) protein chip arrays. The advantage of this method is the ability to analyze crude biological extracts and its high sensitivity (**Wright G.L. Jr. et al. 1999**). The method is based on the peptide masses measurement of proteins adsorbed on the chip surface, which enables protein identification. Additionally, different protein chip arrays that contain chemically (cationic, anionic, hydrophobic, hydrophilic) or biochemically (antibody, receptor, DNA) treated surfaces can be used to further analyze protein of interest. Combined with this method, 2-D electrophoresis should provide reliable results in proteome analysis.

At the end, results in protein changes can be compared to the changes on RNA level to additionally verify the findings. However, it should be emphasized that some changes may exist only on the protein level, without any alterations in gene expression, due to the changes in protein stability and degradation and other posttranscriptional regulatory mechanisms.

3.2. Identified changes in protein expression and connection to vitamin D

All proteins identified to be differentially expressed (downregulated) in kidneys of VDR knock-out mice concern enzymes that are involved in central metabolic processes. For some of them, like malate dehydrogenase, previous reports about regulatory elements in promoter region did not reveal any vitamin D responsive element (**Setoyama C. et al. 1990**). Therefore the question arose about connection between metabolic changes and vitamin D. As already mentioned, it is not necessary that changes on protein level reflect changes in gene expression. However this is not a likely explanation in this case since the changed enzymes are not representing isolated cases but rather show functional connection. Only changes in vitamin D receptor expression can be directly connected with inability of the receptor in knock-out animals to trigger genomic responses, since it was reported that vitamin D regulates production of VDR via VDRE (**Naveh-Many T. et al. 1990**). In all other cases additional explanation should be found.

One, and the most likely, possibility is that VDR deficiency acts secondary to the changes in Ca^{2+} level. It is well known that major role of vitamin D in organism is Ca^{2+} mobilization. Elevation in vitamin D plasma level causes intestinal calcium absorption and at the same time, together with parathyroid hormone (PTH), it also triggers calcium reabsorption in bones and kidneys. This makes vitamin D a regulator of Ca^{2+} homeostasis, and therefore mineral ion homeostasis in organism. Why is this important? Ca^{2+} is essential for a vast array of intra- and extracellular activities and represents a key intracellular second messenger that carries information to virtually all processes important for cell life, like cell proliferation, differentiation and apoptosis, via changes in gene transcription, protein secretion and enzyme activity (**Bootman M.D. et al. 2001**). In the past decades impact of extracellular calcium on metabolism, especially lipid synthesis, was suggested. Substantial downregulation in level of malic enzyme in both, kidney and liver, and additionally lactic enzyme and glucose-6-phosphate dehydrogenase in liver, were observed in parathyroidectomised mice with low extracellular Ca^{2+} level (**Bogin E. and Earon Y. 1985**), but the exact mechanism by which it could act upon cells remained unclear till recently. Cloning of G Protein-Coupled, Extracellular Ca^{2+} (Ca_o^{2+})-Sensing Receptor (CaR) provided an explanation for Ca^{2+} function as a versatile extracellular first messenger (**Brown E.M. 2000; Brown E.M. and MacLeod J.R. 2001**).

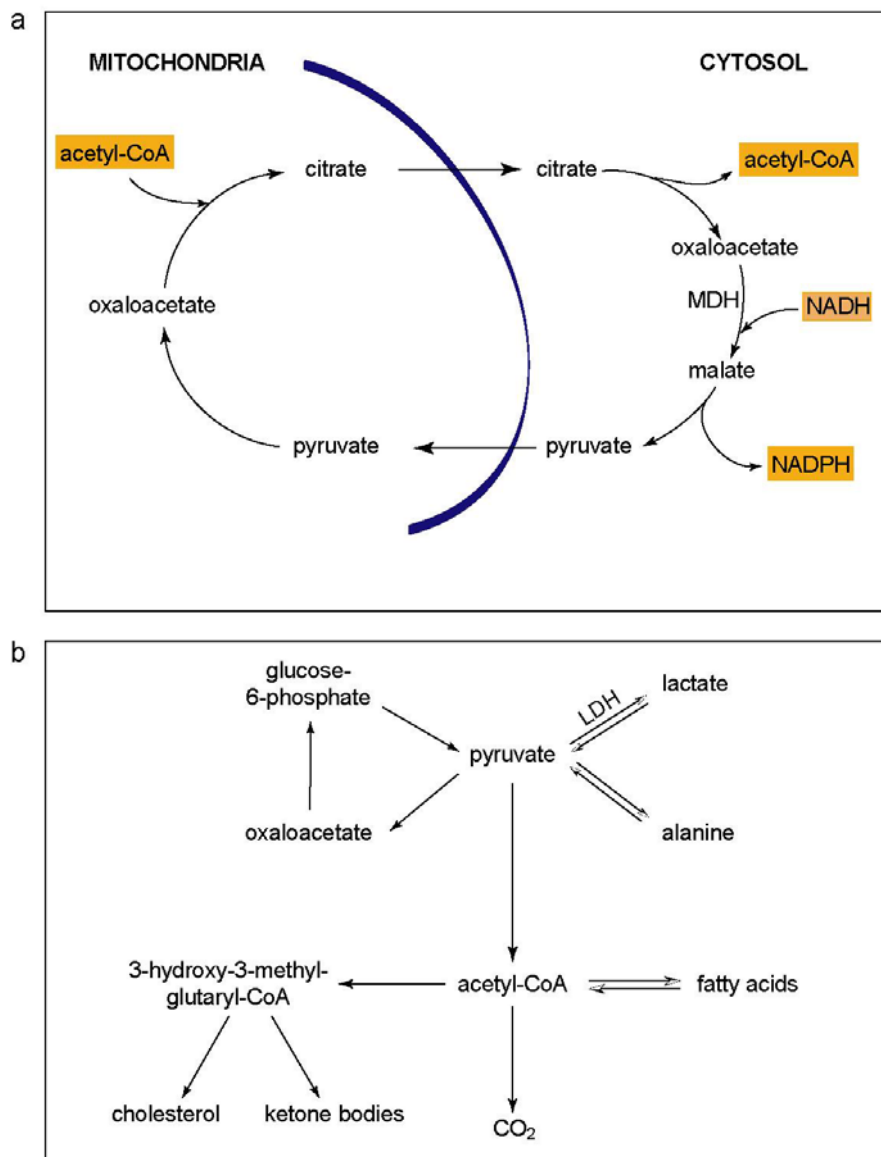


Figure 21. Different metabolic actions in metabolic pathway of mammalian cells. Figure a represents the citrate cycle with stress on the transport of acetyl-CoA from mitochondria into the cytosol, a necessary step in fatty acid synthesis. Figure b shows a schematic connection of different enzymes included in the metabolic pathway with the common aim of lipid metabolism (synthesis of cholesterol, ketone bodies, and fatty acids). MDH – malate dehydrogenase; LDH – lactate dehydrogenase; NADH – *reduced* nicotineamide adenine dinucleotide; NADPH – *reduced* nicotineamide adenine dinucleotide phosphate.

The most prominent features of CaR deficient mice are growth retardation, hyperparathyroidism and rickets (**Brown E.M. and MacLeod J.R. 2001; Sanford C. et al. 2001**), the same features that can be observed in VDR knock-out mice and overcome by rescue calcium diet (**Yoshizawa T. et al. 1997; Kinuta K. et al. 2000; Erben R.G. et al. 2002; Li Y.C. et al. 1998; Amling M. et al. 1999**). These findings suggest that the major effect of VDR deficiency on growth retardation and bone defects are actually secondary, due to low Ca^{2+} level (**Li Y.C. et al. 1998; Donohue M.M. and Demay M.B. 2002**). Only alopecia in VDR knock-out mice could not be corrected by calcium rich diet and was not present in CaR deficiency.

Since low Ca^{2+} level led to the downregulation of malic enzyme in parathyroidectomized rats, the observed changes in expression of cytosolic malate dehydrogenase and lactate dehydrogenase in VDR knock-out kidneys are consistent with previous observations. Malate dehydrogenase (MDHC) plays a pivotal role in malate-aspartate shuttle (**Stryer L. 1996**), operative in the metabolic coordination between cytosol and mitochondria in mammalian tissues. This is very important for fatty acid synthesis, which takes place in the cytosol and requires acetyl-CoA, generated in mitochondria *via* transformation of pyruvate to oxaloacetate. Acetyl-CoA is transported from mitochondria to cytosol in the form of citrate and is regenerated in cytosol in reaction transforming citrate back to oxaloacetate. In following steps oxaloacetate is transformed to malate in reaction catalyzed by malate dehydrogenase and malate is further transformed to pyruvate, by malic enzyme. The entire process is shown in **Figure 21 a** and **b**. Lactate represents a reduced form of pyruvate and is formed in a reaction catalyzed by lactate dehydrogenase (LDH). From all those data the connection between all identified enzymes in the same metabolic pathway is clearly visible. In earlier studies inactivity of the citrate cycle was connected to some forms of leukemias like acute myeloblastic leukemia and chronic myelocytic leukemia (**Belfiore F. et al. 1975**). VDR knock-out mouse used in this study revealed similar symptoms, thus it would be interesting to further investigate this connection. In addition, cytosolic malate dehydrogenase is found to be a regulatory subunit of nucleic acid conducting channel (NACH) and to confers its nucleic acid selectivity. This channel is responsible for nucleic acid uptake in liver and kidney tissue but so far a little is known about this process (**Hanss B. et al. 2002**).

Hydroxyacid oxidase (HAO3), the third metabolic enzyme found to be downregulated in kidneys from VDR knock-out mice is involved in peroxisomal fatty acid α -oxidation (**Jones M.J. et al. 2000**). The oxidative metabolism of fatty acids can proceed by either α - or β -oxidation. While fatty acid β -oxidation generates cellular energy through release of reducing equivalents and acetyl-CoA, the exact contribution of α -oxidation to mammalian metabolism remains unclear. One function of fatty acid α -oxidation, at least in humans, appears to be in converting 3-methyl branched fatty acids to 2-methyl branched fatty acids, which can be further oxidized by both, peroxisomal and mitochondrial β -oxidation pathways. Having in mind the previously mentioned downregulation of citrate cycle enzymes, which in turn can lead to downregulation of fatty acid formation, it is to be expected that similar downregulation would be observed also in the case of fatty acid oxidation.

Adenosine kinase (ADK) participates in ATP production, catalyzing phosphorylation of adenosine to adenosine monophosphate (AMP), which can be further metabolized to adenosine triphosphate (ATP), the major energy source in organism, used for active transport of molecules, synthesis of macromolecules and mechanical movement.

However, although downregulation of the enzymes described above implies lower energy supplies in kidneys of VDR deficient animals, no functional abnormalities could be observed (**Erben R.G., personal comm.**).

3.3. Conclusions

The following conclusions can be drawn from the results presented in this work.

Two-dimensional electrophoresis still has significant limitations that require careful optimization of all protocols. Therefore, only few changes in protein expression in kidney proteome of VDR knock-out mice were found. All proteins identified were downregulated in kidneys of VDR-deficient animals and are involved in central metabolic processes in the cell. These findings imply a significant disturbance of energy metabolism in VDR-deficient cells.

Considering the complex actions of vitamin D in various tissues, it should be additionally checked if proteome changes found are really due to nonfunctional VDR, or are secondary effects of disturbed Ca^{2+} homeostasis. Therefore, VDR knock-out mice represent a good model for studying proteome changes caused by nonfunctional VDR only if secondary effects are excluded, like in VDR knock-out fed with Ca^{2+} rich diet.

Despite the technical limitations of 2-D electrophoresis, it is still the method of choice when it comes to screening of the huge number of proteins at the same time. Many problems of reproducibility could be overcome by extensive replication and computer-aided analysis. Especially in combination with other new protein analysis methods, 2-D electrophoresis represents a most significant step in proteome analysis. This is demonstrated by the successful identification of several down-regulated proteins by the combination of 2-D gels, matchset gel analysis and MALDI-TOF mass spectrometry.

4. MATERIALS AND METHODS

4.1. METHODS

4.1.1. Two-dimensional electrophoresis

Two-dimensional electrophoresis (2-D electrophoresis) is a powerful method for the analysis of complex protein mixtures extracted from cells, tissues, or other biological samples. It sorts proteins according to two independent properties in two discrete steps: the first dimension step, isoelectric focusing (IEF), separates proteins according to their isoelectric points (pI), and the second dimension step, SDS-polyacrylamide gel electrophoresis (SDS-PAGE), separates proteins according to their molecular weights (M_w , relative molecular weight). Each spot on the resulting two-dimensional array corresponds to a single protein species in the sample, and information such as protein pI, and the apparent molecular weight can be obtained. 2-D electrophoresis was first introduced by O'Farrell (**O'Farrell P.H. 1975**) and Klose (**Klose J. 1975**) in 1975. But, only after introduction of immobilized pH gradients and ImmobilineTM reagents (**Bjellquist B. et al. 1982**), and further development of the method by Görg and colleagues (**Görg A. et al. 1985; Görg A. et al. 1988**), it became significant and widely used biochemical separation technique, especially in the proteome analysis. The term "proteome" was used for the first time in 1995 (**Wasinger V.C. et al. 1995**), to describe the expressed protein complement of a genome.

Beside proteome analysis, 2-D electrophoresis application involves cell differentiation, detection of disease markers, monitoring therapies, drug discovery, cancer research, purity checks, and microscale protein purification. Therefore, it is of high importance to use special reagents all the time, with high purity grade, especially when 2-D electrophoresis analysis is followed by protein identification on mass spectrometers.

Sample preparation

In order to characterize specific proteins in a complex protein mixture, the proteins of interest must be completely soluble under electrophoresis conditions. In general, it is advisable to keep sample preparation as simple as possible. Though additional sample preparation steps can improve the quality of the final results, each additional step can result in the selective loss of protein species. Methods that are used depend on the goal of the final 2-D result - is it to view as many proteins as possible - or only a subset of the proteins in the sample of potential interest. Ideally, the process will result in the complete solubilization, disaggregation, denaturation, and reduction of the proteins in the sample.

Kidney isolation

Wild type animals and vitamin D receptor (VDR) knock-out mice (C₅₇BL/6) were purchased from the group of Dr. R. Erben, Institute of Animal Physiology, Ludwig Maximilians University, Munich. The mice were killed by cervical dislocation under anaesthesia. Kidneys were removed and rapidly frozen in liquid nitrogen. They were stored at -80°C till further application.

Protein isolation

Samples were kept all the time at dry ice to avoid protein degradation. Protease inhibition stock solution (25 x conc.) was prepared by dissolving one tablet of protease inhibitor cocktail (Roche #1697498) in 2 ml of deionized water. A 100 µl aliquot was taken and diluted 25x into the working solution (1 x conc.), according to the manufacturer's protocol.

Each kidney (average weight ~500 mg) was overlaid with 500 µl of protease inhibitor working solution and cell disruption was performed by mechanical homogenisation for 5 minutes at 1100 rpm, in a table homogenizer (Potter S homogenizer, B.Braun Biotech International), until all tissue was resuspended. A 50 µl aliquot was removed in the clean Eppendorf tube for measuring the protein concentration and the rest of resuspended tissue was immediately transferred into separate tubes. Each tube was closed with perforated cap, quickly frozen in liquid nitrogen, and samples were lyophilized over the night in a vacuum concentrator (SC210A SpeedVac Concentrator, Savant)

The lyophilized sample was dissolved in 1 ml of lysis buffer and left 30 minutes at room temperature for full denaturation and solubilization. Removal of contaminants, as nucleic acids, polysaccharides, lipids etc. that would interfere with 2-D electrophoresis results, was done by ultracentrifugation at 42000 rpm (150000xg), for 60 minutes, at 20°C (L7-65 Ultracentrifuge, Beckman; rotor SW 50.1). The supernatant was carefully removed into the clean Eppendorf tube and aliquoted before freezing at -80°C.

The lysis buffer is composed of high molar urea (Amersham Biosciences #17-1319-01) that solubilizes and denatures proteins, unfolding them to their full random conformation, with all ionizable groups exposed to solution; a zwitterionic detergent CHAPS (Sigma #C-3023), which is included to ensure complete sample solubilization and to prevent aggregation through hydrophobic interactions; reducing agent dithioerythritol (DTE; Merck #1.24511.0025), for breaking disulfide bonds and maintaining all proteins in their fully reduced state; IPG buffers (Amersham Biosciences) that enhance protein solubility by minimizing protein aggregation due to charge-charge interactions, and improve separations.

Protein concentration measurement

The assay used is a colorimetric assay based on copper ions and Folin-Ciocalteu's phenol reagent for phenolic groups, first described by Lowry, but here, the modified method, according to Markwell (**Markwell M.A. et al. 1981**), was used.

Each sample was diluted to 3 different concentrations (500, 1000 and 5000 dilution fold) of proteins. A dilution series of calibration standard bovine serum albumin (BSA; Sigma #A-8531), in the deionized water (diluted in the same way as samples) were prepared, to give concentration of 0 to 84 µg/µl.

250 µl of each protein-containing sample, or each standard dilution, was mixed with 750 µl of solution C (for details see Materials, Buffers and solutions) and incubated 10 minutes at room temperature. 75 µl of solution D (Folin-Ciocalteu diluted 1:1 with deionized water) was then added to each sample, mixed, and left for 45 minutes in the dark. Within next 45 minutes, the net absorbance at 660 nm (A_{660}) was measured.

A calibration plot was prepared by graphing the net A_{660} values for the standards versus protein concentrations. The protein concentration of samples was determined by interpolation from the plot.

According to the measured values, samples were diluted with lysis buffer to an approximate concentration of 10 mg/ml.

4.1.1.1. First-dimension isoelectric focusing

Isoelectric focusing (IEF) is an electrophoretic method that separates proteins according to their isoelectric points (pI). Proteins, as amphoteric molecules, carry either positive, negative, or zero net charge, depending on the pH of their surrounding. The net charge of a protein is the sum of all negative and positive charges of its amino acid side chains and amino- and carboxyl-termini. The isoelectric point (pI) is the specific pH at which the net charge of the protein is zero.

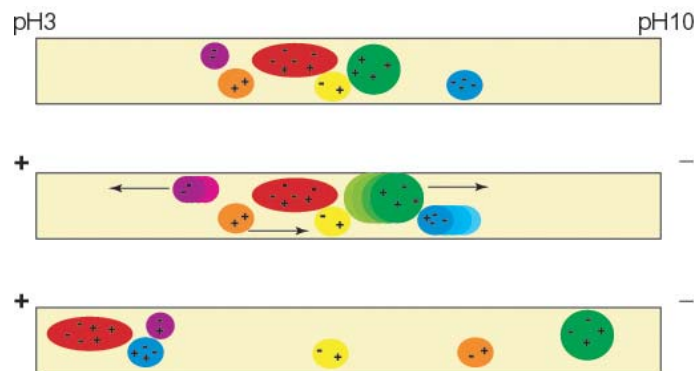


Figure 22. Principle of isoelectric focusing (IEF). After applying an electrical field proteins are moving in the direction of cathode or anode, dependent on their charges.

In a pH gradient, under the influence of an electric field, a protein will move to the position in the gradient where its net charge is zero (**Figure 22**). This is called focusing effect of IEF, which concentrate proteins at their pIs and allows proteins to be separated on the basis of very small charge differences. The slope of the pH gradient and the electric field strength determines the resolution. IEF is therefore performed at high voltages and for a constant number of Volt-hours (Vh), being the integral of the volts applied over the time. The first-dimension isoelectric focusing was done on IPGphor IEF Unit (Amersham Biosciences #80-6414-02).

Immobiline DryStrip gels

Ready-made Immobiline DryStrip gels (IPG strips; Amersham Biosciences), strip length 18 cm, were used. IPG strips contain a pre-formed pH gradient immobilized in a polyacrylamide gel. The gels are cast on a plastic backing and delivered dried. Prior to use, they were rehydrated in rehydration buffer.

Rehydration buffer includes the same substances as lysis buffer (described previously), but in different concentrations, to reduce salts and detergent amount, which could disturb the focusing.

Sample application

Sample can be applied either by including it in the rehydration solution or by applying it directly to the rehydrated IPG strip via sample cups. For IPG strips with pH interval 3-10 and 4-7, samples were applied together with rehydration solution, and for pH interval 6-9, strips were first rehydrated in rehydration solution only, in the reswelling tray (Amersham Biosciences #80-6465-32), over the night, and the sample was applied immediately prior to focusing, anodically in a sample cup.

Each strip holder was washed prior to use with neutral pH detergent by vigorous agitation (Ettan IPGphor Strip Holder Cleaning Solution; Amersham Biosciences #80-6452-78) to remove residual protein, rinsed well with deionized water and air dried thoroughly, before applying the sample.

IPG strips pH 3-10 and pH 4-7

100 μg and 150 μg of total protein (of each sample), for pH 3-10 and pH 4-7, respectively, were resuspended in rehydration buffer to a final volume of 350 μl , and 3 μl of 0,5% bromophenol blue (Biomol #50206), as a tracking dye, was added. Samples were shortly mixed and centrifuged in a tabletop centrifuge (Eppendorf #5415C) for 1 minute at 14000 rpm to remove air bubbles or any insoluble material present.

The whole volume was pipetted into each strip holder (Amersham Biosciences #80-6416-68) at a central point, in the strip holder channel and large bubbles were removed. The protective cover foil was removed from the frozen IPG strip (Amersham Biosciences #17-1234-01 and #17-1233-01) and it was slowly lowered onto the solution, with a gel side down, taking care that the entire strip was wetted equally, and that no air bubbles were trapped under the strip. An IPG strip should make contact with both electrodes, at each end of the holder. Approximately 1 ml of DryStrip Cover Fluid (Amersham Biosciences #17-1335-01) was applied on top of the strip to minimize evaporation and urea crystallization, or burning of the

strip caused by drying during the focusing. Finally, a cover was placed on to the strip holder and focusing was initiated.

Rehydration time was programmed as the first step of an IPGphor protocol, under low voltage (30V), to facilitate the entry of high-molecular weight proteins (**Görg A. et al. 1998**). After rehydration, voltage was gradually increased to the final desired focusing voltage, which was held for several hours (**Table 4**).

IPG strips pH 6-9

350 μ l of rehydration buffer (contains IPG buffer pH6-11; Amersham Biosciences #17-6001-78) was mixed with 3 μ l of bromophenol blue tracking dye and shortly span down to remove air bubbles. The whole volume was pipetted into the slot of the reswelling tray. The protective cover foil was removed from the frozen IPG strip (Amersham Biosciences #17-6001-88), and it was gently lowered on the solution in its slot, with the gel faced down. Possible air bubbles were removed by sliding strip back and forth. Each strip was overlaid with 3 ml of DryStrip Cover Fluid and the reswelling tray was covered with a lid. Strips were left to rehydrate over the night (at least 12 hours) at room temperature.

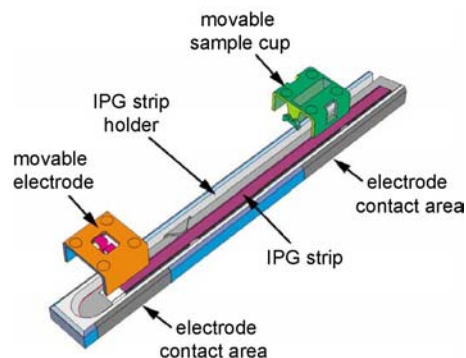


Figure 23. Set up of an IPG strip in a cup loading strip holder. For simplicity only one end of the holder and one movable electrode are shown.

The next day, strips were carefully removed from the tray, briefly rinsed in a stream of deionised water, and the excess of water was removed on a damp filter paper. They were placed in the IPGphor cup loading strip holders (**Figure 23**), with the gel faced up, and overlaid with 4 ml of DryStrip Cover Fluid across the surface. Two electrode pads, 5 mm long, made of IEF electrode strips (Amersham Biosciences #18-1004-40), were wetted with deionised water and placed on the each end of the strip, overlapping it.

Electrodes were put on top of each pad, so that they were in contact with metal plating on the sides of the strip holder. The sample cup was positioned on the anodic (+) end of the IPG strip, so it is sealed against the strip without cutting into it. 150 μg (approximately 15 μl for each sample) of total protein was briefly centrifuged prior to loading, to remove air bubbles, and pipetted into the sample cup. The holder was closed with a plastic cover and isoelectric focusing protocol was started (**Table 4**).

<i>pH range</i>	<i>voltage (V)</i>	<i>(h:min)</i>	<i>mode</i>	<i>volt-hours (kVh)</i>
3-10 and 4-7	30	14:00	step and hold	0.42
	200	1:00	step and hold	0.2
	500	1:00	step and hold	0.5
	1000	1:00	step and hold	1
	8000	0:30	Gradient	2.25
	8000	4:00*	step and hold	up to 37 kVh
6-9	200	1:00	step and hold	0.2
	500	1:00	step and hold	0.5
	1000	1:00	step and hold	1
	8000	0:30	gradient	2.25
	8000	5:30*	step and hold	up to 49 kVh

Table 4. Running protocols for both, rehydration sample load and sample cup load. Voltages, step duration and voltage modes are given. Maximal current was 50 μA /IPG strip, surface temperature 20°C.

* Step duration depended on total current during the step and voltage amount achieved. It was set up for the total kVh of the isoelectric focusing.

IPG strip storage

After isoelectric focusing, if not immediately further processed, IPG strips were frozen at -80°C in equilibration tubes (Amersham Biosciences #80-6467-79). In this way they can be stored for a longer period of time.

4.1.1.2. Second-dimension SDS-PAGE

SDS-PAGE (SDS-polyacrylamide gel electrophoresis) is an electrophoretic method for separating polypeptides according to their molecular weights (M_w). The technique is performed in polyacrylamide gels containing sodium dodecyl sulfate (SDS; Amersham Biosciences #17-1313-01), an anionic detergent that denatures proteins by wrapping the hydrophobic tail around the polypeptide backbone and masking the charge of the proteins, so the formed anionic complexes have nearly a constant net negative charge per unit mass. In that way, migration is determined not by intrinsic electric charge of polypeptides but by molecular weight.

SDS-PAGE in a 2-D electrophoresis

Immediately prior to the second dimension, the IPG strips were equilibrated in equilibration solutions. In the first equilibration step (reduction step), 1% w/v dithioerythritol (Merck #1.24511.0025) was included, and in the second step, alkylation was performed with 4% w/v iodoacetamide (Merck #8.04744.0100). Each step was done in equilibration tubes, with 10 ml of solution per strip, for 15 minutes with gentle shaking (DUOMAX 1030, Heidolph Instruments).

For SDS-PAGE a continuous tris-glycine buffer system was used, on the vertical second-dimension system (Protean II xi multi-cell, BioRad #165-1951). 10x stock solution was prepared and diluted 1:10 with deionised water to working concentration, directly prior the electrophoresis run.

After pouring the gel (thickness 1 mm, total acrylamide concentration 12,5% homogenous, size 20x20 cm), its surface was overlaid with isopropanol (Merck #1.09634.2500) to minimize exposure to oxygen and to create a flat surface. Gels were left to polymerize at least one hour. Afterwards, isopropanol was removed, gel surface was well rinsed with deionized water and excess of water was removed by gel blotting paper (Schleicher & Schuell #GB002).

Equilibrated IPG strips were briefly rinsed in a stream of deionized water, and the water excess was removed with the lint-free tissue. Each strip was placed on top of one vertical SDS-polyacrylamide gel (**Figure 24**), with the gel side of the strip pointing to the front glass of SDS-polyacrylamide gel cassette. A filter paper strip soaked with 20 μ l of protein standard (Prestained Precision Protein Standard, broad range, BioRad #161-0372) was positioned next to the basic end of the IPG strip. Approximately 3 ml of hot (60°C) agarose (Biozym #6036085) solution was poured over the IPG strip, that was then immediately gently pressed to the upper edge of the second-dimension gel by 0,75 mm thick spacer, to enable a close contact between the IPG strip and the gel. After the agarose had set, 4 gels were simultaneously run over the night in the Protean II xi multi-cell.

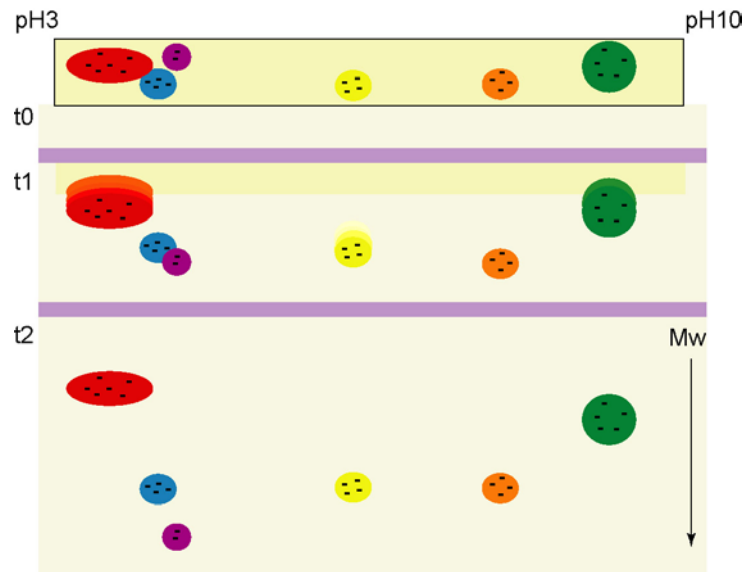


Figure 24. Principle of second dimension separation (SDS-PAGE). Equilibrated IPG strip is placed on the top of SDS-PAGE gel (**t0**). Applying an electrical field (**t1**) causes protein movement through the gel. In the end (**t2**) proteins are separated according to their molecular weights (Mw). Arrow points to the low Mw.

To improve the transfer of polypeptides from IPG strip into the second dimension gel, voltage was first set to 70V for 10-15 minutes. After the bromophenol blue dye had entered the gel the voltage was raised to 100V, and run was carried approximately for 15:30 hours, at room temperature, with the gel holder cores cooled to 15°C.

SDS-PAGE of molecular weight markers

Samples were prepared by dissolving the molecular weight markers in 1xPBS buffer, in three different dilutions. Each sample was mixed 1:1 with 5x Laemmli buffer and incubated for 5 minutes at 95°C. They were cooled on the ice before application on the 10% tricine gel, and electrophoresis run was performed at 90 V, for 1,5 hours. In the end, each protein marker was loaded on the gel in three different amounts: 100 ng, 500 ng, and 1 µg. To visualize the protein bands, gels were incubated with Coomassie stain for 30 min – 1 h, at room temperature, and destained afterwards by boiling in 7% acetic acid. Molecular weight markers used were: bovine serum albumin (66 kDa; Sigma #A-8531), carboanhydrase (29 kDa; Sigma #C-7025), albumin (45 kDa; Fluka #05440), alcohol dehydrogenase (150 kDa; Sigma #A-8656), β-amylase (200 kDa; Sigma #A-8781), apoferritin (443 kDa; Sigma #A-3660), thyroglobulin (669 kDa; Sigma #T-9145), and blue dextran (2000 kDa; Sigma #D-4772).

4.1.1.3. Visualization

When the bromophenol blue front had completely migrated out of the SDS gel, polypeptides were fixed in methanol/acetic acid/water (4/1/5) for at least one hour. Visualization was done by modified silver-staining protocol according to Blum. The complete protocol is presented in **Table 5**.

When proteins were fixed to the polyacrylamide gel and excess of fixing solution was washed out with 30% ethanol (Merck #1.00983.2500) and deionised water, sodium thiosulfate (Merck #1.06509.0100) was used to enhance the contrast between the stained protein spots and background, improving the sensitivity. After sensitisation, the gel was exposed to silver nitrate solution (Merck #1.01512.0025), resulting in formation of silver ions complex with the proteins. In the subsequent developing stage, which is similar to photographic developing, the silver ions complexed with the protein undergo faster reduction than free silver ions. Particles of colloidal silver then form, preferentially at the protein spots at the two surfaces of the gel, making them visible.

After the last washing step, gels were soaked in the preserving solution for at least 90 minutes, before drying. Each gel was laid on sheet of cellophane (BioRad #1651779) and digitized on densitometer (GS710 Calibrated Imaging Densitometer, BioRad), to enable further evaluation of results. Scanned gels were covered with another cellophane sheet and dried in an oven (GelAir Drying System, BioRad #165-1772), in warm air-flow (80°C), for at least 60 minutes. In this way, gels were preserved for longer period of time.

Step	Reagent	Duration (min)
fixing	fixing solution	60
fixing	fixing solution	30
wash	wash solution	2 x 20
wash	deionized water	20
sensitizer	thiosulfate reagent	1
wash	deionized water	3 x 0.3
silver	silver nitrate	20
wash	deionized water	3 x 0.3
development	developer	3-5*
wash	deionized water	0.3
stop	stop reagent	5
wash	deionized water	3 x 10

Table 5. Silver-staining protocol. Each gel was separately stained, all reagents are reagent grade chemicals, and gels were handled using gloves all the time.

* duration of development step was watched and it differed for each gel.

4.1.1.4. Pattern evaluation

As already mentioned, gels were scanned on GS710 densitometer, at 84,7x84,7 microns resolution (300 dpi). The background of the gels was subtracted and computerized 2-D gel analysis (spot detection, spot editing, pattern matching) was performed with the help of PDQuest software version 6.2.0, from BioRad.

Because precast Immobiline DryStrip gels are highly reproducible, the pI of particular protein was estimated from its focusing position along a linear pH gradient IPG strip. pH gradients for each pH range are shown on figures below, although pI of certain protein can differ depending on the experimental conditions used. The second dimension was calibrated using molecular weight marker proteins loaded to the side of the second-dimension gel.

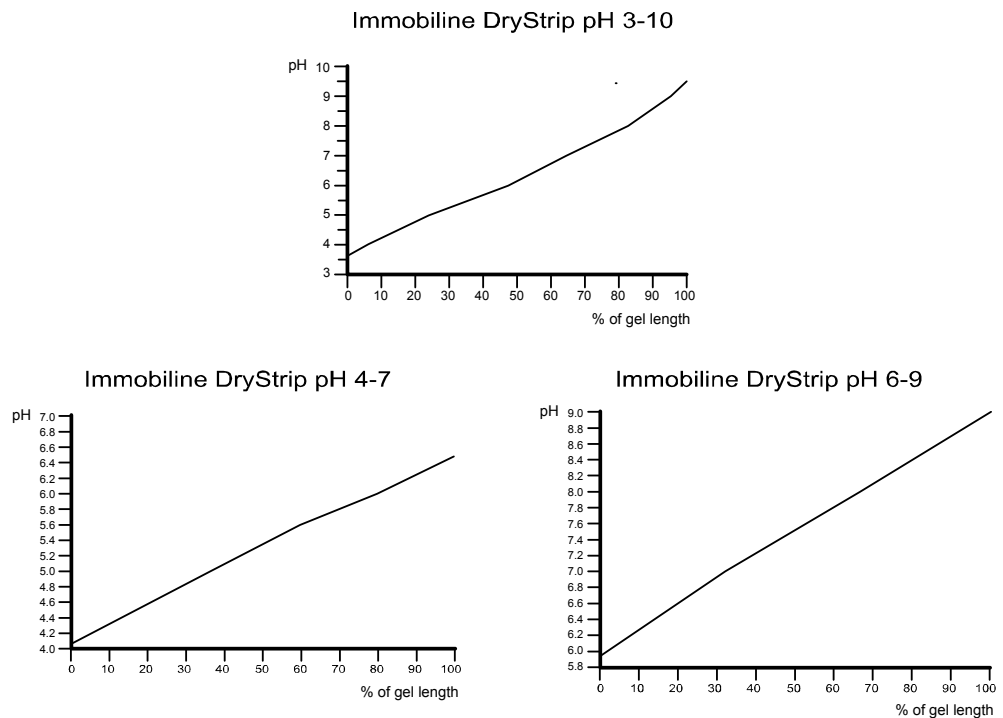


Figure 25. Distribution of pH gradients in different Immobiline DryStrip gels. pI value of a protein can be estimated by relating the position of the protein in the second dimension gel to its original position in the Immobiline DryStrip gel.

4.1.2. In-gel digestion

Before analysing differentially expressed proteins by matrix-assisted laser desorption/ionisation mass spectrometry (MALDI MS), protein spots were excised from the gel and in-gel digested with trypsin. A “negative control” piece was cut from a blank region of the gel and processed in parallel with the samples.

After excising, the gel pieces were destained in destain solution till all colour had disappeared, washed with high purity water (for chromatography; Merck #1.15333.1000) and buffer (100 mM ammonium bicarbonate; Sigma #A-6141), and shrunk by dehydration in acetonitrile (Chromasol V[®] Riedel-deHaen #34851), which was then removed. Gel pieces were dried for 15 minutes at 40°C, afterwards dithiothreitol (DTT; Biomol #04010) solution, in a volume just sufficient to cover the gel pieces was added, and the proteins were reduced for 30 minutes at 40°C. The same volume of iodoacetamide solution was added and the incubation was for 20 minutes at 40°C. After the alkylation step (iodoacetamide), gel pieces were washed once (10 minutes) with buffer, and dehydrated 3x for 5 minutes by addition and removal of acetonitrile.

Trypsin was prepared by dissolving lyophilised trypsin (Promega #V5111) in trypsin resuspension buffer (Promega #V542A). One aliquot was diluted with 1 mM NH₄HCO₃ to the working concentration (1,33 µg/µl). 15 µl of this working solution was added when pretreated gel pieces were completely dry. After 10 minutes on ice, if whole liquid was soaked into the gel pieces, additional 1 mM NH₄HCO₃ buffer (approximately 5 µl) was used to cover them. Sample plate was tightly closed by parafilm (American National Can) and left in the incubator (Heraeus Instruments), at 37°C, overnight, for enzymatic cleavage. Volumes of buffers used and duration of all steps are listed in **Table 6**.

solution	volume (μl) per sample	duration (min)	solution removal
<i>destain</i>			
destain solution	50	5-10	yes
dH ₂ O	100	5	no
acetonitrile	50	5	yes
100 mM NH ₄ HCO ₃	75	5	no
acetonitrile	50	5	yes
<i>reduction-alkylation</i>			
acetonitrile	50	5	yes
evaporation		15	
DTT	50	30	no
iodoacetamide	50	20	no
acetonitrile	100	5	yes
<i>wash-dehydrate</i>			
100 mM NH ₄ HCO ₃	50	10	no
acetonitrile	50	5	yes
acetonitrile	50	5	yes
acetonitrile	50	5	yes
evaporation		5	
<i>trypsin digestion</i>			
trypsin solution	15	overnight	no

Table 6. In-gel digestion of protein spots excised from the 2-D gels.
The whole procedure was done at 40°C, only the trypsin addition was done at ice, and trypsin digestion in incubator, at 37°C.

4.1.3. MALDI-TOF mass spectrometry

Mass spectrometry (MS) is a powerful analytical technique for forming gas-phase ions from intact, neutral molecules and subsequently determining their molecular masses. All mass spectrometers have three essential components: an ion source, a mass analyser, and a detector. Ions are produced from the sample in the ion source using a specific ionisation method, separated in the mass analyser based on their mass-to-charge (M/z) ratios, and then detected. The data system produces a mass spectrum which is a plot of ion abundance versus M/z . The ion source, mass analyser, and detector are usually situated inside a high vacuum chamber.

The matrix-assisted laser desorption/ionisation (MALDI) technique was firstly introduced in the late 80's by Karas and Hillenkamp (**Karas M. and Hillenkamp F. 1988**). The mechanism by which MALDI MS operates is that the sample is mixed with a large molar excess of matrix and bombarded with photons of UV light. The matrix is strongly UV-absorbing compound at the designated wavelength (N₂ laser, 337 nm, for α -cyano-4-hydroxycinnamic acid) where the large excess of matrix separates the analyte molecules from one another, thereby reducing intramolecular interactions. The second role of matrix is that it rapidly absorbs large amounts of energy from the incoming photons, resulting in an explosive breakdown of the matrix-analyte lattice, that substantially results in the transfer of protons from the matrix to the peptide and protein molecules.

The most common application of MALDI, time-of-flight (TOF) mass analyser, that works in reflectron mode (M@LDI, Micromass) was used in this study. A reflectron TOF instrument works by slowing an ion down, at an ion mirror (reflectron), until it stops, turning it around, and then reaccelerating it back out to the second detector, presented in **Figure 26**.

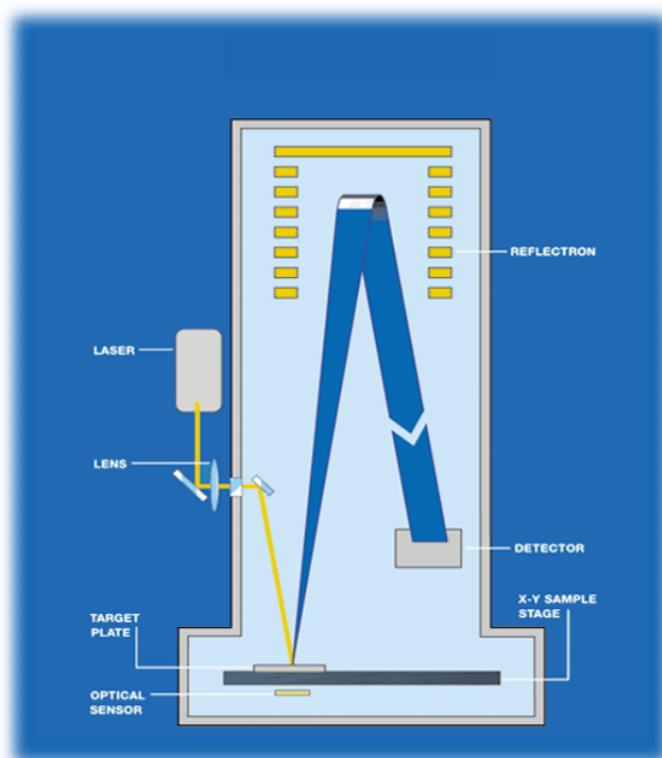


Figure 26. Schematic figure of MALDI-TOF mass spectrometer that works in reflectron mode.

The reflectron improves resolution (ability to distinguish peaks that are close in mass) by allowing ions of the same mass with different energies to arrive at the detector at the same time. For time-of-flight instruments, the resolution is defined by the mass of a peak divided by its width at half-height.

Peptide analysis is one of the most important applications of MALDI MS. The ability to ionise many peptides in a mixture simultaneously makes MALDI MS a popular choice for rapid analysis of protein digests. Although MALDI has been described as a “soft” ionisation technique, that produces singly charged ions, fragmentation often occurs, when operating in a reflector mode. But compared to older techniques, this technique has multiple advantages, including the instruments’ ease of operation and relatively good tolerance of moderate buffers and salt concentration in the analyte mixture.

Matrix mixture

Two parts of α -cyano-4-hydroxycinnamic acid (HCCA; Aldrich Chemical Company #47,687-0) and one part of nitrocellulose (NC; Macherey-Nagel #741280) were dissolved in acetone-isopropanol 4:1 mixture to final concentration of 20 $\mu\text{g}/\mu\text{l}$ HCCA and 10 $\mu\text{g}/\mu\text{l}$ NC.

Internal standard (“spike”)

Adrenocorticotrophic hormone (ACTH; Sigma #A0673) was diluted in water (chromatography grade purity) to 400 pmol/ μl concentration and 2 μl aliquots were stored at -20°C . Immediately before use, one aliquot was diluted 1:400 with 0.5% trifluoroacetic acid (TFA; Aldrich Chemical Company #30,203-1), to the working concentration of 1 pmol/ μl and kept on ice during the whole spotting procedure.

Calibrant (alcohol dehydrogenase)

Buffer was prepared by dissolving 4 mg of ammonium bicarbonate (Sigma #A-6141) to 1 ml of deionised water.

1 mg of alcohol dehydrogenase (ADH; Sigma #A-7011) was dissolved in 300 μl of the buffer solution prepared above by vortexing on Vortex-2 Genie (Scientific Industries).

1 mg of trypsin (Sigma #T-1426) was dissolved in 500 μl of the buffer solution.

5 μl of the trypsin solution was added to the alcohol dehydrogenase solution and mixed by vortexing for 30 seconds. This mixture, containing 100 pmol/ μl of protein, was then incubated for 90 minutes at 37°C .

1 μl aliquot was diluted 1:100 with 0.1% TFA (aqueous), to working concentration of 1 pmol/ μl , directly before spotting it on the target.

Sample preparation for MALDI MS

Before applying the samples, the 96 well target plate (Micromass) was washed by gentle brushing, with mild detergent, to remove the rest of the matrix or previously applied protein samples. After washing in the stream of deionised water, it was cleaned 2 x 10 minutes in the ultrasonic bath (Transsonic 310, ELMA®), completely lowered in 5% formic acid (Aldrich Chemical Company #39,938-8) and 50% acetonitrile, respectively, briefly rinsed in acetone (Merck #1.00014.1000), and left to air dry, protected from impurities of the surrounding.

Samples were applied onto the target using thin-layer method (Kusmann M. et al, 1997). 0,5 µl of the matrix mixture was deposited on each target well in homogenous thin layer and allowed to dry. 1 µl of internal standard (“spike”, adrenocorticotrophic hormone, 1 pmol/µl) was applied on dry layer of matrix and allowed to dry for 10 minutes. On “lock mass” wells, 1 µl of calibrant (alcohol dehydrogenase, 1 pmol/µl) was added, to prepare spots for instrument calibration. On sample wells of the target 1 µl of trypsin digest of each sample was applied and left to dry completely before loading the target plate into the MALDI-TOF MS instrument.

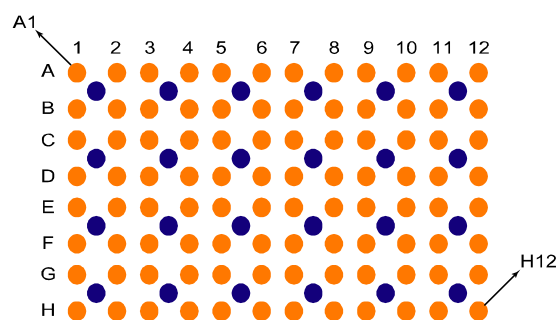


Figure 27. Lay out of MALDI MS target plate. Presented in orange are sample wells (A1-H12), and in blue are lock mass wells that are used for calibration.

Instrument calibration

The calibration of the instrument was performed each time before new set of samples was analysed, so that spectrum used for calibration was acquired under the same conditions as the analyte spectra. The peptide mixture was matched to the reference file that contained the known theoretical MH^+ values for the reference mixture of alcohol dehydrogenase and the mass errors, after fitting the calibration curve through the data points, were in ± 0.01 Daltons range.

Addition of mass standard to the analyte sample (internal calibration) can improve the accuracy to +0.01%, but there is always a risk that internal standard can suppress ionisation of the analyte. Also a matrix peak can be used for a one point calibration adjustment (**Vorm O. and Mann M. 1994**).

MALDI MS data acquisition

All mass spectra were obtained by acquiring the data manually on the benchtop MALDI-TOF mass spectrometer, in reflectron mode (MALDI Reflectron, MicromassUK), using average laser energy of 75%.

20 to 30 separate spectra were combined and 20-40% of background was subtracted by polynomial order 15, at 0,010 tolerance. Afterwards, spectra were smoothed by Savitzky Golay method (± 3 smooth windows, 2 smooths applied), and peaks were centered (minimal peak width at half height was 4, in 80% centroid top manner), to obtain spectrum easier to analyse.

If no spectra were obtained, when there was not enough peptides in the trypsin digest, or if there was no trypsin digest after the overnight incubation, additional extraction was done. 40 μ l of 50% acetonitrile was added to each gel piece, tubes were closed tightly with parafilm and left to incubate on shaker (KS260 basic, IKA[®]), max. 300 rpm, for 60 minutes, at room temperature. The whole volume was transferred into the clean Eppendorf tube and concentrated for 20-30 minutes at 30°C (Concentrator 5301, Eppendorf). When samples were completely dry, they were dissolved in 1 μ l of pure formic acid and diluted with 4 μ l of water (chromatography grade purity). After 10 minutes of incubation at room temperature, 1 μ l was applied on the target, in the same way as described above.

Protein identification

To identify proteins in sequence databases by using mass spectrometric peptide maps, the determined peptide molecular masses (mass fingerprints) were compared with expected values (virtual fingerprints), computed from the protein databases entries, according to the enzyme's cleavage specificity.

Enzyme cleavage specificity, number of matching peptides, mass accuracy, and size of the database are critical parameters that determine the performance of the method. These parameters were entered in the search set-up window of MassLynx 3.5 program.

Query was specified always with trypsin as a digest reagent, and no missed cleavages were included. There was no restriction to the molecular weight of query or certain pH range, considering possible protein changes during the two-dimensional electrophoresis. Oxidation was considered as an optional modification, according to the oxidative silver-destaining step, prior to the in gel digestion. Due to in-gel digestion's reduction and alkylation steps, carbamidomethyl as a fixed modification was included. SWISSPROT database was searched with minimally 3 matched peptides. The results were scored and the ranking suggested one or several candidates.

4.2. MATERIALS

4.2.1. Buffers and solutions

Two-dimensional electrophoresis

Lysis buffer 9 M Urea, 2% w/v CHAPS, 1% w/v DTE, 2.0% v/v IPG buffer pH 3-10 and 10 mM Pefabloc^R (Aminoethyl benzylsulfonyl fluoride, AEBSF; inhibitor of serine protease and some cysteine proteases)

Rehydration buffer 8M Urea, 0.5% w/v CHAPS, 2.5% w/v DTE and 0.5% v/v IPG buffer

NOTE: pH of IPG buffer depends on the pH range of the strip. For IPG strips with pH interval 3-10, 4-7 and 6-9, IPG buffers pH 3-10, 4-7 and 6-9 were used, respectively.

Equilibration solution 50 mM Tris-HCl, pH 8.8, 6 M urea, 30% v/v glycerol, 2% w/v SDS, a trace of bromophenol blue
reduction: 1% w/v DTT
alkylation: 4% w/v iodoacetamide

SDS-PAGE gel (Single-percentage 12,5% gel recipe for 100 ml of total gel solution)

38,9 ml acrylamide/bisacrylamide
37,5 ml Tris-HCl buffer, pH 8.8
0,5 ml 20% SDS
22,2 ml deionized water
0,8 ml 10% ammonium persulfate
32 µl TEMED

SDS-PAGE buffer 192 mM glycine, 25 mM Tris, 0.1% w/v SDS

SDS-PAGE agarose 0,5% agarose in electrophoresis buffer, prepared fresh

MATERIALS AND METHODS

SDS-PAGE for molecular weight markers

1 x PBS	10 mM sodium phosphate, 150 mM sodium chloride, pH 7.4
5 x Laemmli buffer	50% v/v glycerol, 4% w/v SDS, 0.2 M Tris-HCl, 0.1% w/v Coomassie blue G250, pH 6.8
Gel buffer	3 M Tris, 0.3% w/v SDS, pH 8.5
Stacking gel (4%)	0.67 ml acrylamide/bisacrylamide 0.67 ml gel buffer 3.6 ml deionised water 45 µl 10% ammonium persulfate 10 µl TEMED
Resolving gel (10%)	3.3 ml acrylamide/bisacrylamide 3 ml gel buffer 2.5 ml glycine 1 ml deionised water 60 µl 10% ammonium persulfate 20 µl TEMED
Two-system buffer (catode)	0.1 M Tris, 0.1 M Tricine, 0.1% w/v SDS 0.2 M Tris-HCl, pH 8.9 (anode)
Coomassie staining	200 ml methanol, 5 ml acetic acid, 295 ml deionised water, 500 mg Coomassie blue G250 (filtrate)

Protein concentration measurement

Solution A	2% sodium carbonate, 0.7% sodium hydroxide, 0.16% sodium tartarate, 1% sodium dodecylsulfate
Solution B	4% cupper sulfate pentahydrate
Solution C	100A + 1B
Solution D	Folin-Ciocalteau diluted 1:1 with deionized water

Standard solution	Bovine serum albumin (BSA) in concentration 0.1 mg/ml
Sample solution	Each sample diluted in 3 different concentrations, less than 0.1 mg/ml proteins

Silver staining

Fixing solution	40% methanol, 10% acetic acid, 50% deionized water
Wash solution	30% ethanol, 70% deionized water
Thiosulfate reagent	0.02% sodium thiosulfate
Silver nitrate reagent	0.2% silver nitrate, 0.02% formaldehyde (37%)
Developer	3% sodium carbonate, 0.05% formaldehyde (37%), 0.0005% sodium thiosulfate
Stop reagent	0.5% glycine
Preserving solution	20% ethanol, 2% glycerol

In-gel digestion

Buffer	100 mM ammonium bicarbonate (NH_4HCO_3)
Silver-destain solution	1:1 mixture of 100 mM sodium thiosulfate and 30 mM potassium ferricyanide in deionised water
Coomassie-destain	1:1 mixture of 100 mM ammonium bicarbonate and 50% acetonitrile
Reduction buffer	10 mM dithiothreitol (DTT) in 100 mM NH_4HCO_3
Alkylation buffer	55 mM iodoacetamide in 100 mM NH_4HCO_3
Trypsin resusp. buffer	50 mM acetic acid
Trypsin working solution	1,33 $\mu\text{g}/\mu\text{l}$ trypsin in 1 mM NH_4HCO_3

MALDI-TOF MS

Target washing reagents

Formic acid	5% formic acid in deionised water
Acetonitrile	50% acetonitrile in deionised water
Acetone	100% acetone

Matrix mixture

α -cyano-4-hydroxycinnamic acid (HCCA) and nitrocellulose (NC) mixed 2:1 in acetone-isopropanol (4:1) mixture to final concentration of 20 $\mu\text{g}/\mu\text{l}$ HCCA and 10 $\mu\text{g}/\mu\text{l}$ NC

“Spike”

1 pmol/ μl adrenocorticotrophic hormone (ACTH) in 0.5% trifluoroacetic acid (TFA; aqueous)

Calibrant

1 pmol/ μl alcohol dehydrogenase (ADH) tryptic peptides in 0.1% TFA (aqueous)

Additional extraction

Acetonitrile	50% acetonitrile
Formic acid	99% formic acid
Water	chromatography grade water

4.2.2. Chemicals

4.2.2.1. General

α -cyano-4-hydroxycinnamic acid	Aldrich Chemical Co.
Acetic acid (glacial, 100%)	Merck
Acetone p.a.	Merck
Acetonitrile, for HPLC, gradient grade	Chromasol V [®]
Acrylamide	Biomol
Agarose	Biozym
Ammonium bicarbonate	Sigma
Ammonium persulphate	Amersham Bioscien.
Bromophenol Blue	Biomol
CHAPS	Sigma
Coomassie Blue G250	Biomol
Copper sulfate pentahydrate	Merck
Dithioerythritol	Merck
Dithiothreitol	Biomol
Ethanol (absolute)	Merck
Folin & Ciocalteu's phenol reagent	Sigma
Formalin (37% formaldehyde solution)	Merck
Formic acid	Aldrich Chemical Co.
Glycerol	Biomol
Glycine	Amersham Bioscien.
HCl	Merck
Iodoacetamide	Merck
Isopropanol p.a.	Merck
Methanol	Merck
Potassium Ferricyanide	Sigma
Rotiphorese Gel 30 (Acrylamid/Bisacrylamid)	Roth
Silver nitrate	Merck
Sodium carbonate	Merck
Sodium chloride	Merck
Sodium dodecylsulfate	Amersham Bioscien.
Sodium hydroxide	Merck
Sodium phosphate	Merck
Sodium tartrate dihydrate	Merck
Sodium thiosulfate pentahydrate	Sigma
Sodium thiosulfate pentahydrate (silver-stain.)	Merck
TEMED	BioRad
Trifluoroacetic acid	Aldrich Chemical Co.
Tricine	Biomol
Tris	Amersham Bioscien.
Trypsin Resuspension Buffer	Promega
Urea	Amersham Bioscien.

4.2.2.2. Standards

Adrenocorticotrophic hormone	Sigma
Alcohol dehydrogenase	Sigma
Bovine serum albumin	Sigma
Precision Protein Standard, Prestained	BioRad

4.2.3. Enzymes

Complete proteinase inhibitor cocktail	Roche
Pefabloc ^R	Sigma
Sequencing Grade Modified Trypsin, Porcine	Promega
Trypsin	Sigma

4.2.4. IEF material

DryStrip Cover Fluid	Amersham Bioscien.
Etan IPGphor Strip Cleaning Solution	Amersham Bioscien.
Equilibration tube set	Amersham Bioscien.
IEF electrode strips	Amersham Bioscien.
Immobiline DryStrip Reswelling tray	Amersham Bioscien.
IPG buffer	Amersham Bioscien.
IPG Cup Loading Strip Holder	Amersham Bioscien.
IPG Strip Holder	Amersham Bioscien.
IPG Strips	Amersham Bioscien.
IPGphor Isoelectric Focusing Unit	Amersham Bioscien.
Sample cups, Electrodes	Amersham Bioscien.

4.2.5. SDS-PAGE material

Frames, clamps, spacers (for SDS-PAGE)	BioRad
Frames, clamps (for Gel dryer system)	BioRad
PROTEAN II xi multi-cell	BioRad

4.2.6. Other material

Cellophane	Biorad
CryoTube TM Vials	NalgeNunc
International	
Deionised water	
Dry ice	
Eppendorf tubes	

Filter paper	Wick
Gel-blotting paper	Schleicher & Schuell
Liquid nitrogen	
Nitrocellulose membrane Porablot NCP	Macherey-Nagel
Parafilm	American National Can
Water for chromatography	Merck

4.2.7. Animals

Mice C₅₇BL/6 wild type and VDR knock-out were kindly provided by group of Dr. R. Erben, Institute of Animal Physiology, Ludwig Maximilians University, Munich

4.2.8. Software

MassLynx 3.5 (MALDI Analysis Software)	Micromass
PDQuest (2-D Gel Analysis Software)	BioRad

4.2.9. Devices

Concentrator 5301	Eppendorf
Gel Air Drying System	BioRad
GS-710 Calibrated Imaging Densitometer	BioRad
Incubator 37°C	Heraeus Instruments
MALDI mass spectrometer	Micromass
PotterS homogenizer	B.Braun Biotech Int.
Power supply POWERPAC 1000	BioRad
SC210A SpeedVac Concentrator	Savant
Shaker DUOMAX 1030	Heidolph Instruments
Shaker KS260 basic	IKA®
Tabletop centrifuge 5415C	Eppendorf
Ultracentrifuge L7-65	Beckman
Vortex-2 Genie	Scientific Industries
Water bath K20/DC10	HAAKE

LITERATURE

Akiyoshi-Shibata, M., Sakaki, T., Ohyama, Y., Noshiro, M., Okuda, K. and Yabusaki, Y. (1994) Further oxidation of hydroxycalcidiol by calcidiol 24-hydroxylase: a study with the mature enzyme expressed in *Escherichia coli*.

Eur J Biochem 224, 335-343.

Amling, M., Priemel, M., Holzmann, T., Chapin, K., Rueger, J.M., Baron, R. and Demay, M.B. (1999) Rescue of the skeletal phenotype of vitamin D receptor-ablated mice in the setting of normal mineral ion homeostasis: formal histomorphometric and biomechanical analyses.

Endocrinology 140, 4982-4987.

Beckman, M., Tadikonda, P., Werner, E., Prah, J.M., Yamada, S. and DeLuca, H.F. (1996) Human 25-hydroxyvitamin D₃-24-hydroxylase, a multicatalytic enzyme.

Biochemistry 35, 8465-8472.

Belfiore, F., Borzi, V., Lo Vecchio, L., Napoli, E. and Rabuazzo, A.M. (1975) Enzyme activities of NADPH-forming metabolic pathways in normal and leukemic leukocytes.

Clin Chem 21, 880-883.

Beno, D.W., Brady, L.M., Bissonnette, M. and Davis, B.H. (1995) Protein kinase C and mitogen-activated protein kinase are required for 1,25-dihydroxyvitamin D₃-stimulated Egr induction.

J Biol Chem 270, 3642-3647.

Berry, D.M., Antochi, R., Bhatia, M. and Meckling-Gill, K.A. (1996) 1,25-dihydroxyvitamin D₃ stimulates expression and translocation of protein kinase C(α) and C(δ) via a nongenomic mechanism and rapidly induces phosphorylation of a 33-kDa protein in acute promyelocytic NB4 cells.

J Biol Chem 271, 16090-16096.

Bjellquist, B., Ek, K., Righetti, P.G., Gianazza, E., Görg, A., Westermeier, R. and Postel, W. (1982) Isoelectric focusing in immobilized pH gradients: principle, methodology and some applications. *J Biochem Biophys Methods* 6, 317-339.

Bootman, M.D., Collins, T.J., Peppiatt, C.M., Prothero, L.S., MacKenzie, L., De Smet, P., Travers, M., Tovey, S.C., Seo, J.T., Berridge, M.J., Ciccolini, F. and Lipp, P. (2001) Calcium signalling-an overview. *Semin Cell Dev Biol* 12, 3-10.

Bouhtiauy, I., Lajeunesse, D., Christakos, S. and Brunette, M.G. (1994a) Two vitamin D₃-dependent calcium binding proteins increase calcium reabsorption by different mechanism. I. Effect of CaBP 28K. *Kidney Int* 45, 461-468.

Bouhtiauy, I., Lajeunesse, D., Christakos, S. and Brunette, M.G. (1994b) Two vitamin D₃-dependent calcium binding proteins increase calcium reabsorption by different mechanism. II. Effect of CaBP 9K. *Kidney Int* 45, 469-474.

Brown, E.M. (2000) G protein-coupled, extracellular Ca²⁺ (Ca_o²⁺)-sensing receptor enables Ca_o²⁺ to function as a versatile extracellular first messenger. *Cell Biochem Biophys* 33, 63-95.

Brown, E.M. and MacLeod, R.J. (2001) Extracellular calcium sensing and extracellular calcium signalling. *Psychiol Rev* 81, 239-297.

Cantorna, M.T., Humpal-Winter, J. and DeLuca, H.F. (2000) *In vivo* upregulation of interleukin-4 is one mechanism underlying the immunoregulatory effects of 1,25-dihydroxyvitamin D₃. *Arch Biochem Biophys* 377, 135-138.

Chen, H., Lin, R.J., Schiltz, R.L., Chakravarti, D., Nash, A., Nagy, L., Privalsky, M.L., Nakatani, Y. and Evans, R.M. (1997) Nuclear receptor coactivator ACTR is a novel histone acetyltransferase and forms a multimeric activation complex with P/CAF and CBP/p300. *Cell* 90, 569-580.

Chertow, B.S., Sivitz, W.I., Baranetsky, N.G., Clark, S.A., Waite, A. and DeLuca, H.F. (1983) Cellular mechanisms of insulin release: the effects of vitamin D deficiency and repletion on rat insulin secretion. *Endocrinology* 113, 1511-1518.

- Donohue, M.M. and Demay, M.B.** (2002) Rickets in VDR null mice is secondary to decreased apoptosis of hypertrophic chondrocytes. *Endocrinology* 143, 3691-3694.
- Erben, R.G., Soegiarto, D.W., Weber, K., Zeitz, U., Lieberherr, M., Gniadecki, R., Moller, G., Adamski, J. and Balling, R.** (2002) Deletion of deoxyribonucleic acid binding domain of the vitamin D receptor abrogates genomic and nongenomic functions of vitamin D. *Mol Endocrinol* 16, 1524-1537.
- Görg, A., Postel, W., Günther, S. and Weser, J.** (1985) Improved horizontal two-dimensional electrophoresis with hybrid isoelectric focusing in immobilized pH gradients in the first dimension and laying-on transfer to the second dimension. *Electrophoresis* 6, 599-546.
- Görg, A., Postel, W. and Günther, S.** (1988) The current state of the two-dimensional electrophoresis with immobilized pH gradients. *Electrophoresis* 9, 531-546.
- Görg, A., Boguth, G., Obermaier, C., Harder, A. and Weiss, W.** (1998) 2-D electrophoresis with immobilized pH gradients using IPGphor isoelectric focusing system. *Life Science News* 1, 4-6.
- Hanss, B., Leal-Pinto, E., Teixeira, A., Christian, R.E., Shabanowitz, J., Hunt, D.F. and Klotman, P.E.** (2001) Cytosolic malate dehydrogenase confers selectivity of the nucleic acid-conducting channel. *PNAS* 99, 1707-1712.
- Hoenderop, J.G., Dardenne, O., Van Abel, M., Van Der Kemp, A.W., Van Os, C.H., St-Arnaud, R. and Bindels, R.J.** (2002) Modulation of renal Ca^{2+} transport protein genes by dietary Ca^{2+} and 1,25-dihydroxyvitamin D_3 in 25-hydroxyvitamin D_3 -1 α -hydroxylase knockout mice. *FASEB J* 16, 1398-1406.
- Jones, G., Strugnelli, S.A. and DeLuca, H.F.** (1998) Current understanding of the molecular actions of vitamin D. *Physiol Rev* 78, 1193-1231. *Review.*
- Jones, J.M., Morrell, J.C. and Gould, S.J.** (2000) Identification and characterization of HAOX1, HAOX2, and HAOX3, three human peroxisomal 2-hydroxy acid oxidases. *J Biol Chem* 275, 12590-12597.

Karas, M. and Hillenkamp, F. (1988) Laser desorption ionization of proteins with molecular masses exceeding 10,000 daltons. *Anal Chem* 60, 2299-2301.

Kimmel-Jehan, C., Jehan, F. and DeLuca, H.F. (1997) Salt concentration determines 1,25-dihydroxyvitamin D₃ dependency of vitamin D receptor-retinoid X receptor--vitamin D-responsive element complex formation. *Arch Biochem Biophys* 341, 75-80.

Kimmel-Jehan, C., Darwish, H.M., Strugnelli, S.A., Jehan, F., Wiefeling, B. and DeLuca, H.F. (1999) DNA bending is induced by binding of vitamin D receptor-retinoid X receptor heterodimers to vitamin D response elements. *J Cell Biochem* 74, 220-228.

Kinuta, K., Tanaka, H., Moriwake, T., Aya, K., Kato, S. and Seino, Y. (2000) Vitamin D is an important factor in estrogen biosynthesis of both female and male gonads. *Endocrinology* 141, 1317-1324.

Klose, J. (1975) Protein mapping by combined isoelectric focusing and electrophoresis of mouse tissues. A novel approach to testing for induced point mutation in mammals. *Humangenetik* 26, 231-243.

Kusmann, M., Nordhoff, E., Rahbek-Nielsen, H., Haebel, S., Rossel-Larsen, M., Jakobsen, L., Gobom, J., Mirgorodskaya, E., Kroll-Kristensen, A., Palm, L. and Roepstorff, P. (1997) Matrix-assisted laser desorption/ionization mass spectrometry sample preparation techniques designed for various peptide and protein analytes. *J Mass Spectrom* 32, 593-601.

Li, Y.C., Pirro, A.E., Amling, M., Delling, G., Baron, R., Bronson, R. and Demay, M.B. (1997) Targeted ablation of the vitamin D receptor: an animal model of vitamin D-dependent rickets type II with alopecia. *Proc Natl Acad Sci USA* 94, 9831-9835.

Li, Y.C., Amling, M., Pirro, A.E., Priemel, M., Meuse, J., Baron, R., Delling, G. and Demay, M.B. (1998) Normalization of mineral ion homeostasis by dietary means prevents hyperparathyroidism, rickets, and osteomalacia, but not alopecia in vitamin D receptor-ablated mice. *Endocrinology* 139, 4391-4396.

- Lottspeich, F. and Zorba H.** (1998) Bioanalytik
Spektrum Akademische Verlag GmbH Heidelberg · Berlin
ISBN 3-8274-0041-4
- Markwell, M.A., Haas, S.M., Tolbert, N.E. and Bieber, L.L.** (1981)
Protein determination in membrane and lipoprotein samples : manual and
automated procedures.
Methods Enzymol 72, 296-303.
- Naveh-Many, T., Marx, R., Keshet, E., Pike, J.W. and Silver, J.** (1990)
Regulation of 1,25-dihydroxyvitamin D₃ receptor gene expression by 1,25-
dihydroxyvitamin D₃ in the parathyroid in vivo.
J Clin Invest 86, 1968-1975.
- Norman, A.W., Henry, H.L., Bishop, J.E., Song, X.D., Bula, C. and
Okamura, W.H.** (2001) Different shapes of the steroid hormone 1 α ,
25(OH)₂-vitamin D₃ act as agonists for two different receptors in the
vitamin D endocrine system to mediate genomic and rapid responses.
Steroids 66, 147-158.
- O'Farrell, P.H.** (1975) High resolution two-dimensional electrophoresis of
proteins.
J Biol Chem 250, 4007-4021.
- O'Kelly, J., Hisatake, J., Hisatake, Y., Bishop, J., Norman, A. and
Koeffler, H.P.** (2002) Normal myelopoiesis but abnormal T lymphocyte
responses in vitamin D receptor knockout mice.
J Clin Invest 109, 1091-1099.
- Polly, P., Herdick, M., Moehren, U., Baniahmad, A., Heinzl, T. and
Carlberg, C.** (2000) VDR-Alien: a novel, DNA-selective vitamin D₃
receptor-corepressor partnership.
FASEB J. 14, 1455-1463.
- Purroy, J. and Spurr, N.K.** (2002) Molecular genetics of calcium sensing
in bone cells.
Hum Mol Genet 11, 2377-2384.
- Rabilloud, T.** (1990) Mechanism of protein silver staining in
polyacrylamide gels: a 10-year synthesis.
Electrophoresis 11, 785-794.

Setoyama, C., Ding, S.-H., Choudhury, B.K., Joh, T., Takeshima, H., Tsuzuki, T. and Shimada, K. (1990) Regulatory regions of the mitochondrial and cytosolic isoenzyme genes participating in the malate-aspartate shuttle.

J Biol Chem 265, 1293-1299.

Shevchenko, A., Wilm, M., Vorm, O. and Mann, M. (1996) Mass spectrometric sequencing of proteins from silver-stained polyacrylamide gels.

Anal Chem 68, 850-858.

Shinki, T., Hin, C.H., Nishimura, A., Nagai, Y., Ohyama, Y., Noshiro, M., Okuda, K. and Suda, T. (1992) Parathyroid hormone inhibits 25-hydroxyvitamin D₃ in rat kidney but not in intestine.

J Biol Chem 267, 13757-13762.

Shinki, T., Shimada, H., Wankino, S., Anazawa, H., Hayashi, M., Saruta, T., DeLuca, H.F. and Suda, T. (1998) Cloning and expression of rat 25-hydroxyvitamin D₃-1 α -hydroxylase cDNA.

Proc Natl Acad Sci USA 94, 12920-12925.

Song, X., Bishop, J.E., Okamura, W.H. and Norman, A.W. (1998) Stimulation of phosphorylation of mitogen-activated protein kinase by 1 α ,25-dihydroxyvitamin D₃ in promyelocytic NB4 leukemia cells: a structure-function study.

Endocrinology 139, 457-465.

Stryer, L. (1996) Biochemie

Spektrum Akademische Verlag GmbH Berlin · Heidelberg · Oxford

ISBN 3-86025-346-8

Sunn, K.L., Cock, T.A., Crofts, L.A., Eisman, J.A. and Gardiner, E.M. (2001) Novel N-terminal variant of human VDR.

Mol Endocrinol 15, 1599-1609.

Tagami, T., Lutz, W.H., Kumar, R. and Jameson, J.L. (1998) The interaction of the vitamin D receptor with nuclear receptor corepressors and coactivators.

Biochem Biophys Res Commun 253, 358-363.

Torchia, J., Glass, C. and Rosenfeld, M.G. (1998) Co-activators and co-repressors in the integration of transcriptional responses.

Curr Opin Cell Biol 10, 373-383. Review.

Ünlü, M., Morgan, M.E. and Minden, J.S. (1997) Difference gel electrophoresis: a single gel method for detecting changes in protein extracts.

Electrophoresis 18, 2071-2077.

Van Cromphaut, S.J., Dewerchin, M., Hoenderop, J.G., Stockmans, I., Van Herck, E., Kato, S., Bindels, R.J., Collen, D., Carmeliet, P., Bouillon, R. and Carmeliet, G. (2001) Duodenal calcium absorption in vitamin D receptor-knockout mice: functional and molecular aspects.

Proc Natl Acad Sci USA 98, 13324-13329.

Vorm, O. and Mann, M. (1994) Improved mass accuracy in matrix-assisted laser desorption/ionization time-of-flight mass spectrometry of peptides.

J Am Soc Mass Spectrom 5, 955-958.

Wasinger, V.C., Cordwell, S.J., Cerpa-Poljak, A., Yan, J.X., Gooley, A.A., Wilkins, M.R., Duncan, M.W., Harris, R., Williams, K.L. and Humphery-Smith, I. (1995) Progress with gene-product mapping of the Mollicutes: *Mycoplasma genitalium*.

Electrophoresis 16, 1090-1099.

Wilson, J.D. and Foster, D.W. (1992) Williams textbook of endocrinology. W.B. Saunders Company

ISBN 0-7216-9514-0

Wright, G.L. Jr., Cazares, L.H., Leung, S.-M., Nasim, S., Adam, B.-L., Yip, T.-T., Schellhammer, P.F., Gong, L. and Vlahou, A. (1999) Proteinchip® surface enhanced laser desorption/ionization (SELDI) mass spectrometry: a novel protein biochip technology for detection of prostate cancer biomarkers in complex protein mixtures.

Prostate Cancer Prostatic Dis 2, 264-276.

Yoshizawa, T., Handa, Y., Uematsu, Y., Takeda, S., Sekine, K., Yoshihara, Y., Kawakami, T., Arioka, K., Sato, H., Uchiyama, Y., Masushige, S., Fukamizu, A., Matsumoto, T. and Kato, S. (1997) Mice lacking the vitamin D receptor exhibit impaired bone formation, uterine hypoplasia and growth retardation after weaning.

Nat Genet 16, 391-396.

Zanello, L.P. and Norman, A.W. (1997) Stimulation by $1\alpha,25(\text{OH})_2$ -vitamin D₃ of whole cell chloride currents in osteoblastic ROS 17/2.8 cells. A structure-function study.

J Biol Chem 272, 22617-22622.

List of figures

Figure 1.	Activation and inactivation steps in vitamin D metabolism	12
Figure 2.	Vitamin D mediated genomic and nongenomic response	15
Figure 3.	Schematic structure of vitamin D receptor	16
Figure 4.	Analysis of wild type mice kidney proteome by 2-D electrophoresis (wild type)	22
Figure 5.	Analysis of wild type mice kidney proteome by 2-D electrophoresis (VDR knock-out)	23
Figure 6.	Set of 2-D electrophoresis gels with differentially modified second dimension SDS-PAGE	24
Figure 7.	2-D electrophoresis gel with reduced proteolysis and protein diffusion	26
Figure 8.	PDQuest analysis of wild type 2-D electrophoresis gels	28
Figure 9.	PDQuest analysis of knock-out 2-D electrophoresis gels	29
Figure 10.	“Zoom-in” 2-D electrophoresis gels (pH 4-7)	33
Figure 11.	“Zoom-in” 2-D electrophoresis gels (pH 6-9)	33
Figure 12.	PAGE of different molecular weight protein markers	34
Figure 13.	Reflectron MALDI-TOF spectrum of test protein spot	35
Figure 14.	2-D electrophoresis gel of a wild type mouse kidney proteome	36
Figure 15.	Reflectron MALDI-TOF mass spectrometry of peptides obtained by in-gel trypsin digestion of 2-D electrophoresis gel spots	39
Figure 16.	Reflectron MALDI-TOF mass spectrometry of peptides obtained by in-gel trypsin digestion of 2-D electrophoresis gel spots	41
Figure 17.	Reflectron MALDI-TOF mass spectrometry of adenosine kinase peptides	42

Figure 18. Reflectron MALDI-TOF mass spectrometry of vitamin D receptor peptides	44
Figure 19. Amino acid sequences of proteins identified by MALDI-TOF MS	45
Figure 20. Amino acid sequence alignments of human and mouse proteins	46
Figure 21. Different metabolic actions in metabolic pathway of mammalian cells	52
Figure 22. Principle of isoelectric focusing (IEF)	60
Figure 23. Set up of an IPG strip in a cup loading strip holder	62
Figure 24. Principle of second dimension separation (SDS-PAGE)	65
Figure 25. Distribution of pH gradients in different Immobiline DryStrip gels	67
Figure 26. Schematic figure of MALDI-TOF mass spectrometer that works in reflectron mode	70
Figure 27. Lay out of MALDI MS target plate	72
Figure 5.1. A calibration plot for protein concentration measurement	91

List of tables

Table 1. List of the proteins that were differentially expressed in the VDR knock-out kidney samples	31
Table 2. List of tryptic peptide fragments peaks of all analysed protein samples	37
Table 3. List of different parameters for all proteins identified by MALDI-TOF MS	39
Table 4. Running protocols for both rehydration and sample cup load	63
Table 5. Silver-staining protocol	66
Table 6. In-gel digestion of protein spots excised from the 2-D gels	69
Table 5.1. Absorbences data for 5 wild type (wt) and 5 VDR knock-out (ko) kidney protein isolates	92

5. APPENDIX

5.1. Protein concentration measurement

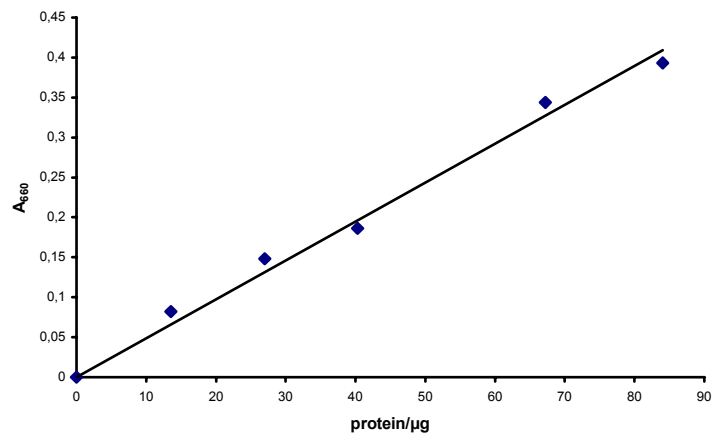


Figure 5.1. A calibration plot for protein concentration measurement. On the axis x are micrograms (μg) of protein, and on the axis y are absorbences (A_{660}) at 660 nm. Calibration curve is made of data for dilution series of calibration standard.

APPENDIX

Sample	A ₁	A ₂	A _{mean}	Dilution (n-fold)	Protein concentration (mg/ml)	Average concentration (mg/ml)
wt1	0.075	0.051	0.063	5000	51.436	51.4
wt1	0.158	0.114	0.136	1000	23.566	22.6
wt1	0.239	0.237	0.238	500	21.620	
wt2	0.069	0.027	0.048	5000	38.093	38.1
wt2	0.118	0.148	0.133	1000	23.010	22.3
wt2	0.219	0.257	0.238	500	21.620	
wt3	0.062	0.055	0.059	5000	47.424	47.4
wt3	0.108	0.133	0.121	1000	20.701	18.9
wt3	0.178	0.205	0.192	500	17.040	
wt4	0.073	0.075	0.074	5000	61.278	61.3
wt4	0.156	0.119	0.138	1000	23.845	22.9
wt4	0.239	0.242	0.241	500	21.871	
wt5	0.066	0.026	0.046	5000	36.320	36.3
wt5	0.152	0.113	0.133	1000	22.917	23.3
wt5	0.260	0.256	0.258	500	23.647	
ko1	0.052	0.054	0.053	5000	42.531	42.5
ko1	0.131	0.127	0.129	1000	22.269	19.9
ko1	0.200	0.194	0.197	500	17.572	
ko2	0.029	0.065	0.047	5000	37.206	37.2
ko2	0.165	0.153	0.159	1000	27.873	24.7
ko2	0.228	0.248	0.238	500	21.620	
ko3	0.051	0.056	0.054	5000	42.975	43.0
ko3	0.165	0.093	0.078	1000	12.884	12.5
ko3	0.140	0.138	0.139	500	12.062	
ko4	0.021	0.064	0.043	5000	33.221	33.2
ko4	0.124	0.154	0.139	1000	24.124	21.8
ko4	0.219	0.214	0.217	500	19.480	
ko5	0.019	0.068	0.044	5000	34.106	34.1
ko5	0.131	0.096	0.114	1000	19.415	18.2
ko5	0.191	0.189	0.190	500	16.895	

Table 5.1. Absorbences data for 5 wild type (wt) and 5 VDR knock-out (ko) kidney protein isolates. Each sample was diluted to the three different concentrations and A₆₆₀ was measured for each sample dilution in duplicates. The mean absorbance value (A_{mean}) was used for interpolation of the data from the calibration plot. Protein concentration was calculated for each dilution factor separately and expressed in mg/ml of total protein. The average concentration for 1000 and 500 fold dilutions was used to estimate the concentration for each sample. 5000x diluted samples were unreliable, most probably due to the high dilution factor, so they were excluded.

Acknowledgements

My special thanks goes to:

PD Dr. Jerzy Adamski, my supervisor, for giving me the chance to do my Ph.D. work in his lab and for all support he gave me during that time,

Dr. Rainer Breitling, first of all for being a friend, but also for giving me his critical observations from the beginning of my work, especially at the end, for all his support and long talks.

I would like to thank,

- Dr. Hans Zischka, for continuous help with 2-D electrophoresis and MALDI by giving me directions and tips, and for all the time he spend unselfishly on my questions,
- Dr. R. Erben, for providing me with mice samples.

I would also like to thank all my colleagues for a nice working atmosphere and scientific support, but most of all:

- Dr. Gabriele Möller for taking care of me from the very beginning, for helping me to cope with all bureaucratic problems and for all given support, especially at the end of the work
- (soon to be Dr.) Florian Grädler for tasteful dinners, nice parties and for being a friend all the time.

At the end my very special thanks goes to my best female friend, flatmate and working colleague Zrinka Marijanovic, for all support she gave me, in scientific and private life, but most of all for being a true friend; to Nikica for understanding, patience and love; to all my friends that helped me to cope more easily with the distance; and the most important to my parents and brothers for their trust in me and for all love they gave me – HVALA.